UNIVERSIDAD DE CONCEPCIÓN

Centro de Investigación en Ingeniería Matemática (CI^{2}MA)

A priori and a posteriori error analyses of a high order unfitted mixed-FEM for Stokes flow

Ricardo Oyarzúa, Manuel Solano, Paulo Zuñiga

PREPRINT 2019-15

SERIE DE PRE-PUBLICACIONES

A priori and a posteriori error analyses of a high order unfitted mixed-FEM for Stokes flow☆

Ricardo Oyarzúa[a,b], Manuel Solano[b,c], Paulo Zúñiga[b,c]

[a]*GIMNAP-Departamento de Matemática, Facultad de Ciencias, Universidad del Bío-Bío, Casilla 5-C, Concepción, Chile*
[b]*Centro de Investigación en Ingeniería Matemática, CI²MA, Universidad de Concepción, Casilla 160-C, Concepción, Chile*
[c]*Departamento de Ingeniería Matemática, Facultad de Ciencias Físicas y Matemáticas, Universidad de Concepción, Casilla 160-C, Concepción, Chile*

Abstract

We propose and analyze a high order unfitted mixed finite element method for the pseudostress-velocity formulation of the Stokes problem with Dirichlet boundary condition on a fluid domain Ω with curved boundary Γ. The method consists of approximating Ω by a polygonal subdomain D_h, with boundary Γ_h, where a Galerkin method is applied to approximate the solution, and on a transferring technique, based on integrating the extrapolated discrete gradient of the velocity, to approximate the Dirichlet boundary data on the computational boundary Γ_h. The associated Galerkin scheme is defined by Raviart–Thomas elements of order $k \geq 0$ for the pseudostress and discontinuous polynomials of degree k for the velocity. Provided suitable hypotheses on the mesh near the boundary Γ, we prove well-posedness of the Galerkin scheme by means of the Babuška–Brezzi theory and establish the corresponding optimal convergence $\mathcal{O}(h^{k+1})$. Moreover, for the case when Γ_h is constructed through a piecewise linear interpolation of Γ, we propose a reliable and quasi-efficient residual-based a posteriori error estimator. Its definition makes use of a postprocessed velocity with enhanced accuracy to achieve the same rate of convergence of the method when the solution is smooth enough. Numerical experiments illustrate the performance of the scheme, show the behaviour of the associated adaptive algorithm and validate the theory.

Keywords: curved domain, high order, Stokes flow, unfitted methods, mixed finite element method, a posteriori error analysis
2010 MSC: 65N30, 65N12, 65N15, 76D07

1. Introduction

It is well-known that standard Galerkin procedures devised to solve PDEs on curved domains Ω do not achieve high order accuracy whenever Ω is approximated by a nearby domain D_h. In principle, neither the regularity of the solution nor the smoothness of the curved boundary Γ are the reasons behind the loss of accuracy. Instead, the difficulties arise from the *variational crimes* (see, e.g. [9, Chapter 10]) given by an eventual noncoforming method. A natural way to avoid the lack of accuracy is to use isoparametric finite elements (see, e.g. [38]) where the mesh of D_h fits the PDE domain under an explicit parametrization of

☆R. Oyarzúa acknowledges partial support from CONICYT-Chile through project Fondecyt 1161325 and project AFB170001 of the PIA Program: Concurso Apoyo a Centros Científicos y Tecnológicos de Excelencia con Financiamiento Basal and from Universidad del Bío-Bío through DIUBB project GI 171508/VC. M. Solano acknowledges partial support from CONICYT-Chile through project Fondecyt 1160320 and project AFB170001 of the PIA Program: Concurso Apoyo a Centros Científicos y Tecnológicos de Excelencia con Financiamiento Basal. P. Zúñiga acknowledges support from CONICYT-Chile through project AFB170001 of the PIA Program: Concurso Apoyo a Centros Científicos y Tecnológicos de Excelencia con Financiamiento Basal and from Becas-CONICYT-Chile through PFCHA/Doctorado/2016–21160446.

Email addresses: `royarzua@ubiobio.cl` (Ricardo Oyarzúa), `msolano@ing-mat.udec.cl` (Manuel Solano), `pzuniga@ci2ma.udec.cl` (Paulo Zúñiga)

Γ. However, these meshes are not easy to construct and remeshing is expensive, especially for complicated geometries or evolving domains.

Alternatively, when the geometry is implicitly described by a level set function, *unfitted methods*, such as the cut finite element method (CutFEM [11]), minimize the complexity of mesh generation by, for instance, immersing Ω in a background uniform mesh and setting D_h as the union of all the elements of the mesh that lie inside Ω. While these methods are convenient for general curved domains, its major drawback is to retain the high order accuracy of the approximation, since the computational boundary $\Gamma_h := \partial \mathrm{D}_h$ is "far" from Γ.

Provided a domain Ω with Lipschitz continuous and picewise $\mathcal{C}^2$ boundary Γ, a novel high order *unfitted method* for Dirichlet boundary value problems has been proposed in the context of hybridizable discontinuous Galerkin (HDG) methods [18, 19, 21]. More precisely, denoting by u the variable such that $\sigma := \nabla u$ in Ω and $u = g$ on Γ, it consists of transferring the Dirichlet datum g from Γ to Γ_h by integrating σ along a family of segments joining both boundaries, which are usually referred as *transferring paths*. At the discrete level, the transferred data, say $\widetilde{g}$, is approximated by $\widetilde{g}_h$ obtained by integrating the extrapolation of the discrete approximation of σ along the transferring paths. Thus, the problem is solved in D_h and its solution is extended by local extrapolations to D_h^c. It is remarkable that the method keeps high order accuracy when the distance $d(\Gamma, \Gamma_h)$ between Γ and Γ_h is only of order of the meshsize h. Also, it covers the case where Γ_h is constructed through a picewiese linear interpolation of Γ. In addition, also in the context of HDG methods, this *transferring technique* has been successfully applied to a wide variety of problems in continuum mechanics, including exterior diffusion equations [20], convection-diffusion problems [22], the semi-linear Grad–Shafranov equation [42], the Stokes equations for incompressible flow [44], and the Oseen equations [43]. It has been also extended to a diffusion problem with mixed boundary conditions and to an elliptic transmission problem where the interface is not piecewise flat, for which we refer to [40].

On the other hand, we have recently proposed and analyzed in [39] the first high order *unfitted mixed finite element method* for diffusion problems where the Dirichlet datum is transferred according to the above technique. Considering general finite dimensional subspaces, we showed the well-posed of the discrete formulation by means of the classical Babuška–Brezzi theory (see, e.g. [29]). In particular, we showed that Raviart–Thomas elements of order order $k \geq 0$ for the vectorial variable and discontinuous polynomials of degree k for the scalar variable, ensure unique solvability and optimal convergence $\mathcal{O}(h^{k+1})$ of the associated Galerkin scheme, which rely only on some hypotheses involving the "closeness" between Γ and Γ_h.

According to the above discussion, our first goal in this paper is to additionally contribute in the direction of [39] and provide a high order unfitted mixed-FEM for the incompressible Stokes equations in which the pseudostress tensor [12] and the fluid velocity are the only unknowns, whereas the pressure is computed via a postprocessing procedure. We refer the reader to the early work of Gatica et al. [30] (see also [13]), for the analysis of this problem in polygonal/polyhedral domains. A few points for this choice deserve comments. First, the pseudostress tensor has been widely used to overcome the well-known disadvantages of considering the symmetric stress tensor (see, e.g. [3, 5, 6, 10]). Indeed, in the modeling equations the pseudostress take the place of the stress without requiring symmetry. In addition, an accurate direct calculation of further physical quantities such as the velocity gradient, the vorticity and the stress, can be expressed in terms of the pseudostress discretization via a simple postprocessing procedure, and with the same accuracy. Finally, we remark that, different from the work by Solano and Vargas in [44], here the novelty lies on the treatment of the pseudostress approximation in D_h.

Now, in addition to the loss of accuracy over curved domains, the numerical approximation could be deteriorated by singularities or high gradients of the solution, often as a result of domains with re-entrant corners or solutions having interior/boundary layers. In order to guarantee a good convergence behaviour in that cases, one usually needs to apply an adaptive mesh refinement near the critical region; for a survey, we refer the reader to [48]. The elements to be refined are marked according to a global estimator Θ given in terms of local indicators Θ_T on each element T of a given mesh. The estimator Θ is said to be efficient (resp. reliable) if there exists $C_{\mathrm{eff}} > 0$ (resp. $C_{\mathrm{rel}} > 0$), independent of the meshsizes, such that

$$C_{\mathrm{eff}}\Theta + \text{h.o.t.} \leq \|\text{error}\| \leq C_{\mathrm{rel}}\Theta + \text{h.o.t.},$$

where h.o.t. is a generic expression denoting one or several high order terms. In particular, concerning our problem of interest, a residual-based *a posteriori* error estimator has been developed by [30]. However, in all the proofs, Ω has been assumed to be polygonal (or polyhedral in 3D).

In this paper, provided Γ is interpolated by a piecewise linear function, we further contribute in developing the first residual-based *a posteriori* error analysis for Stokes flow where the above mentioned transferring technique is employed. Unlike the polygonal case, our estimator is efficient up to calculable terms involving curved segments and a postprocessed velocity with enhanced accuracy. It is import to remark that the literature regarding high order approximations and adaptive mesh refinement on curved domains is scarce. Up to the authors's knowledge, probably the only work treating this matter was carried out in [2], where the Poisson problem was solved by using the *hp* finite element method [6] along with isoparametric elements fitting a Lipschitz continuous and piecewise $\mathcal{C}^{k+2}$ boundary Γ (for $k \geq 0$). However, the associated *hp* adaptivity strategy is difficult to implement. Indeed, at each refinement step and on each marked element, it must be decided whether to refine the mesh (h-version of FEM) or increase the polynomial degree (p-version of FEM). By contrast, in our analysis the assumption on Γ can be relaxed to piecewise $\mathcal{C}^2$ only. Moreover, our adaptive algorithm keeps the polynomial degree fixed and improves the accuracy of the approximation by refining the mesh without the need of using isoparametric elements, thus reducing the complexity for implementation.

Outline. The rest of this paper is organized as follows. In the remaining of the present section we recall some recurrent notation and general definitions. Next, in Section 2 we present the model problem and recall its classical dual-mixed formulation, having the pseudostress tensor and the fluid velocity as main unknowns. In Section 3, the fluid domain Ω is approximated by a polygonal subdomain D_h where a high order Galerkin scheme is introduced and analyzed. An *a priori* error analysis, involving hypotheses of "closeness" between Γ and Γ_h, is derived in Section 4. Moreover, in Section 5 we derive our *a posteriori* error estimator and establish its main properties, as long as Γ is interpolated by a piecewise linear function. Finally, in Section 6 we present numerical experiments validating the theory.

Preliminaries. In the sequel, when no confusions arises, $|\cdot|$ will denote the Euclidean norm in $\mathbb{R}^2$. In turn, given tensor fields $\boldsymbol{\sigma} := (\sigma_{ij})_{i,j=1,2}$ and $\boldsymbol{\tau} := (\tau_{ij})_{i,j=1,2}$, we let $\mathbf{div}\,\boldsymbol{\tau}$ be the divergence operator div acting along the rows of $\boldsymbol{\tau}$, and define the trace $\mathrm{tr}\,(\boldsymbol{\tau}) := \sum_{i=1}^{2} \boldsymbol{\tau}_{ii}$, the inner product $\boldsymbol{\sigma} : \boldsymbol{\tau} := \sum_{i,j=1}^{2} \sigma_{ij}\tau_{ij}$, and the deviatoric tensor $\boldsymbol{\tau}^{\mathrm{d}} := \boldsymbol{\tau} - \frac{1}{2}\mathrm{tr}\,(\boldsymbol{\tau})\mathbb{I}$, where $\mathbb{I}$ stand for the identity tensor in $\mathbb{R}^{2\times 2}$. Also, we adopt standard simplified terminology for Sobolev spaces and norms, where spaces of vector-valued and tensor-valued functions are denoted in bold face and blackboard bold face, respectively. For instance, if $\mathcal{O}$ is a domain in $\mathbb{R}^2$, $\mathscr{C}$ is an open or closed Lipschitz curve, and $s \in \mathbb{R}$, we define

$$\mathbf{H}^s(\mathcal{O}) := [\mathrm{H}^s(\mathcal{O})]^2\,, \quad \mathbb{H}^s(\mathcal{O}) := [\mathrm{H}^s(\mathcal{O})]^{2\times 2}\,, \quad \text{and} \quad \mathbf{H}^s(\mathscr{C}) := [\mathrm{H}^s(\mathscr{C})]^2\,,$$

with the conventions $\mathbf{H}^0(\mathcal{O}) = \mathbf{L}^2(\mathcal{O})$, $\mathbb{L}^2(\mathcal{O}) = \mathbb{H}^0(\mathcal{O})$ and $\mathbf{L}^2(\mathscr{C}) = \mathbf{H}^0(\mathscr{C})$. The corresponding norms are denoted by $\|\cdot\|_{s,\mathcal{O}}$ and $\|\cdot\|_{s,\mathscr{C}}$, whereas the seminorm is denoted by $|\cdot|_{s,\mathcal{O}}$. Furthermore, we recall that

$$\mathbb{H}(\mathbf{div};\mathcal{O}) := \{\boldsymbol{\tau} \in \mathbb{L}^2(\mathcal{O}) :\ \mathbf{div}\,\boldsymbol{\tau} \in \mathbf{L}^2(\mathcal{O})\},$$

equipped with the norm $\|\cdot\|_{\mathbf{div},\mathcal{O}} := (\|\cdot\|_{0,\mathcal{O}}^2 + \|\mathbf{div}\,(\cdot)\|_{0,\mathcal{O}}^2)^{1/2}$, is a Hilbert space. Note that if $\boldsymbol{\tau} \in \mathbb{H}(\mathbf{div};\mathcal{O})$, then $\boldsymbol{\tau}\mathbf{n}_{\partial\mathcal{O}} \in \mathbf{H}^{-1/2}(\partial\mathcal{O})$, where $\mathbf{H}^{1/2}(\partial\mathcal{O})$ is the space of traces of $\mathbf{H}^1(\mathcal{O})$, $\mathbf{H}^{-1/2}(\partial\mathcal{O})$ corresponds to the dual space of $\mathbf{H}^{1/2}(\partial\mathcal{O})$, and $\mathbf{n}_{\partial\mathcal{O}}$ denotes the outward unit normal vector on $\partial\mathcal{O}$. Hereafter, $\langle\cdot,\cdot\rangle_{\partial\mathcal{O}}$ denotes the duality pairing between $\mathbf{H}^{-1/2}(\partial\mathcal{O})$ and $\mathbf{H}^{1/2}(\partial\mathcal{O})$ with respect to the $\mathbf{L}^2(\mathcal{O})$-inner product. The following estimate (see, e.g. [29, Theorem 1.7]) holds:

$$\|\boldsymbol{\tau}\mathbf{n}\|_{-1/2,\partial\mathcal{O}} \leq \|\boldsymbol{\tau}\|_{\mathbf{div},\mathcal{O}} \quad \forall\,\boldsymbol{\tau} \in \mathbb{H}(\mathbf{div};\mathcal{O}). \tag{1.1}$$

In addition, by $\mathbf{0}$ we will refer to the generic null vector (including the null functional and operator), and we will denote by C and c, with or without subscripts, bars, tildes or hats, generic constants independent of the meshsize, but might depend on the polynomial degree, the shape-regularity of the triangulation and the domain. Furthermore, for quantities A and B, we write $A \lesssim B$, whenever there exists $C > 0$ such that $A \leq CB$. Finally, $A \simeq B$ stands for both $A \lesssim B$ and $B \lesssim A$ being satisfied.

2. The continuous problem

2.1. Governing equations

Let Ω be a bounded and open, not necessarily polygonal region with boundary Γ, which we assume to be piecewise $\mathcal{C}^2$ and Lipschitz continuous. We are interested in approximating, by a mixed finite element method, the Stokes equations describing a steady viscous incompressible fluid flow occupying Ω, under the action of external forces, given by

$$\begin{aligned} &\boldsymbol{\sigma} = 2\mu\nabla\mathbf{u} - p\mathbb{I} \quad \text{in} \quad \Omega, \quad \mathbf{div}\,\boldsymbol{\sigma} = -\mathbf{f} \quad \text{in} \quad \Omega, \\ &\mathrm{div}\,\mathbf{u} = 0 \quad \text{in} \quad \Omega, \quad \mathbf{u} = \mathbf{g} \quad \text{on} \quad \Gamma, \quad \int_\Omega p = 0. \end{aligned} \tag{2.1}$$

Here, the unknowns are the fluid velocity $\mathbf{u}$, the fluid pressure p, and the so-called pseudostress tensor $\boldsymbol{\sigma}$; the given data are a volume force $\mathbf{f} \in \mathbf{L}^2(\Omega)$ and the boundary velocity $\mathbf{g} \in \mathbf{H}^{1/2}(\Gamma)$, while the kinematic viscosity μ is a positive constant. Note that the incompressibility constraint $\mathrm{div}\,\mathbf{u} = 0$ in Ω, which expresses the conservation of mass, enforces that $\mathbf{g}$ must satisfy the compatibility condition

$$\int_\Gamma \mathbf{g}\cdot\mathbf{n}_\Gamma = 0, \tag{2.2}$$

where $\mathbf{n}_\Gamma$ stands for the outward unit normal vector to Γ. Furthermore, the last condition in (2.1) is added to ensure uniqueness of solution, and this will lead us to the introduction of the space $\mathrm{L}^2_0(\Omega) := \big\{ q \in \mathrm{L}^2(\Omega) : \int_\Omega q = 0 \big\}$.

2.2. The pseudostress-velocity formulation

In what follows, we briefly recall the pseudostress-velocity formulation employed in [13] and [30] for the Stokes problem described in the precious section. Let us first remark that taking the matrix trace operator in the first equation and using the incompressibility condition, we easily obtain the postprocessing formula

$$p = -\frac{1}{2}\mathrm{tr}\,(\boldsymbol{\sigma}) \quad \text{in} \quad \Omega. \tag{2.3}$$

In this way, using (2.3) we can eliminate p from (2.1), obtaining

$$\begin{aligned} &\frac{1}{2\mu}\boldsymbol{\sigma}^{\mathrm{d}} = \nabla\mathbf{u} \quad \text{in} \quad \Omega, \quad \mathbf{div}\,\boldsymbol{\sigma} = -\boldsymbol{f} \quad \text{in} \quad \Omega, \\ &\mathbf{u} = \mathbf{g} \quad \text{on} \quad \Gamma, \quad \int_\Omega \mathrm{tr}\,(\boldsymbol{\sigma}) = 0. \end{aligned} \tag{2.4}$$

Notice that the last condition is a consequence of (2.3) and of the requirement on the pressure space, and this therefore suggests the introduction of the space $\mathbb{H}_0(\mathbf{div};\Omega) := \big\{\boldsymbol{\tau} \in \mathbb{H}(\mathbf{div};\Omega) : \int_\Omega \mathrm{tr}\,(\boldsymbol{\tau}) = 0\big\}$ satisfying $\mathbb{H}(\mathbf{div}\,;\Omega) = \mathbb{H}_0(\mathbf{div};\Omega) \oplus \mathrm{P}_0(\Omega)\mathbb{I}$, where $\mathrm{P}_0(\Omega)$ is the space of constant polynomials defined on Ω. More precisely, each $\boldsymbol{\tau} \in \mathbb{H}(\mathbf{div};\Omega)$ can be decomposed uniquely as $\boldsymbol{\tau} = \boldsymbol{\tau}_0 + c\mathbb{I}$, with

$$\boldsymbol{\tau}_0 := \boldsymbol{\tau} - \left(\frac{1}{2|\Omega|}\int_\Omega \mathrm{tr}\,(\boldsymbol{\tau})\right)\mathbb{I} \in \mathbb{H}_0(\mathbf{div};\Omega) \quad \text{and} \quad c := \frac{1}{2|\Omega|}\int_\Omega \mathrm{tr}\,(\boldsymbol{\tau}) \in \mathbb{R}.$$

As a consequence of the above, from (2.4) it is not difficult to obtain the following variational formulation of (2.4): Find $(\boldsymbol{\sigma},\mathbf{u}) \in \mathbb{H}_0(\mathbf{div};\Omega) \times \mathbf{L}^2(\Omega)$ such that

$$\begin{aligned} a(\boldsymbol{\sigma},\boldsymbol{\tau}) + b(\boldsymbol{\tau},\mathbf{u}) &= \langle \boldsymbol{\tau}\mathbf{n}_\Gamma, \mathbf{g}\rangle_\Gamma \quad \forall\,\boldsymbol{\tau} \in \mathbb{H}_0(\mathbf{div};\Omega), \\ b(\boldsymbol{\sigma},\mathbf{v}) &= -\int_\Omega \mathbf{f}\cdot\mathbf{v} \quad \forall \in \mathbf{L}^2(\Omega), \end{aligned} \tag{2.5}$$

where $\mathbf{n}_\Gamma$ stands for the outward unit normal vector on Γ, whereas the bounded bilinear forms $a : \mathbb{H}(\mathbf{div};\Omega)\times\mathbb{H}(\mathbf{div};\Omega)\to\mathbb{R}$ and $b : \mathbb{H}(\mathbf{div};\Omega)\times\mathbf{L}^2(\Omega)$ are given, respectively, by

$$a(\boldsymbol{\sigma},\boldsymbol{\tau}) := \frac{1}{2\mu}\int_\Omega \boldsymbol{\sigma}^{\mathrm{d}} : \boldsymbol{\tau}^{\mathrm{d}} \quad\text{and}\quad b(\boldsymbol{\tau},\mathbf{v}) := \int_\Omega \mathbf{v}\cdot\mathbf{div}\,\boldsymbol{\tau}.$$

We refer the reader to [30, Theorem 2.1] for the well-posedness analysis of this problem. In particular, the respective continuous dependence result provided by the classical Babuška–Brezzi theorem (see, for instance [30, Theorem 2.3]), implies that the following global inf-sup conditions holds:

$$\|(\boldsymbol{\zeta},\mathbf{w})\|_{\mathbb{H}(\mathbf{div};\Omega)\times\mathbf{L}^2(\Omega)} \lesssim \sup_{\substack{(\boldsymbol{\tau},\mathbf{v})\in\mathbb{H}_0(\mathbf{div};\Omega)\times\mathbf{L}^2(\Omega)\\(\boldsymbol{\tau},\mathbf{v})\neq\mathbf{0}}} \frac{|a(\boldsymbol{\zeta},\boldsymbol{\tau})+b(\boldsymbol{\tau},\mathbf{w})+b(\boldsymbol{\zeta},\mathbf{v})|}{\|(\boldsymbol{\tau},\mathbf{v})\|_{\mathbb{H}(\mathbf{div};\Omega)\times\mathbf{L}^2(\Omega)}} \tag{2.6}$$

for all $(\boldsymbol{\zeta},\mathbf{w})\in\mathbb{H}_0(\mathbf{div};\Omega)\times\mathbf{L}^2(\Omega)$, where $\|(\cdot,\cdot)\|_{\mathbb{H}(\mathbf{div};\Omega)\times\mathbf{L}^2(\Omega)} := (\|\cdot\|^2_{\mathbf{div},\Omega}+\|\cdot\|^2_{0,\Omega})^{1/2}$. The specific purpose of this estimate will become clear below in Section 5 when dealing with the a posteriori error analysis.

To end this section, we remark that the solution of (2.5) solves the original problem (2.4) in the sense of the following lemma. The proof is omitted because is straightforward.

Lemma 2.1. *Let $(\boldsymbol{\sigma},\mathbf{u})\in\mathbb{H}_0(\mathbf{div};\Omega)\times\mathbf{L}^2(\Omega)$ be the unique solution of (2.5). It satisfies in a distributional sense, $(2\mu)^{-1}\boldsymbol{\sigma}^{\mathrm{d}}=\nabla\mathbf{u}$ in Ω, and $\mathbf{div}\,\boldsymbol{\sigma}=-\mathbf{f}$ in Ω. Moreover, $\mathbf{u}\in\mathbf{H}^1(\Omega)$ and satisfies the boundary condition described in (2.4).*

3. The Galerkin scheme

3.1. Preliminary results

In the context of curved domains, we now proceed as in [39] (see also [19, 21] for HDG methods) and suppose that there exist a family of subdomains D_h of the fluid region Ω having a polygonal boundary $\Gamma_h := \partial\mathrm{D}_h$, which may not necessarily fit the true boundary Γ. The index h will refer to the size of a given triangulation of $\overline{\mathrm{D}_h}$. For ease of presentation, in this section we develop the theory and postpone the construction of D_h to Sections 5 and 6.

As a consequence of Lemma 2.1, we can infer that the solution of (2.5) satisfies in a distributional sense,

$$\frac{1}{2\mu}\boldsymbol{\sigma}^{\mathrm{d}} = \nabla\mathbf{u} \quad\text{in}\quad \mathrm{D}_h, \qquad \mathbf{div}\,\boldsymbol{\sigma} = -\mathbf{f} \quad\text{in}\quad \mathrm{D}_h. \tag{3.1}$$

In turn, following the approach of [21], the trace of $\mathbf{u}$ on Γ_h, denoted by $\widetilde{\mathbf{g}}$, can be conveniently rewritten in terms of $\boldsymbol{\sigma}$. Indeed, integrating componentwise $(2\mu)^{-1}\boldsymbol{\sigma}^{\mathrm{d}}=\nabla\mathbf{u}$ along a segment, say $\mathscr{C}(\mathbf{x})$, starting at $\mathbf{x}\in\Gamma_h$ and ending at $\widetilde{\mathbf{x}}\in\Gamma$, which is often referred as *transferring path* and whose definition will be detailed in Section 3.2, we get

$$\widetilde{\mathbf{g}}(\mathbf{x}) = \overline{\mathbf{g}}(\mathbf{x}) - \frac{1}{2\mu}\int_{\mathscr{C}(\mathbf{x})} \boldsymbol{\sigma}^{\mathrm{d}}\,\mathbf{m}(\mathbf{x})\,d\eta, \tag{3.2}$$

where $\overline{\mathbf{g}}(\mathbf{x}) := \mathbf{g}(\widetilde{\mathbf{x}}(\mathbf{x}))$ and $\mathbf{m}(\mathbf{x})$ is the unit tangent vector to $\mathscr{C}(\mathbf{x})$. Clearly, this definition coincides with the trace of $\mathbf{u}$ on Γ_h, as it does not depend on the integration path. Moreover, when high order accuracy is required, the line integral in (3.2) allows us to obtain a better approximation of $\widetilde{\mathbf{g}}$ than the trace of the finite element solution associated to $\mathbf{u}$ on Γ_h.

Next, after reducing the equations of (3.1) to a weak form and using (3.2), it readily follows that the solution of (2.5) satisfies

$$\int_{\mathrm{D}_h} \mathrm{tr}\,(\boldsymbol{\sigma}) = -\int_{\mathrm{D}_h^c} \mathrm{tr}\,(\boldsymbol{\sigma}) \quad\text{with}\quad \mathrm{D}_h^c := \Omega\setminus\overline{\mathrm{D}_h}, \tag{3.3}$$

and

$$\begin{aligned} a_h(\boldsymbol{\sigma}, \boldsymbol{\tau}) + b_h(\boldsymbol{\tau}, \mathbf{u}) &= \langle \boldsymbol{\tau}\mathbf{n}_{\Gamma_h}, \widetilde{\mathbf{g}} \rangle_{\Gamma_h} \quad && \forall\, \boldsymbol{\tau} \in \mathbb{H}(\mathbf{div}; \mathrm{D}_h), \\ b_h(\boldsymbol{\sigma}, \mathbf{v}) &= F_h(\mathbf{v}) && \forall\, \mathbf{v} \in \mathbf{L}^2(\mathrm{D}_h), \end{aligned} \tag{3.4}$$

where $\mathbf{n}_{\Gamma_h}$ denotes the unit vector pointing in the outward normal direction of Γ_h with respect to D_h, and $a_h(\cdot,\cdot)$ on $\mathbb{H}(\mathbf{div}; \mathrm{D}_h) \times \mathbb{H}(\mathbf{div}; \mathrm{D}_h)$, $b_h(\cdot,\cdot)$ on $\mathbb{H}(\mathbf{div}; \mathrm{D}_h) \times \mathbf{L}^2(\mathrm{D}_h)$, and $F_h(\cdot)$ on $\mathbb{H}(\mathbf{div}; \mathrm{D}_h)$, denote the forms defined, respectively, by

$$a_h(\boldsymbol{\sigma}, \boldsymbol{\tau}) := \frac{1}{2\mu} \int_{\mathrm{D}_h} \boldsymbol{\sigma}^{\mathrm{d}} : \boldsymbol{\tau}^{\mathrm{d}}, \quad b_h(\boldsymbol{\tau}, \mathbf{v}) := \int_{\mathrm{D}_h} \mathbf{v} \cdot \mathbf{div}\, \boldsymbol{\tau}, \quad F_h(\mathbf{v}) := -\int_{\mathrm{D}_h} \mathbf{f} \cdot \mathbf{v}. \tag{3.5}$$

However, defining $\boldsymbol{\sigma}_0 \in \mathbb{H}(\mathbf{div}; \mathrm{D}_h)$ by

$$\boldsymbol{\sigma}_0 := \boldsymbol{\sigma}|_{\mathrm{D}_h} - \left(\frac{\gamma}{2|\mathrm{D}_h|} \right) \mathbb{I} \quad \text{with} \quad \gamma := -\int_{\mathrm{D}_h^c} \mathrm{tr}\,(\boldsymbol{\sigma}), \tag{3.6}$$

it is not difficult to see that $\boldsymbol{\sigma}_0 \in \mathbb{H}_0(\mathbf{div}; \mathrm{D}_h)$ if and only if (3.3) holds, and therefore, the equations (3.3)-(3.4) can be rewritten, equivalently, as:

$$\begin{aligned} a_h(\boldsymbol{\sigma}_0, \boldsymbol{\tau}) + b_h(\boldsymbol{\tau}, \mathbf{u}) &= \langle \boldsymbol{\tau}\mathbf{n}_{\Gamma_h}, \widetilde{\mathbf{g}} \rangle_{\Gamma_h} \quad && \forall\, \boldsymbol{\tau} \in \mathbb{H}_0(\mathbf{div}; \mathrm{D}_h), \\ b_h(\boldsymbol{\sigma}_0, \mathbf{v}) &= F_h(\mathbf{v}) && \forall\, \mathbf{v} \in \mathbf{L}^2(\mathrm{D}_h), \end{aligned} \tag{3.7}$$

provided that the compatibility condition $\int_{\Gamma_h} \widetilde{\mathbf{g}} \cdot \mathbf{n}_{\Gamma_h} = 0$ is satisfied. The latter is, indeed, a consequence of Gauss' divergence theorem and the equation $\mathrm{div}\, \mathbf{u} = 0$ in D_h, obtained from the first equation of (3.1) by applying the matrix trace operator. In addition, let us observe that since $\boldsymbol{\sigma}^{\mathrm{d}} = \boldsymbol{\sigma}_0^{\mathrm{d}}$, (3.2) can be written in terms of $\boldsymbol{\sigma}_0$ as

$$\widetilde{\mathbf{g}}(\mathbf{x}) = \overline{\mathbf{g}}(\mathbf{x}) - \frac{1}{2\mu} \int_{\mathscr{C}(\mathbf{x})} \boldsymbol{\sigma}_0^{\mathrm{d}}\, \mathbf{m}(\mathbf{x})\, d\eta, \tag{3.8}$$

Therefore, in what follows we propose a Galerkin scheme for (3.7). Before discussing further this matter, in the next section we introduce notation that will be useful to define our approximation in the region D_h^c.

3.2. Meshes and transferring paths

We consider a shape-regular family of triangulations $\{\mathcal{T}_h\}_{h>0}$ that subdivides the polygonal region $\overline{\mathrm{D}_h}$ into triangles T of diameter h_T and outward unit normal vector $\mathbf{n}_T$. Here, the index $h > 0$, refers to the meshsize $h := \max\{h_T :\ T \in \mathcal{T}_h\}$. Furthermore, we denote by $\mathcal{E}_h^i$ and $\mathcal{E}_h^\partial$ the sets of interior and boundary edges, respectively, and denote $\mathcal{E}_h = \mathcal{E}_h^i \cup \mathcal{E}_h^\partial$. Given $e \in \mathcal{E}_h$, we denote by T^e the element of $\mathcal{T}_h$ having e as an edge. In addition, to emphasize that a unit vector is normal to Γ_h or to an edge $e \in \mathcal{E}_h^\partial$, we will write $\mathbf{n}_{\Gamma_h}$ and $\mathbf{n}_e$, respectively.

We now turn to specify the family of transferring paths connecting Γ_h and Γ. Given $e \in \mathcal{E}_h^\partial$, let $\mathbf{p}_1$ and $\mathbf{p}_2$ its two vertices. To each of them, we assign a unique point in Γ, denoted by $\widetilde{\mathbf{p}}_1$ and $\widetilde{\mathbf{p}}_2$, respectively. In the numerical experiment section we will describe how $\widetilde{\mathbf{p}}_i$ $(i = 1, 2)$ can be obtained. Now, let $\widehat{\mathbf{m}}^{\mathbf{p}_i} := \widetilde{\mathbf{p}}_i - \mathbf{p}_i$. We set $\mathbf{m}^{\mathbf{p}_i} := \widehat{\mathbf{m}}^{\mathbf{p}_i}/|\widehat{\mathbf{m}}^{\mathbf{p}_i}|$ if $|\widehat{\mathbf{m}}^{\mathbf{p}_i}| \neq 0$ and $\mathbf{m}^{\mathbf{p}_i} = \mathbf{n}_e$, otherwise. Given $\mathbf{x} \in e$, $\mathscr{C}(\mathbf{x})$ is determined as a convex combination of those paths originated from the vertices of e. More precisely, for $\theta \in [0, 1]$, we write $\mathbf{x} = \mathbf{p}_1(1-\theta) + \theta\mathbf{p}_2$ and define $\widehat{\mathbf{m}} := \mathbf{m}^{\mathbf{p}_1}(1-\theta) + \theta\mathbf{m}^{\mathbf{p}_2}$. Then, we write $\mathbf{m} := \widehat{\mathbf{m}}/|\widehat{\mathbf{m}}|$ if $|\widehat{\mathbf{m}}| \neq 0$ and $\mathbf{m} := \mathbf{n}_e$, otherwise. Thus, we set $\widetilde{\mathbf{x}}$ as the closest intersection between the boundary Γ and the ray starting at $\mathbf{x}$ whose unit tangent vector is $\mathbf{m}$. In other words, the transferring path connecting a point $\mathbf{x} \in \Gamma_h$ to a point $\widetilde{\mathbf{x}} \in \Gamma$, is given by

$$\mathscr{C}(\mathbf{x}) := \{\mathbf{x} + \eta\mathbf{m}(\mathbf{x}) :\ 0 \leq \eta \leq \ell(\mathbf{x}) := |\widetilde{\mathbf{x}} - \mathbf{x}|\}\,.$$

In addition, concerning our approximate solution outside D_h, we consider, for each boundary edge e with vertices $\mathbf{p}_1$ and $\mathbf{p}_2$, the cones

$$\begin{aligned} \mathrm{C}_{\mathbf{p}_1}^e &:= \left\{\mathbf{p}_1 + \varepsilon_1(\widetilde{\mathbf{p}}_1 - \mathbf{p}_1) + \varepsilon_2(\mathbf{p}_2 - \mathbf{p}_1) :\ \varepsilon_1, \varepsilon_2 \in \mathbb{R}^+\right\}, \\ \mathrm{C}_{\mathbf{p}_2}^e &:= \left\{\mathbf{p}_2 + \varepsilon_1(\widetilde{\mathbf{p}}_2 - \mathbf{p}_2) + \varepsilon_2(\mathbf{p}_1 - \mathbf{p}_2) :\ \varepsilon_1, \varepsilon_2 \in \mathbb{R}^+\right\}, \end{aligned}$$

and define, for $e \in \mathcal{E}_h^\partial$,

$$\widetilde{T}_{ext}^e := \{\mathscr{C}(\mathbf{x}) : \ \mathbf{x} \in e\} \cap \mathrm{C}_{\mathbf{p}_1}^e \cap \mathrm{C}_{\mathbf{p}_2}^e \cap \mathrm{D}_h^c.$$

Also, it will be convenient to write Γ_e to denote the intersection between Γ and the closure of the region $\widetilde{T}_{ext}^e$.

Finally, given $e \in \mathcal{E}_h^\partial$, the exterior region $\widetilde{T}_{ext}^e$ is said to be an *admissible set* if for every $\mathbf{x} \in e$, the intersection of the ray $\{\mathbf{x} + \varepsilon(\widetilde{\mathbf{x}} - \mathbf{x}) : \ \varepsilon \in \mathbb{R}^+\}$ with Γ is a single point (see left panel of Figure 1). According to the above and for the sake for simplicity, from now on we assume that $\widetilde{T}_{ext}^e$ is an *admissible set*, and denote by $\widetilde{\mathcal{T}}_h$ the partition of D_h^c into those sets. Therefore, for instance, cases like the one on the right of Figure 1 are not considered.

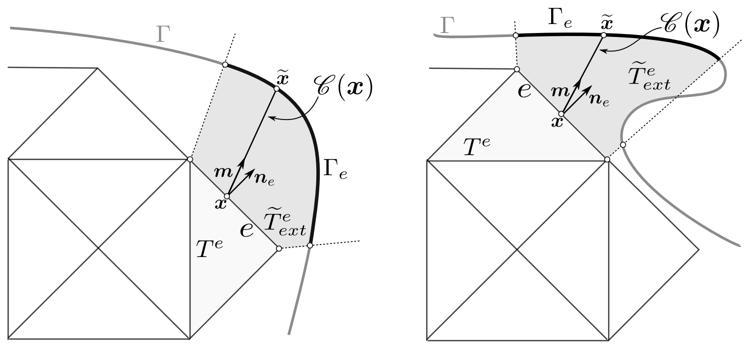

Figure 1: Examples of sets $\widetilde{T}_{ext}^e$. The *admissible case* is the one on the left.

3.3. Statement of the Galerkin scheme

In this section we specify the Galerkin approximation of (3.7). It requires first some definitions. Given an integer $l \geq 0$ and a subset $\mathcal{O}$ of $\mathbb{R}^2$, we let $\mathrm{P}_l(\mathcal{O})$ (resp. $\widetilde{\mathrm{P}}_l(\mathcal{O})$) be the space of polynomials of degree at most l defined on $\mathcal{O}$ (resp. of degree equal to l) and according to the terminology described in Section 1, we set $\mathbf{P}_l(\mathcal{O}) := [\mathrm{P}_l(\mathcal{O})]^2$ and $\mathbb{P}_l(\mathcal{O}) := [\mathrm{P}_l(\mathcal{O})]^{2\times 2}$. Then, for each integer $k \geq 0$ and for each $T \in \mathcal{T}_h$, we define the local Raviart–Thomas space of order k (see, e.g. [10, 29]) as:

$$\mathbf{RT}_k(T) := \mathbf{P}_k(T) \oplus \widetilde{\mathrm{P}}_k(T)\mathbf{x},$$

where $\mathbf{x} := (x_1, x_2)^{\mathbf{t}}$ is a generic vector of $\mathbb{R}^2$. In agreement with the previous notation, the space of matrix-valued functions whose rows belong to $\mathbf{RT}_k(T)$ will be denoted by $\mathbb{RT}_k(T)$. Also, we let

$$\mathbb{H}_h(\mathrm{D}_h) := \{\boldsymbol{\tau} \in \mathbb{H}(\mathbf{div}\,; \mathrm{D}_h) : \ \boldsymbol{\tau}|_T \in \mathbb{RT}_k(T) \quad \forall\, T \in \mathcal{T}_h\},$$

and

$$\mathbf{Q}_h(\mathrm{D}_h) := \left\{\mathbf{v} \in \mathbf{L}^2(\mathrm{D}_h) : \ \mathbf{v}|_T \in \mathbf{P}_k(T) \quad \forall\, T \in \mathcal{T}_h\right\}.$$

Notice that $\mathbb{H}(\mathrm{D}_h) = \mathbb{H}_{0,h}(\mathrm{D}_h) \oplus \mathbb{R}\mathbb{I}$, where $\mathbb{H}_{0,h}(\mathrm{D}_h) := \mathbb{H}_h(\mathrm{D}_h) \cap \mathbb{H}_0(\mathbf{div}; \Omega)$. In this way, we propose to approximate the solution of (3.7) by $(\boldsymbol{\sigma}_{0,h}, \mathbf{u}_h) \in \mathbb{H}_{0,h}(\mathrm{D}_h) \times \mathbf{Q}_h(\mathrm{D}_h)$, satisfying

$$\begin{aligned} (a_h + d_h)\,(\boldsymbol{\sigma}_{0,h}, \boldsymbol{\tau}_h) + b_h(\boldsymbol{\tau}_h, \mathbf{u}_h) &= G_h(\boldsymbol{\tau}_h) \quad \forall\, \boldsymbol{\tau}_h \in \mathbb{H}_{0,h}(\mathrm{D}_h), \\ b_h(\boldsymbol{\sigma}_{0,h}, \mathbf{v}_h) &= F_h(\mathbf{v}_h) \quad \forall\, \mathbf{v}_h \in \mathbf{Q}_h(\mathrm{D}_h), \end{aligned} \tag{3.9}$$

where a_h, b_h and F_h are given by (3.5),

$$G_h(\boldsymbol{\tau}_h) := \sum_{e \in \mathcal{E}_h^\partial} \int_e \overline{\mathbf{g}} \cdot (\boldsymbol{\tau}_h \mathbf{n}_e)\, d\mathcal{S}_{\mathbf{x}}, \tag{3.10}$$

and

$$d_h(\boldsymbol{\xi}_h,\boldsymbol{\tau}_h) := \frac{1}{2\mu}\sum_{e\in\mathcal{E}_h^\partial}\int_e\left(\int_0^{\ell(\mathbf{x})}\mathbf{E}_h\left(\boldsymbol{\xi}_h^{\mathrm{d}}\right)(\mathbf{x}+\eta\mathbf{m})\,\mathbf{m}\,d\eta\right)\cdot(\boldsymbol{\tau}_h\mathbf{n}_e)\,d\mathcal{S}_{\mathbf{x}}, \tag{3.11}$$

where we recall that $\overline{\mathbf{g}}(\mathbf{x}) := \mathbf{g}(\widetilde{\mathbf{x}}(\mathbf{x}))$. Above, $\mathbf{E}_h$ is the extrapolation operator given by

$$\mathbf{E}_h : \mathbb{P}_n(\mathcal{T}_h) \ni \boldsymbol{\tau}_h \longmapsto \mathbf{E}_h(\boldsymbol{\tau}_h)(\mathbf{y}) := \begin{cases} \boldsymbol{\tau}_h(\mathbf{y}) & \forall\,\mathbf{y}\in T, \quad \forall\, T\in\mathcal{T}_h, \\ \boldsymbol{\tau}_h|_{T^e}(\mathbf{y}) & \forall\,\mathbf{y}\in\widetilde{T}^e_{ext}, \quad \forall\, e\in\mathcal{E}_h^\partial, \end{cases} \tag{3.12}$$

where for any integer $n \geq 0$, $\mathbb{P}_n(\mathcal{T}_h) := \prod_{T\in\mathcal{T}_h}\mathbb{P}_n(T)$. We observe that $\mathbf{E}_h(\boldsymbol{\sigma}^{\mathrm{d}}_{0,h})$ is well-defined since $\boldsymbol{\sigma}_{0,h}|_T \in \mathbb{RT}_k(T) \subseteq \mathbb{P}_{k+1}(T)$ for all $T\in\mathcal{T}_h$. We also observe that above we are implicitly using the following approximation of $\widetilde{\mathbf{g}}$ (cf. (3.8)):

$$\widetilde{\mathbf{g}}_h(\mathbf{x}) := \overline{\mathbf{g}}(\mathbf{x}) - \frac{1}{2\mu}\int_0^{\ell(\mathbf{x})}\mathbf{E}_h\big(\boldsymbol{\sigma}^{\mathrm{d}}_{0,h}\big)(\mathbf{x}+\eta\mathbf{m})\,\mathbf{m}\,d\eta, \tag{3.13}$$

for any edge $e\in\mathcal{E}_h^\partial$ and for each $\mathbf{x}\in e$. Note that if $\Omega = \mathrm{D}_h$ is a polygonal domain, then $\widetilde{\mathbf{g}}_h = \mathbf{g}$ and $d_h \equiv 0$. Hence, (3.9) would be reduced to the standard approach to approximate the saddle-point problem (2.5).

We end this section by recalling the approximation properties of the corresponding discrete spaces. To that end, we first introduce the $\mathbf{L}^2(\mathrm{D}_h)$-orthogonal projector onto $\mathbf{Q}_h(\mathrm{D}_h)$, $\boldsymbol{\mathcal{P}}_h^k : \mathbf{L}^2(\mathrm{D}_h) \to \mathbf{Q}_h(\mathrm{D}_h)$, which for each $\mathbf{v}\in\mathbf{H}^l(\mathrm{D}_h)$, with $0\leq l\leq k+1$, satisfies the approximation property

$$\|\mathbf{v} - \boldsymbol{\mathcal{P}}_h^k(\mathbf{v})\|_{0,T} \lesssim h_T^l|\mathbf{v}|_{l,T} \quad \forall\, T\in\mathcal{T}_h. \tag{3.14}$$

In turn, we recall the classical Raviart–Thomas interpolation operator $\boldsymbol{\Pi}_h^k : \mathbb{H}^1(\mathrm{D}_h) \to \mathbb{H}_h(\mathrm{D}_h)$, which, given $\boldsymbol{\tau}\in\mathbb{H}^1(\mathrm{D}_h)$, is characterized by the identities

$$\begin{aligned} \int_T \boldsymbol{\Pi}_h^k(\boldsymbol{\tau}) : \boldsymbol{\xi}_h &= \int_T \boldsymbol{\tau} : \boldsymbol{\xi}_h && \forall\,\boldsymbol{\xi}_h\in\mathbb{P}_{k-1}(T),\ \forall\, T\in\mathcal{T}_h, \quad \text{when } k\geq 1, \\ \int_e \left(\boldsymbol{\Pi}_h^k(\boldsymbol{\tau})\mathbf{n}_e\right)\cdot\boldsymbol{\psi}_h &= \int_e (\boldsymbol{\tau}\mathbf{n}_e)\cdot\boldsymbol{\psi}_h && \forall\,\boldsymbol{\psi}_h\in\mathbf{P}_k(e),\ \forall\, e\in\mathcal{E}_h, \quad \text{when } k\geq 0, \end{aligned}$$

whence it is easy to show that $\mathbf{div}\,(\boldsymbol{\Pi}_h^k(\boldsymbol{\tau})) = \boldsymbol{\mathcal{P}}_h^k(\mathbf{div}\,\boldsymbol{\tau})$ for all $\boldsymbol{\tau}\in\mathbb{H}^1(\mathrm{D}_h)$. In addition, the local approximation properties of $\boldsymbol{\Pi}_h^k$ (see, e.g. [10, 41]) satisfy

- For each $\boldsymbol{\tau}\in\mathbb{H}^l(\mathrm{D}_h)$, with $1\leq l\leq k+1$, there holds

$$\|\boldsymbol{\tau} - \boldsymbol{\Pi}_h^k(\boldsymbol{\tau})\|_{0,T} \lesssim h_T^l|\boldsymbol{\tau}|_{l,T} \quad \forall\, T\in\mathcal{T}_h. \tag{3.15}$$

- For each $\boldsymbol{\tau}\in\mathbb{H}^1(\mathrm{D}_h)$ such that $\mathbf{div}\,\boldsymbol{\tau}\in\mathbf{H}^l(\mathrm{D}_h)$, with $0\leq l\leq k+1$,

$$\left\|\mathbf{div}\,(\boldsymbol{\tau} - \boldsymbol{\Pi}_h^k(\boldsymbol{\tau}))\right\|_{0,T} \lesssim h_T^l|\mathbf{div}\,\boldsymbol{\tau}|_{l,T} \quad \forall\, T\in\mathcal{T}_h. \tag{3.16}$$

- For each $\boldsymbol{\tau}\in\mathbb{H}^1(\mathrm{D}_h)$, there holds

$$\|(\boldsymbol{\tau} - \boldsymbol{\Pi}_h^k(\boldsymbol{\tau}))\mathbf{n}_e\|_{0,e} \lesssim h_e^{1/2}\|\boldsymbol{\tau}\|_{1,T^e} \quad \forall\, e\in\mathcal{E}_h. \tag{3.17}$$

Moreover, the interpolation operator $\boldsymbol{\Pi}_h^k$ can be defined as a bounded linear operator from the larger space $\mathbb{H}^s(\mathrm{D}_h)\cap\mathbb{H}(\mathbf{div},\mathrm{D}_h)$ into $\mathbb{H}_h(\mathrm{D}_h)$ for all $s\in(0,1]$ (see, e.g. [37, Theorem 3.1]) and in that case, the approximation property reduces to

$$\|\boldsymbol{\tau} - \boldsymbol{\Pi}_h^k(\boldsymbol{\tau})\|_{\mathbf{div},T} \lesssim h_T^s\left(\|\boldsymbol{\tau}\|_{s,T} + \|\mathbf{div}\,\boldsymbol{\tau}\|_{s,T}\right) \quad \forall\, T\in\mathcal{T}_h. \tag{3.18}$$

3.4. *Well-posedness*

We first introduce some hypotheses regarding the *closeness* between Γ and Γ_h. We remark that most of the notations and ideas here are closely connected to the ones of [19] and [39].

Let $e \in \mathcal{E}_h^{\partial}$. We define $\widetilde{r}_e := \widetilde{H}_e/h_e^{\perp}$, where $\widetilde{H}_e := \max_{\mathbf{x}\in e} \ell(\mathbf{x})$ and $h_e^{\perp}$ is the distance between the vertex, opposite to e, and the plane determined by e. In turn, for each $T \in \mathcal{T}_h$, we introduce $\mathbf{S}_k(\partial T) := \prod_{e\in\mathcal{E}(T)} \mathbf{P}_k(e)$, and for each edge $e \in \mathcal{E}_h^{\partial}$, we set

$$C_{eq}^e := h_{T^e}^{1/2} \sup_{\substack{\mathbf{v}_h\in\mathbf{S}_k(\partial T^e)\\ \mathbf{v}_h\neq\mathbf{0}}} \frac{\|\mathbf{v}_h\|_{0,\partial T^e}}{\|\mathbf{v}_h\|_{-1/2,\partial T^e}}, \tag{3.19}$$

$$\widetilde{C}_{ext}^e := (\widetilde{r}_e)^{-1/2} \sup_{\substack{\boldsymbol{\tau}_h\in\mathbb{P}_n(T^e)\\ \boldsymbol{\tau}_h\neq\mathbf{0}}} \frac{|\!|\!|\mathbf{E}_h(\boldsymbol{\tau}_h)|\!|\!|_e}{\|\boldsymbol{\tau}_h\|_{0,T^e}}, \tag{3.20}$$

where the mapping

$$\boldsymbol{\xi} \longmapsto |\!|\!|\boldsymbol{\xi}|\!|\!|_e := \left(\int_e \int_0^{\ell(\mathbf{x})} |\boldsymbol{\xi}(\mathbf{x}+\eta\mathbf{m}(\mathbf{x}))|^2 \, d\eta \, \mathcal{S}_{\mathbf{x}}\right)^{1/2} \tag{3.21}$$

defines a norm over the space $\mathbb{L}^2(\widetilde{T}_{ext}^e)$, which is equivalent to the standard $\mathbb{L}^2(\widetilde{T}_{ext}^e)$-norm (see [39, Lemma 3.4]) if we assume that

- **(i)** $\mathbf{m}^{\mathbf{p}_1} \cdot \mathbf{m}^{\mathbf{p}_2} \geq 0$,
- **(ii)** there exists a constant δ_e, independent of h, such that $\mathbf{m}(\theta) \cdot \mathbf{n}_e \geq \delta_e > 0$ for all $\theta \in [0,1]$; and
- **(iii)** $\mathbf{m}^{\mathbf{p}_1} \cdot (\mathbf{m}^{\mathbf{p}_2})^{\perp} \geq 0$, with $(\mathbf{m}^{\mathbf{p}_2})^{\perp}$ being the vector obtained from $\mathbf{m}^{\mathbf{p}_2}$ through a counterclockwise rotation by $\pi/2$ about the origin.

We notice that both norms coincide when $\mathbf{m}^{\mathbf{p}_1}$ is parallel to $\mathbf{m}^{\mathbf{p}_2}$, and in such a case, conditions **(i)**-**(iii)** are no longer required. On the other hand, (3.19) is inspired by the equivalence between the norms $\|\cdot\|_{-1/2,\partial T^e}$ and $\|\cdot\|_{0,\partial T^e}$ (see, e.g. [23, Lemma 3.2]), whereas (3.20) was originally introduced by [19] with the $\mathbb{L}^2(\widetilde{T}_{ext}^e)$-norm, and later generalized to the norm $|\!|\!|\cdot|\!|\!|_e$ by [39]. We also recall that both C_{eq}^e and $\widetilde{C}_{ext}^e$ are independent of the meshsize h, but depend on the shape-regularity constant and the polynomial degree. In turn, we denote $R := \max_{e\in\mathcal{E}_h^{\partial}} \widetilde{r}_e$ and assume

(A1) $R \leq C$, where $C > 0$ is independent of h; and

(A2) $\max_{e\in\mathcal{E}_h^{\partial}} \left\{\widetilde{r}_e \widetilde{C}_{ext}^e C_{eq}^e\right\} \leq C_1/4C_2$.

Above, C_1 and C_2 are positive constants, depending only on D_h, such that

$$C_1\|\boldsymbol{\tau}\|_{0,\mathrm{D}_h}^2 \leq \|\boldsymbol{\tau}^{\mathrm{d}}\|_{0,\mathrm{D}_h}^2 + \|\mathbf{div}\,\boldsymbol{\tau}\|_{0,\mathrm{D}_h}^2 \quad \forall\, \boldsymbol{\tau} \in \mathbb{H}_0(\mathbf{div};\mathrm{D}_h) \tag{3.22}$$

and

$$\|\boldsymbol{\tau}^{\mathrm{d}}\|_{0,\mathrm{D}_h} \leq C_2\|\boldsymbol{\tau}\|_{\mathbf{div},\mathrm{D}_h} \quad \forall\, \boldsymbol{\tau} \in \mathbb{H}(\mathbf{div},\mathrm{D}_h). \tag{3.23}$$

In particular, the proof of (3.22) can be found in [4, Lemma 3.1] (see also [10, Proposition 3.1]).

Let us briefly discuss the implications of these constraints. Assumption **(A1)** indicates that $d(\Gamma,\Gamma_h) \lesssim h$. In addition, Assumption **(A2)** holds true when, for instance, Γ_h is constructed by interpolating Γ by a picewise linear function because r_e for h is small enough.

We have then the following result.

Lemma 3.1. *Suppose that* **(A1)** *and* **(A2)** *hold. There exist positive constants* $\widetilde{C}_d$ *and* $\widetilde{\alpha}$*, independent of the meshsize* h*, such that*

$$|d_h(\boldsymbol{\xi}_h, \boldsymbol{\tau}_h)| \leq \widetilde{C}_d \|\boldsymbol{\xi}_h\|_{\mathbf{div},\mathrm{D}_h} \|\boldsymbol{\tau}_h\|_{\mathbf{div},\mathrm{D}_h} \quad \forall\, \boldsymbol{\xi}_h, \boldsymbol{\tau}_h \in \mathbb{H}_{0,h}(\mathrm{D}_h), \tag{3.24}$$

$$(a_h + d_h)(\boldsymbol{\tau}_h, \boldsymbol{\tau}_h) \geq \widetilde{\alpha} \|\boldsymbol{\tau}_h\|^2_{\mathbf{div},\mathrm{D}_h} \quad \forall \boldsymbol{\tau}_h \in \mathbb{V}_h(\mathrm{D}_h), \tag{3.25}$$

where $\mathbb{V}_h(\mathrm{D}_h) := \{\boldsymbol{\tau}_h \in \mathbb{H}_{0,h}(\mathrm{D}_h) : \; b_h(\boldsymbol{\tau}_h, \mathbf{v}_h) = 0 \quad \forall\, \mathbf{v}_h \in \mathbf{Q}_h(\mathrm{D}_h)\}$.

Proof. We proceed analogously to [39, Section 2.4]. In fact, having in mind the estimation of d_h, let us first define for any $\boldsymbol{\xi}_h \in \mathbb{H}_{0,h}(\mathrm{D}_h)$ and any edge $e \in \mathcal{E}_h^{\partial}$,

$$\mathbf{w}_h(\mathbf{x}) := \int_0^{\ell(\mathbf{x})} \mathbf{E}_h(\boldsymbol{\xi}_h^{\mathtt{d}})(\mathbf{x} + \eta \mathbf{m})\, \mathbf{m}\, d\eta \quad \forall\, \mathbf{x} \in e.$$

Integrating this vector-valued function over the edge e, applying the Cauchy–Schwarz inequality, using the constants $\widetilde{C}^e_{ext}$ of (3.20) to bound the term in the norm $|\!|\!|\cdot|\!|\!|_e$, employing the estimate in (3.23) and the fact that $h_e^{\perp} \leq h_{T^e}$, yield

$$\begin{aligned} \|\mathbf{w}_h\|^2_{0,e} &\leq \int_e \ell(\mathbf{x}) \int_0^{\ell(\mathbf{x})} |\mathbf{E}_h(\boldsymbol{\xi}_h^{\mathtt{d}})(\mathbf{x} + \eta \mathbf{m})|^2\, d\eta\, d\mathcal{S}_{\mathbf{x}} \leq \widetilde{r}_e \widetilde{H}_e \left(\widetilde{C}^e_{ext}\right)^2 \|\boldsymbol{\xi}_h^{\mathtt{d}}\|^2_{0,T^e} \\ &\leq h_{T^e} \left(\widetilde{r}_e \widetilde{C}^e_{ext}\right)^2 \|\boldsymbol{\xi}_h^{\mathtt{d}}\|^2_{0,T^e} \leq h_{T^e} \left(\widetilde{r}_e \widetilde{C}^e_{ext} C_2\right)^2 \|\boldsymbol{\xi}_h\|^2_{\mathbf{div},T^e}. \end{aligned} \tag{3.26}$$

Then, applying the Cauchy–Schwarz inequality together with (3.26), we have

$$|d_h(\boldsymbol{\xi}_h, \boldsymbol{\tau}_h)| \leq \frac{1}{2\mu} \sum_{e \in \mathcal{E}_h^{\partial}} \|\mathbf{w}_h\|_{0,e} \|\boldsymbol{\tau}_h \mathbf{n}\|_{0,\partial T^e} \leq \frac{C_2}{2\mu} \|\boldsymbol{\xi}_h\|_{\mathbf{div},\mathrm{D}_h} \sum_{e \in \mathcal{E}_h^{\partial}} \widetilde{r}_e \widetilde{C}^e_{ext} h_{T^e}^{1/2} \|\boldsymbol{\tau}_h \mathbf{n}\|_{0,\partial T^e}$$

for all $\boldsymbol{\xi}_h, \boldsymbol{\tau}_h \in \mathbb{H}_{0,h}(\mathrm{D}_h)$. In view of this, by the definition of C^e_{eq} (cf. (3.19)) together with the estimate (1.1), and after some algebraic manipulations, we have from Assumption **(A1)** that (3.24) holds. On the other hand, to obtain the coercivity of $(a_h + d_h)$ on $\mathbb{V}_h(\mathrm{D}_h)$, we note that $\boldsymbol{\tau}_h \in \mathbb{V}_h(\mathrm{D}_h)$ implies $\mathbf{div}\, \boldsymbol{\tau}_h \equiv \mathbf{0}$ in D_h, since $\mathbf{div}\, \mathbb{H}_{0,h}(\mathrm{D}_h) \subseteq \mathbf{Q}_h(\mathrm{D}_h)$. Consequently, from the inequality (3.22), the boundedness of d_h and Assumption **(A2)**, it follows that

$$(a_h + d_h)(\boldsymbol{\tau}_h, \boldsymbol{\tau}_h) \geq \frac{1}{2\mu} \|\boldsymbol{\tau}_h^{\mathtt{d}}\|^2_{0,\Omega} - \frac{C_1}{8\mu} \|\boldsymbol{\tau}_h\|^2_{\mathbf{div};\mathrm{D}_h} \geq \frac{3C_1}{8\mu} \|\boldsymbol{\tau}_h\|^2_{\mathbf{div},\mathrm{D}_h}$$

for all $\boldsymbol{\tau}_h \in \mathbb{V}_h(\mathrm{D}_h)$, showing that (3.25) is satisfied with $\widetilde{\alpha} = 3C_1/8\mu$ and concluding the proof. $\square$

Remark 3.1. *The boundedness of the functional* G_h *in* (3.10) *can be deduced from the continuity of the mapping* $\widetilde{\mathbf{x}} : \Gamma_h \to \Gamma$ *(cf. Section 3.2). In fact, since* $\overline{\mathbf{g}}(\cdot) = \mathbf{g}(\widetilde{\mathbf{x}}(\cdot))$ *belongs to* $\mathbf{H}^{1/2}(\Gamma_h)$*, we apply the continuity of the normal trace operator and the estimate* (1.1) *to obtain* $|G_h(\boldsymbol{\tau}_h)| \leq \|\overline{\mathbf{g}}\|_{1/2,\Gamma_h} \|\boldsymbol{\tau}_h\|_{\mathbf{div},\mathrm{D}_h}$ *for all* $\boldsymbol{\tau}_h \in \mathbb{H}_{0,h}(\mathrm{D}_h)$*, as required.*

Let us now recall that the pair $(\mathbb{H}_{h,0}(\mathrm{D}_h), \mathbf{Q}_h(\mathrm{D}_h))$ satisfies the following discrete inf-sup condition (see, for instance [30, Lemma 3.2]):

$$\inf_{\substack{\boldsymbol{\tau}_h \in \mathbb{H}_{0,h}(\mathrm{D}_h) \\ \boldsymbol{\tau}_h \neq \mathbf{0}}} \frac{b_h(\boldsymbol{\tau}_h, \mathbf{v}_h)}{\|\boldsymbol{\tau}_h\|_{\mathbf{div},\Omega}} \geq \hat{\beta} \|\mathbf{v}_h\|_{0,\Omega} \quad \forall\, \mathbf{v}_h \in \mathrm{Q}_h(\mathrm{D}_h), \tag{3.27}$$

with $\hat{\beta} > 0$, independent of h.

We are now ready to state the main result concerning the well-posedness of (3.9).

Theorem 3.2. *Suppose that* **(A1)** *and* **(A2)** *hold. Given* $\mathbf{f} \in \mathbf{L}^2(\Omega)$ *and* $\mathbf{g} \in \mathbf{H}^{1/2}(\Gamma)$*, there exists a unique* $(\boldsymbol{\sigma}_{0,h}, \mathbf{u}) \in \mathbb{H}_{h,0}(\mathrm{D}_h) \times \mathbf{Q}_h(\mathrm{D}_h)$ *solution to the problem* (3.9)*, which satisfies*

$$\|(\boldsymbol{\sigma}_{0,h}, \mathbf{u}_h)\|_{\mathbb{H}(\mathbf{div}\,;\mathrm{D}_h)\times \mathbf{L}^2(\mathrm{D}_h)} \lesssim \|F_h\|_{[\mathbb{H}_{0,h}(\mathrm{D}_h)]'} + \|G_h\|_{[\mathbf{Q}_h(\mathrm{D}_h)]'}.$$

Proof. The proof is a straightforward application of the discrete version of the Babuška–Brezzi theorem (see, e.g. [29, Section 2.5]). □

We end this section by providing a postprocessing technique for approximating the pseudostress $\boldsymbol{\sigma}$ and the pressure p in the computational domain D_h. To that end, we let $(\boldsymbol{\sigma}_{0,h}, \mathbf{u}_h) \in \mathbb{H}_{h,0}(\mathrm{D}_h) \times \mathbf{Q}_h(\mathrm{D}_h)$ be the unique solution of (3.9) and based on the definition (3.6), we propose the following approximations of $\boldsymbol{\sigma}$ and p:

$$\boldsymbol{\sigma}_h := \boldsymbol{\sigma}_{0,h} + \left(\frac{\gamma_h}{2|\mathrm{D}_h|}\right)\mathbb{I}, \tag{3.28}$$

and

$$p_h := -\frac{1}{2}\mathrm{tr}\,(\boldsymbol{\sigma}_h), \tag{3.29}$$

where

$$\gamma_h := -\int_{\mathrm{D}_h^c} \mathrm{tr}\,\left(\mathbf{E}_h(\boldsymbol{\sigma}_{0,h}) - \left(\frac{1}{2|\Omega|}\int_{\mathrm{D}_h^c} \mathrm{tr}\,\left(\mathbf{E}_h(\boldsymbol{\sigma}_{0,h})\right)\right)\mathbb{I}\right), \tag{3.30}$$

and $\mathbf{E}_h(\boldsymbol{\sigma}_{0,h})$ denotes the extrapolation of $\boldsymbol{\sigma}_{0,h}$ (cf. (3.12)). Notice that the following identity holds:

$$\int_{\mathrm{D}_h} \mathrm{tr}\,(\boldsymbol{\sigma}_h) = \gamma_h. \tag{3.31}$$

4. A priori error bounds

Given $(\boldsymbol{\sigma}, \mathbf{u}) \in \mathbb{H}_0(\mathbf{div};\Omega) \times \mathbf{L}^2(\Omega)$ and $(\boldsymbol{\sigma}_{0,h}, \mathbf{u}_h) \in \mathbb{H}_{0,h}(\mathrm{D}_h) \times \mathbf{Q}_h(\mathrm{D}_h)$ solutions of (2.5) and (3.9), respectively, we are now interested in obtaining upper bounds for

$$\|\boldsymbol{\sigma} - \boldsymbol{\sigma}_h\|_{\mathbf{div},\mathrm{D}_h}, \quad \|\mathbf{u} - \mathbf{u}_h\|_{0,\mathrm{D}_h} \quad \text{and} \quad \|p - p_h\|_{0,\mathrm{D}_h},$$

where $\boldsymbol{\sigma}_h$ and p_h are given by (3.28) and (3.29), respectively. These errors, as we shall see below, depend on a Céa-type estimate for $\|\boldsymbol{\sigma}_0 - \boldsymbol{\sigma}_{0,h}\|_{\mathbf{div},\mathrm{D}_h}$, with $\boldsymbol{\sigma}_0$ defined as in (3.6). For this reason, we follow the strategy of [39]: we first derive the corresponding Céa estimate, then apply it to derive error bounds for the main variables, even on the complement D_h^c, and finally infer the theoretical rate of convergence result.

4.1. Estimates on D_h

We begin with a Céa-type estimate for our Galerkin scheme (3.9). For its proof we proceed similarly to the proof of [39, Theorem 3.3].

Theorem 4.1. *Let* $(\boldsymbol{\sigma}, \mathbf{u}) \in \mathbb{H}_0(\mathbf{div};\Omega) \times \mathbf{L}^2(\Omega)$ *and* $(\boldsymbol{\sigma}_{0,h}, \mathbf{u}_h)$ *be the unique solutions of* (2.5) *and* (3.9)*, respectively. Let* $\boldsymbol{\sigma}_0$ *be defined as in* (3.6) *and suppose that hypotheses of Theorem 3.2 are satisfied. Then, there holds*

$$\begin{aligned}&\|(\boldsymbol{\sigma}_0 - \boldsymbol{\sigma}_{0,h}, \mathbf{u} - \mathbf{u}_h)\|_{\mathbb{H}(\mathbf{div};\mathrm{D}_h)\times\mathbf{L}^2(\mathrm{D}_h)} \\ &\qquad \lesssim \inf_{\mathbf{v}_h\in\mathbf{Q}_h(\mathrm{D}_h)} \|\mathbf{u} - \mathbf{v}_h\|_{0,\mathrm{D}_h} + \inf_{\boldsymbol{\xi}_{0,h}\in\mathbb{H}_{0,h}(\mathrm{D}_h)} \left(\|\boldsymbol{\sigma}_0 - \boldsymbol{\xi}_{0,h}\|_{\mathbf{div},\mathrm{D}_h} + \sum_{e\in\mathcal{E}_h^\partial} |||\boldsymbol{\sigma}^{\mathrm{d}} - \mathbf{E}_h(\boldsymbol{\xi}_{0,h}^{\mathrm{d}})|||_e\right).\end{aligned}$$

Proof. Recalling that $(\boldsymbol{\sigma}_0, \mathbf{u})$ solves (3.7), and rearranging conveniently (3.9), it follows that

$$\begin{aligned} a_h(\boldsymbol{\sigma}_0,\boldsymbol{\tau}) + b_h(\boldsymbol{\tau},\mathbf{u}) &= \langle \boldsymbol{\tau}\mathbf{n}_{\Gamma_h}, \widetilde{\mathbf{g}}\rangle_{\Gamma_h} \quad && \forall\, \boldsymbol{\tau} \in \mathbb{H}_0(\mathbf{div}\,;\mathrm{D}_h),\\ b_h(\boldsymbol{\sigma}_0,\mathbf{v}) &= F_h(\mathbf{v}) && \forall\, \mathbf{v} \in \mathbf{L}^2(\mathrm{D}_h), \end{aligned}$$

and

$$\begin{aligned} a_h(\boldsymbol{\sigma}_{0,h},\boldsymbol{\tau}_h) + b_h(\boldsymbol{\tau}_h,\mathbf{u}_h) &= G_h(\boldsymbol{\tau}_h) - d_h(\boldsymbol{\sigma}_{0,h},\boldsymbol{\tau}_h) \quad && \forall\, \boldsymbol{\tau}_h \in \mathbb{H}_{0,h}(\mathrm{D}_h),\\ b_h(\boldsymbol{\sigma}_{0,h},\mathbf{v}_h) &= F_h(\mathbf{v}_h) && \forall\, \mathbf{v}_h \in \mathbf{Q}_h(\mathrm{D}_h). \end{aligned}$$

It should be noted that the structure of these problems differ only in the functionals concerning the Dirichlet boundary condition. This leads us to apply the well-known Strang-type estimate to obtain our preliminary error bounds as done in [39, Section 3.1] (see also [25, Lemma 5.2] or [33, Section 4.1]):

$$\begin{aligned} \|\boldsymbol{\sigma}_0 - \boldsymbol{\sigma}_{0,h}\|_{\mathbf{div},\mathrm{D}_h} \le \left(1 + \frac{\|a_h\|}{\hat\alpha}\right)\left(1 + \frac{\|b_h\|}{\hat\beta}\right) \inf_{\boldsymbol{\xi}_{0,h}\in\mathbb{H}_{0,h}(\mathrm{D}_h)} \|\boldsymbol{\sigma}_0 - \boldsymbol{\xi}_{0,h}\|_{\mathbf{div},\mathrm{D}_h}\\ + \frac{\|b_h\|}{\hat\alpha} \inf_{\mathbf{w}_h\in\mathbf{Q}_h(\mathrm{D}_h)} \|\mathbf{u}-\mathbf{w}_h\|_{0,\mathrm{D}_h} + \frac{1}{\hat\alpha}\mathbb{T}^{\boldsymbol{\sigma}}, \end{aligned} \tag{4.1}$$

and

$$\begin{aligned} \|\mathbf{u}-\mathbf{u}_h\|_{0,\mathrm{D}_h} \le \frac{\|a_h\|}{\hat\beta}\left(1 + \frac{\|a_h\|}{\hat\alpha}\right)\left(1 + \frac{\|b_h\|}{\hat\beta}\right) \inf_{\boldsymbol{\xi}_{0,h}\in\mathbb{H}_{0,h}(\mathrm{D}_h)} \|\boldsymbol{\sigma}_0 - \boldsymbol{\xi}_{0,h}\|_{\mathbf{div},\mathrm{D}_h}\\ + \left(1 + \frac{\|b_h\|}{\hat\beta} + \frac{\|b_h\|\,\|a_h\|}{\hat\beta\hat\alpha}\right) \inf_{\mathbf{w}_h\in\mathbf{Q}_h(\mathrm{D}_h)} \|\mathbf{u}-\mathbf{w}_h\|_{0,\mathrm{D}_h} + \frac{1}{\hat\beta}\left(1 + \frac{\|a_h\|}{\hat\alpha}\right)\mathbb{T}^{\boldsymbol{\sigma}}, \end{aligned} \tag{4.2}$$

where $\hat\alpha$ is the coercivity constant of the bilinear form a_h (actually, $\hat\alpha = C_1/2\mu$), $\hat\beta$ is the positive constant satisfying (3.27), $\|\cdot\|$ denotes the norm of the corresponding bilinear forms, and $\mathbb{T}^{\boldsymbol{\sigma}}$ is the error of the boundary condition on Γ_h given by

$$\mathbb{T}^{\boldsymbol{\sigma}} := \sup_{\substack{\boldsymbol{\tau}_h\in\mathbb{H}_{0,h}(\mathrm{D}_h)\\ \boldsymbol{\tau}_h\neq\mathbf{0}}} \frac{|\langle \boldsymbol{\tau}_h\mathbf{n}_{\Gamma_h}, \widetilde{\mathbf{g}}\rangle_{\Gamma_h} - (G_h(\boldsymbol{\tau}_h) - d_h(\boldsymbol{\sigma}_{0,h},\boldsymbol{\tau}_h))|}{\|\boldsymbol{\tau}_h\|_{\mathbf{div},\mathrm{D}_h}} = \sup_{\substack{\boldsymbol{\tau}_h\in\mathbb{H}_{0,h}(\mathrm{D}_h)\\ \boldsymbol{\tau}_h\neq\mathbf{0}}} \frac{|\langle \boldsymbol{\tau}_h\mathbf{n}_{\Gamma_h}, \widetilde{\mathbf{g}} - \widetilde{\mathbf{g}}_h\rangle_{\Gamma_h}|}{\|\boldsymbol{\tau}_h\|_{\mathbf{div},\mathrm{D}_h}}.$$

It remains therefore to upper bound $\mathbb{T}^{\boldsymbol{\sigma}}$. To this end, using the Cauchy–Schwarz inequality, the constant C^e_{eq} of (3.19), the definition of $\widetilde{r}_e$, and the norm given in (3.21), it follows that

$$\mathbb{T}^{\boldsymbol{\sigma}} \le \frac{1}{2\mu}\sum_{e\in\mathcal{E}_h^\partial} C^e_{eq} h_{T^e}^{-1/2} \|\widetilde{\mathbf{g}} - \widetilde{\mathbf{g}}_h\|_{0,e} \le \frac{1}{2\mu}\sum_{e\in\mathcal{E}_h^\partial} C^e_{eq} (\widetilde{r}_e)^{1/2} \left|\!\left|\!\left| \boldsymbol{\sigma}^{\mathtt{d}} - \mathbf{E}_h\left(\boldsymbol{\sigma}_h^{\mathtt{d}}\right)\right|\!\right|\!\right|_e, \tag{4.3}$$

where we recall that $\boldsymbol{\sigma}_h$ has been defined in (3.28) and $\boldsymbol{\sigma}_h^{\mathtt{d}} = \boldsymbol{\sigma}_{0,h}^{\mathtt{d}}$.

Now, we will establish an upper bound for $|\!|\!|\boldsymbol{\sigma}^{\mathtt{d}} - \mathbf{E}_h(\boldsymbol{\sigma}_h^{\mathtt{d}})|\!|\!|_e$. Inspired by (3.28), let $\boldsymbol{\xi}_{0,h} \in \mathbb{H}_{0,h}(\mathrm{D}_h)$ and

$$\boldsymbol{\xi}_h := \boldsymbol{\xi}_{0,h} + \left(\frac{c_h}{2|\mathrm{D}_h|}\right)\mathbb{I}, \tag{4.4}$$

with constant c_h being defined as γ_h in (3.30) by replacing $\boldsymbol{\sigma}_{0,h}$ by $\boldsymbol{\xi}_{0,h}$. Then, adding and subtracting $\mathbf{E}_h(\boldsymbol{\xi}_h^{\mathtt{d}})$ in (4.3), using the constants $\widetilde{C}^e_{ext}$ and C_2 (cf. (3.20) and (3.23), respectively), and also employing the Assumption **(A2)**, we have

$$\mathbb{T}^{\boldsymbol{\sigma}} \le \frac{1}{2\mu}\sum_{e\in\mathcal{E}_h^\partial} C^e_{eq}(\widetilde{r}_e)^{1/2} |\!|\!|\boldsymbol{\sigma}^{\mathtt{d}} - \mathbf{E}_h(\boldsymbol{\xi}_h^{\mathtt{d}})|\!|\!|_e + \frac{C_1}{8\mu}\|\boldsymbol{\sigma}_h - \boldsymbol{\xi}_h\|_{\mathbf{div},\mathrm{D}_h},$$

from which, adding and subtracting $\boldsymbol{\sigma}$ and considering the identity $\boldsymbol{\xi}_h^{\mathtt{d}} = \boldsymbol{\xi}_{0,h}^{\mathtt{d}}$, it holds

$$\mathbb{T}^{\boldsymbol{\sigma}} \leq \frac{1}{2\mu} \sum_{e \in \mathcal{E}_h^{\partial}} C_{eq}^{e} (\widetilde{r}_e)^{1/2} |||\boldsymbol{\sigma}^{\mathtt{d}} - \mathbf{E}_h(\boldsymbol{\xi}_{0,h}^{\mathtt{d}})|||_e + \frac{C_1}{8\mu} \left(\|\boldsymbol{\sigma} - \boldsymbol{\xi}_h\|_{\mathbf{div},\mathrm{D}_h} + \|\boldsymbol{\sigma} - \boldsymbol{\sigma}_h\|_{\mathbf{div},\mathrm{D}_h} \right). \tag{4.5}$$

Furthermore, according to definition (3.6), we know that $\boldsymbol{\sigma}|_{\mathrm{D}_h} = \boldsymbol{\sigma}_0 + \left(\frac{\gamma}{2|\mathrm{D}_h|}\right) \mathbb{I}$ and $\int_{\mathrm{D}_h} \operatorname{tr}(\boldsymbol{\sigma}) = \gamma$. Thus, concerning the last term in (4.5), we use (3.31) to infer

$$\begin{aligned}
\|\boldsymbol{\sigma} - \boldsymbol{\sigma}_h\|_{\mathbf{div},\mathrm{D}_h} &\leq \|\boldsymbol{\sigma}_0 - \boldsymbol{\sigma}_{0,h}\|_{\mathbf{div},\mathrm{D}_h} + \left\| \left(\frac{\gamma - \gamma_h}{2|\mathrm{D}_h|} \right) \mathbb{I} \right\|_{0,\mathrm{D}_h} \\
&= \|\boldsymbol{\sigma}_0 - \boldsymbol{\sigma}_{0,h}\|_{\mathbf{div},\mathrm{D}_h} + \left\| \frac{1}{2|\mathrm{D}_h|} \left(\int_{\mathrm{D}_h} \operatorname{tr}(\boldsymbol{\sigma} - \boldsymbol{\sigma}_h) \right) \mathbb{I} \right\|_{0,\mathrm{D}_h} \\
&\leq \|\boldsymbol{\sigma}_0 - \boldsymbol{\sigma}_{0,h}\|_{\mathbf{div},\mathrm{D}_h} + \frac{1}{\sqrt{2}} \|\boldsymbol{\sigma} - \boldsymbol{\sigma}_h\|_{\mathbf{div},\mathrm{D}_h},
\end{aligned}$$

and hence,

$$\|\boldsymbol{\sigma} - \boldsymbol{\sigma}_h\|_{\mathbf{div},\mathrm{D}_h} \leq \left(\frac{2}{2 - \sqrt{2}} \right) \|\boldsymbol{\sigma}_0 - \boldsymbol{\sigma}_{0,h}\|_{\mathbf{div},\mathrm{D}_h}. \tag{4.6}$$

Similarly, we have

$$\|\boldsymbol{\sigma} - \boldsymbol{\xi}_h\|_{\mathbf{div},\mathrm{D}_h} \leq \left(\frac{2}{2 - \sqrt{2}} \right) \|\boldsymbol{\sigma}_0 - \boldsymbol{\xi}_{0,h}\|_{\mathbf{div},\mathrm{D}_h}. \tag{4.7}$$

Therefore, from (4.1), (4.5), (4.6) and (4.7), we deduce, after simple algebraic manipulations and recalling that $\hat{\alpha} = C_1/2\mu$, that

$$\begin{aligned}
&\left(\frac{3 - 2\sqrt{2}}{4 - 2\sqrt{2}} \right) \|\boldsymbol{\sigma}_0 - \boldsymbol{\sigma}_{0,h}\|_{\mathbf{div},\mathrm{D}_h} \\
&\qquad \lesssim \inf_{\mathbf{w}_h \in \mathbf{Q}_h(\mathrm{D}_h)} \|\mathbf{u} - \mathbf{w}_h\|_{0,\mathrm{D}_h} + \|\boldsymbol{\sigma}_0 - \boldsymbol{\xi}_{0,h}\|_{\mathbf{div},\mathrm{D}_h} + \sum_{e \in \mathcal{E}_h^{\partial}} |||\boldsymbol{\sigma}^{\mathtt{d}} - \mathbf{E}_h\left(\boldsymbol{\xi}_{0,h}^{\mathtt{d}}\right)|||_e.
\end{aligned} \tag{4.8}$$

Finally, dividing (4.8) by $\left(\frac{3-2\sqrt{2}}{4-2\sqrt{2}}\right) > 0$, placing the resulting inequality together with (4.2), one easily arrives at the result claimed. □

Corollary 4.2. *Suppose that hypotheses of Theorem 4.1 hold. Then,*

$$\begin{aligned}
&\|p - p_h\|_{0,\mathrm{D}_h} + \|\boldsymbol{\sigma} - \boldsymbol{\sigma}_h\|_{\mathbf{div},\mathrm{D}_h} \\
&\qquad \lesssim \inf_{\mathbf{v}_h \in \mathbf{Q}_h(\mathrm{D}_h)} \|\mathbf{u} - \mathbf{v}_h\|_{0,\mathrm{D}_h} + \inf_{\boldsymbol{\xi}_{0,h} \in \mathbb{H}_{0,h}(\mathrm{D}_h)} \left(\|\boldsymbol{\sigma}_0 - \boldsymbol{\xi}_{0,h}\|_{\mathbf{div},\mathrm{D}_h} + \sum_{e \in \mathcal{E}_h^{\partial}} |||\boldsymbol{\sigma}^{\mathtt{d}} - \mathbf{E}_h\left(\boldsymbol{\xi}_{0,h}^{\mathtt{d}}\right)|||_e \right).
\end{aligned}$$

Proof. A direct application of definitions (2.3) and (3.29), and the estimate (4.6), imply

$$\|p - p_h\|_{0,\mathrm{D}_h} + \|\boldsymbol{\sigma} - \boldsymbol{\sigma}_h\|_{\mathbf{div},\mathrm{D}_h} \leq \left(\frac{3}{2 - \sqrt{2}} \right) \|\boldsymbol{\sigma}_0 - \boldsymbol{\sigma}_{0,h}\|_{\mathbf{div},\mathrm{D}_h}.$$

The rest of the proof follows from Theorem 4.1. □

4.2. Approximation in D_h^c and rate of convergence

We now turn to provide approximations of the pseudostress $\boldsymbol{\sigma}$, the velocity $\mathbf{u}$ and the pressure p outside D_h. To alleviate the notation, these approximations will be also denoted by $\boldsymbol{\sigma}_h$, $\mathbf{u}_h$ and p_h, respectively.

In order to approximate $\boldsymbol{\sigma}$ in D_h^c, we follow the idea in [19, Section 2.1.3]. To that end, given $(\boldsymbol{\sigma}_{0,h}, \mathbf{u}_h) \in \mathbb{H}_{0,h}(\mathrm{D}_h) \times \mathbf{Q}_h(\mathrm{D}_h)$ the unique solution of (3.9), let $\boldsymbol{\sigma}_h$ be the tensor defined in (3.28). Then, for each $e \in \mathcal{E}_h^\partial$ and any $\mathbf{y} \in \widetilde{T}_{ext}^e$, we set

$$\boldsymbol{\sigma}_h(\mathbf{y}) := \mathbf{E}_h(\boldsymbol{\sigma}_h)(\mathbf{y}). \tag{4.9}$$

Remark 4.1. *From (3.30), we have that $\int_{\mathrm{D}_h^c} \mathrm{tr}\,(\mathbf{E}_h(\boldsymbol{\sigma}_{0,h})) = -\frac{|\Omega|}{|\mathrm{D}_h|}\gamma_h$, thus*

$$\int_{\mathrm{D}_h^c} \mathrm{tr}\,(\boldsymbol{\sigma}_h) = \int_{\mathrm{D}_h^c} \mathrm{tr}\,(\mathbf{E}_h(\boldsymbol{\sigma}_{0,h})) + \left(\frac{\gamma_h}{|\mathrm{D}_h|}\right)|\mathrm{D}_h^c| = -\gamma_h,$$

and by (3.31) we conclude that $\int_\Omega \mathrm{tr}\,(\boldsymbol{\sigma}_h) = 0$. In addition, we can write

$$\boldsymbol{\sigma}_h = \mathbf{E}_h(\boldsymbol{\sigma}_{0,h}) - \left(\frac{1}{2|\Omega|}\int_{\mathrm{D}_h^c} \mathrm{tr}\,(\mathbf{E}_h(\boldsymbol{\sigma}_{0,h}))\right)\mathbb{I} \quad \textit{in} \quad \Omega. \tag{4.10}$$

When Assumption **(A1)** and definition (4.9) (or equivalently, (4.10)) are considered, it is important to point out that since, in D_h^c, the normal component of the extrapolated $\boldsymbol{\sigma}_h$ is, in general, discontinuous across the transferring paths $\{\mathscr{C}(\mathbf{x})\}_{\mathbf{x}\in\Gamma_h}$ (cf. Section 3.2), the method ensures that, at least, $\boldsymbol{\sigma}_h$ belongs to the broken Sobolev space (see, e.g. [28, Section 1.2.6])

$$\mathbb{H}(\mathbf{div}; \widetilde{\mathcal{T}}_h) := \left\{\boldsymbol{\tau} \in \mathbb{L}^2(\mathrm{D}_h^c) : \ \boldsymbol{\tau}|_{\widetilde{T}_{ext}^e} \in \mathbb{H}\big(\mathbf{div}; \widetilde{T}_{ext}^e\big) \quad \forall\, e \in \mathcal{E}_h^\partial\right\}$$

endowed with the broken norm $\|\cdot\|_{\mathbf{div},\widetilde{\mathcal{T}}_h} := \left(\sum_{e\in\mathcal{E}_h^\partial}\|\cdot\|^2_{\mathbf{div},\widetilde{T}_{ext}^e}\right)^{1/2}$, where $\widetilde{\mathcal{T}}_h$ is the mesh defined in Section 3.2.

On the other hand, by defining

$$p_h := -\frac{1}{2}\mathrm{tr}\,(\boldsymbol{\sigma}_h) \quad \text{in} \quad \mathrm{D}_h^c, \tag{4.11}$$

it is clear from Remark 4.1 that $\int_\Omega p_h = 0$. Moreover, from definitions (2.3) and (4.11), we have

$$\|p - p_h\|_{0,\mathrm{D}_h^c} \leq \frac{1}{2}\|\boldsymbol{\sigma} - \boldsymbol{\sigma}_h\|_{0,\mathrm{D}_h^c}. \tag{4.12}$$

The latter suggests to establish firstly the error estimate associated to the pseudostress.

Let us start by introducing the following intermediate result.

Lemma 4.3. *Let $(\boldsymbol{\sigma}, \mathbf{u}) \in \mathbb{H}_0(\mathbf{div}; \Omega) \times \mathbf{L}^2(\Omega)$ be the unique solution of (2.5) and assume that hypotheses of Theorem 4.1 hold. Suppose further that there exists an integer $l \geq 0$ such that $\boldsymbol{\sigma} \in \mathbb{H}^{l+1}(\Omega)$, with $\mathbf{div}\,\boldsymbol{\sigma} \in \mathbf{H}^{l+1}(\Omega)$. Then, for any $\boldsymbol{\xi}_h \in \mathbb{H}_h(\mathrm{D}_h)$, we have*

$$\sum_{e\in\mathcal{E}_h^\partial} \|\boldsymbol{\sigma} - \mathbf{E}_h(\boldsymbol{\xi}_h)\|_{0,\widetilde{T}_{ext}^e} \lesssim \|\boldsymbol{\sigma} - \boldsymbol{\xi}_h\|_{0,\mathrm{D}_h} + h^{l+1}\|\boldsymbol{\sigma}\|_{l+1,\Omega}, \tag{4.13}$$

and

$$\sum_{e\in\mathcal{E}_h^\partial} \|\boldsymbol{\sigma} - \mathbf{E}_h(\boldsymbol{\xi}_h)\|_{\mathbf{div},\widetilde{T}_{ext}^e} \lesssim \|\boldsymbol{\sigma} - \boldsymbol{\xi}_h\|_{\mathbf{div},\mathrm{D}_h} + h^{l+1}\left(\|\boldsymbol{\sigma}\|_{l+1,\Omega} + \|\mathbf{div}\,\boldsymbol{\sigma}\|_{l+1,\Omega}\right). \tag{4.14}$$

Proof. The proof makes use of the averaged Taylor polynomials (cf. [9, Chapter 4]) in the neighborhood of the curved boundary Γ, and their well-known approximation properties. For details of the proof we refer to [39, Lemma 3.5]. $\square$

The following lemma allows us to deduce upper bounds for $(\boldsymbol{\sigma} - \boldsymbol{\sigma}_h)$ in the $\mathbf{L}^2$-norm, as well as in the broken $\mathbb{H}(\mathbf{div})$-norm on D_h^c. The general idea of the proof is inspired by [39, Lemma 3.6].

Lemma 4.4. *Assume the same hypotheses of Theorem 4.1. Let $(\boldsymbol{\sigma}, \mathbf{u}) \in \mathbb{H}_0(\mathbf{div}; \Omega) \times \mathbf{L}^2(\Omega)$ and $(\boldsymbol{\sigma}_{0,h}, \mathbf{u}_h) \in \mathbb{H}_{0,h}(\mathrm{D}_h) \times \mathbf{Q}_h(\mathrm{D}_h)$ be the unique solutions of (2.5) and (3.9), respectively. Let $\boldsymbol{\sigma}_h$ be defined as in (4.9). Suppose further that there exists an integer $l \geq 0$ such that $\boldsymbol{\sigma} \in \mathbb{H}^{l+1}(\Omega)$, with $\mathbf{div}\,\boldsymbol{\sigma} \in \mathbf{H}^{l+1}(\Omega)$. Then, we have*

$$\|\boldsymbol{\sigma} - \boldsymbol{\sigma}_h\|_{0,\mathrm{D}_h^c} \lesssim \inf_{\mathbf{w}_h \in \mathbf{Q}_h(\mathrm{D}_h)} \|\mathbf{u} - \mathbf{w}_h\|_{0,\mathrm{D}_h} + \inf_{\boldsymbol{\xi}_{0,h} \in \mathbb{H}_{0,h}(\mathrm{D}_h)} \|\boldsymbol{\sigma}_0 - \boldsymbol{\xi}_{0,h}\|_{0,\mathrm{D}_h} + h^{l+1}\|\boldsymbol{\sigma}\|_{l+1,\Omega}, \tag{4.15}$$

and

$$\begin{aligned} &\|\boldsymbol{\sigma} - \boldsymbol{\sigma}_h\|_{\mathbf{div},\widetilde{\mathcal{T}}_h} \\ &\quad\lesssim \inf_{\mathbf{w}_h \in \mathbf{Q}_h(\mathrm{D}_h)} \|\mathbf{u} - \mathbf{w}_h\|_{0,\mathrm{D}_h} + \inf_{\boldsymbol{\xi}_{0,h} \in \mathbb{H}_{0,h}(\mathrm{D}_h)} \|\boldsymbol{\sigma}_0 - \boldsymbol{\xi}_{0,h}\|_{\mathbf{div},\mathrm{D}_h} + h^{l+1}\left(\|\boldsymbol{\sigma}\|_{l+1,\Omega} + \|\mathbf{div}\,\boldsymbol{\sigma}\|_{l+1,\Omega}\right). \end{aligned} \tag{4.16}$$

Proof. Let $\boldsymbol{\xi}_h$ be given by (4.4). By adding and subtracting convenient terms, applying the estimate (4.13), using the definition of $\widetilde{C}^e_{ext}$ in (3.20), and making use of Assumption **(A1)**, we obtain

$$\begin{aligned} \|\boldsymbol{\sigma} - \boldsymbol{\sigma}_h\|_{0,\mathrm{D}_h^c} &\leq \sum_{e \in \mathcal{E}_h^\partial} \left(\|\boldsymbol{\sigma} - \mathbf{E}_h(\boldsymbol{\xi}_h)\|_{0,\widetilde{T}^e_{ext}} + \|\mathbf{E}_h(\boldsymbol{\xi}_h) - \boldsymbol{\sigma}_h\|_{0,\widetilde{T}^e_{ext}} \right) \\ &\lesssim h^{l+1}\|\boldsymbol{\sigma}\|_{l+1,\Omega} + \|\boldsymbol{\sigma} - \boldsymbol{\xi}_h\|_{0,\mathrm{D}_h} + \sum_{e \in \mathcal{E}_h^\partial} \widetilde{C}^e_{ext}(\widetilde{r}_e)^{1/2}\|\boldsymbol{\sigma}_h - \boldsymbol{\xi}_h\|_{0,T^e} \\ &\lesssim h^{l+1}\|\boldsymbol{\sigma}\|_{l+1,\Omega} + \|\boldsymbol{\sigma} - \boldsymbol{\xi}_h\|_{0,\mathrm{D}_h} + \|\boldsymbol{\sigma} - \boldsymbol{\sigma}_h\|_{0,\mathrm{D}_h}. \end{aligned} \tag{4.17}$$

On the other hand, the same arguments as for (4.6) and (4.7) imply

$$\|\boldsymbol{\sigma} - \boldsymbol{\xi}_h\|_{0,\mathrm{D}_h} + \|\boldsymbol{\sigma} - \boldsymbol{\sigma}_h\|_{0,\mathrm{D}_h} \leq \left(\frac{2}{2-\sqrt{2}}\right)\left(\|\boldsymbol{\sigma}_0 - \boldsymbol{\sigma}_{0,h}\|_{0,\mathrm{D}_h} + \|\boldsymbol{\sigma}_0 - \boldsymbol{\xi}_{0,h}\|_{0,\mathrm{D}_h}\right). \tag{4.18}$$

Combining (4.17) and (4.18), and employing the error estimate given by Lemma 4.1, it yields

$$\begin{aligned} \|\boldsymbol{\sigma} - \boldsymbol{\sigma}_h\|_{0,\mathrm{D}_h^c} \lesssim h^{l+1}\|\boldsymbol{\sigma}\|_{l+1,\Omega} &+ \sum_{e \in \mathcal{E}_h^\partial} \left|\!\left|\!\left| \boldsymbol{\sigma}^{\mathtt{d}} - \mathbf{E}_h(\boldsymbol{\xi}^{\mathtt{d}}_{0,h}) \right|\!\right|\!\right|_e \\ &+ \|\boldsymbol{\sigma}_0 - \boldsymbol{\xi}_{0,h}\|_{0,\mathrm{D}_h} + \inf_{\mathbf{v}_h \in \mathbf{Q}_h(\mathrm{D}_h)} \|\mathbf{u} - \mathbf{v}_h\|_{0,\mathrm{D}_h}. \end{aligned} \tag{4.19}$$

In turn, by using the fact that $\|\cdot\|_{0,\widetilde{T}^e_{ext}}$ and $|\!|\!|\cdot|\!|\!|_e$ are equivalents norms over $\mathbb{L}^2(\widetilde{T}^e_{ext})$ (cf. Section 3.4), and noting that $\|\boldsymbol{\tau}^{\mathtt{d}}\|_{0,\widetilde{T}^e_{ext}} \lesssim \|\boldsymbol{\tau}\|_{0,\widetilde{T}^e_{ext}}$ holds for all $\boldsymbol{\tau} \in \mathbb{H}(\mathbf{div}; \widetilde{T}^e_{ext})$, we get

$$\begin{aligned} \sum_{e \in \mathcal{E}_h^\partial} \left|\!\left|\!\left| \boldsymbol{\sigma}^{\mathtt{d}} - \mathbf{E}_h(\boldsymbol{\xi}^{\mathtt{d}}_{0,h}) \right|\!\right|\!\right|_e &= \sum_{e \in \mathcal{E}_h^\partial} \left|\!\left|\!\left| \boldsymbol{\sigma}^{\mathtt{d}} - \mathbf{E}_h(\boldsymbol{\xi}^{\mathtt{d}}_{h}) \right|\!\right|\!\right|_e \\ &\lesssim \sum_{e \in \mathcal{E}_h^\partial} \|\boldsymbol{\sigma}^{\mathtt{d}} - \mathbf{E}_h(\boldsymbol{\xi}^{\mathtt{d}}_h)\|_{0,\widetilde{T}^e_{ext}} \lesssim \sum_{e \in \mathcal{E}_h^\partial} \|\boldsymbol{\sigma} - \mathbf{E}_h(\boldsymbol{\xi}_h)\|_{0,\widetilde{T}^e_{ext}} \\ &\lesssim h^{l+1}\|\boldsymbol{\sigma}\|_{l+1,\Omega} + \|\boldsymbol{\sigma} - \boldsymbol{\xi}_h\|_{0,\mathrm{D}_h} \lesssim h^{l+1}\|\boldsymbol{\sigma}\|_{l+1,\Omega} + \|\boldsymbol{\sigma}_0 - \boldsymbol{\xi}_{0,h}\|_{0,\mathrm{D}_h}. \end{aligned} \tag{4.20}$$

Therefore, (4.15) is obtained by gathering (4.19) and (4.20), and by noting, thanks to the identity (3.6), that $\|\boldsymbol{\sigma}_0\|_{l+1,\mathrm{D}_h} \lesssim \|\boldsymbol{\sigma}\|_{l+1,\Omega}$. The estimate (4.16) is obtained analogously to (4.15), but considering the estimate (4.14) instead of (4.13). □

The following result is a direct consequence of the inequalities (4.12) and (4.15).

Corollary 4.5. *Let us suppose that hypotheses of Lemma 4.4 are satisfied. Let p and p_h be defined as in (2.3) and (4.11), respectively. There holds*

$$\|p - p_h\|_{0,\mathrm{D}_h^c} \lesssim \inf_{\mathbf{w}_h \in \mathbf{Q}_h(\mathrm{D}_h)} \|\mathbf{u} - \mathbf{w}_h\|_{0,\mathrm{D}_h} + \inf_{\boldsymbol{\xi}_{0,h} \in \mathbb{H}_{0,h}(\mathrm{D}_h)} \|\boldsymbol{\sigma}_0 - \boldsymbol{\xi}_{0,h}\|_{0,\mathrm{D}_h} + h^{l+1}\|\boldsymbol{\sigma}\|_{l+1,\Omega}.$$

To conclude this section, it remains to specify $\mathbf{u}_h$ in D_h^c. In doing so, we proceed exactly as in [19, Section 2.1.3]. In fact, given an edge $e \in \mathcal{E}_h^{\partial}$, it is easy to see that for each point $\mathbf{y} \in \widetilde{T}_{ext}^e$ there exists a transferring path $\mathscr{C}(\mathbf{x})$, starting at $\mathbf{x} \in \Gamma_h$ and ending at $\widetilde{\mathbf{x}} \in \Gamma$, such that $\mathbf{y} = \mathbf{x} + (\varepsilon/\ell(\mathbf{x}))(\widetilde{\mathbf{x}} - \mathbf{x})$ for some $\varepsilon \in [0, \ell(\mathbf{x})]$. As a result, the definition of $\mathbf{u}_h$ in D_h^c can be stated similarly to the one of $\widetilde{\mathbf{g}}_h$, that is,

$$\mathbf{u}_h(\mathbf{y}) := \mathbf{u}(\widetilde{\mathbf{y}}) - \frac{1}{2\mu} \int_0^{|\widetilde{\mathbf{y}} - \mathbf{y}|} \boldsymbol{\sigma}_h^{\mathtt{d}}(\mathbf{y} + \eta\mathbf{k}(\mathbf{y}))\mathbf{k}(\mathbf{y})\, d\eta, \tag{4.21}$$

where $\boldsymbol{\sigma}_h$ is defined as in (4.9), $\widetilde{\mathbf{y}} := \widetilde{\mathbf{x}}$ and $\mathbf{k}(\mathbf{y}) := (\widetilde{\mathbf{y}} - \mathbf{y})/|\widetilde{\mathbf{y}} - \mathbf{y}|$. Actually, it is possible to define $\mathbf{u}_h$ with either $\boldsymbol{\sigma}_h$ or $\boldsymbol{\sigma}_{0,h}$ upon taking into account the identity $\boldsymbol{\sigma}_h^{\mathtt{d}} = \boldsymbol{\sigma}_{0,h}^{\mathtt{d}}$.

The next lemma provides an upper bound for $(\mathbf{u} - \mathbf{u}_h)$ in the $\mathbf{L}^2$-norm on D_h^c. The proof, which involves the estimate (4.15), is basically the same as for Lemma 3.7 in [39], and for this reason is omitted.

Lemma 4.6. *Suppose that the hypotheses of Lemma 4.4 are satisfied. Then, there holds*

$$\|\mathbf{u} - \mathbf{u}_h\|_{0,\mathrm{D}_h^c} \lesssim Rh \left(\inf_{\mathbf{w}_h \in \mathbf{Q}_h(\mathrm{D}_h)} \|\mathbf{u} - \mathbf{w}_h\|_{0,\mathrm{D}_h} + \inf_{\boldsymbol{\xi}_{0,h} \in \mathbb{H}_{0,h}(\mathrm{D}_h)} \|\boldsymbol{\sigma}_0 - \boldsymbol{\xi}_{0,h}\|_{0,\mathrm{D}_h} \right) + Rh^{l+2}\|\boldsymbol{\sigma}\|_{l+1,\Omega}.$$

Finally, the following theorem provides the theoretical rate of convergence of our Galerkin scheme (3.9) and the main unknowns, provided the usual regularity assumptions on the exact solution.

Theorem 4.7. *In addition to the hypotheses of Theorem 4.1 and Lemma 4.4, let us assume that there exists $s \in (0, k+1]$ such that $\boldsymbol{\sigma} \in \mathbb{H}^s(\Omega)$, $\mathbf{div}\,\boldsymbol{\sigma} \in \mathbf{H}^s(\Omega)$ and $\mathbf{u} \in \mathbf{H}^s(\Omega)$. Then, there hold*

$$\|(\boldsymbol{\sigma}_0 - \boldsymbol{\sigma}_{0,h}, \mathbf{u} - \mathbf{u}_h)\|_{\mathbb{H}(\mathbf{div};\mathrm{D}_h)\times\mathbf{L}^2(\mathrm{D}_h)} \lesssim h^s \left(\|\boldsymbol{\sigma}\|_{s,\Omega} + \|\mathbf{div}\,\boldsymbol{\sigma}\|_{s,\Omega} + \|\mathbf{u}\|_{s,\Omega}\right),$$

and

$$\|\boldsymbol{\sigma} - \boldsymbol{\sigma}_h\|_{\mathbf{div},\mathrm{D}_h} + \|p - p_h\|_{0,\mathrm{D}_h} \lesssim h^s \left(\|\boldsymbol{\sigma}\|_{s,\Omega} + \|\mathbf{div}\,\boldsymbol{\sigma}\|_{s,\Omega} + \|\mathbf{u}\|_{s,\Omega}\right).$$

Moreover, in the non-meshed region D_h^c, we have

$$\|\boldsymbol{\sigma} - \boldsymbol{\sigma}_h\|_{\mathbf{div},\widetilde{\mathcal{T}}_h} + \|p - p_h\|_{0,\mathrm{D}_h^c} \lesssim h^s \left(\|\boldsymbol{\sigma}\|_{s,\Omega} + \|\mathbf{div}\,\boldsymbol{\sigma}\|_{s,\Omega} + \|\mathbf{u}\|_{s,\Omega}\right),$$

and

$$\|\mathbf{u} - \mathbf{u}_h\|_{0,\mathrm{D}_h^c} \lesssim Rh^{s+1} \left(\|\boldsymbol{\sigma}\|_{s,\Omega} + \|\mathbf{div}\,\boldsymbol{\sigma}\|_{s,\Omega} + \|\mathbf{u}\|_{s,\Omega}\right).$$

Proof. It is concluded from Theorem 4.1, Corollary 4.2, Lemma 4.4, Corollary 4.5, Lemma 4.6, the approximations properties (3.14)-(3.16), and (3.18), and the usual interpolation estimates. $\square$

It is interesting to note here that the extra power of h related to $\|\mathbf{u} - \mathbf{u}_h\|_{0,\mathrm{D}_h^c}$ follows exclusively from Assumption **(A1)**, i.e., from the fact that in (4.21) the maximum length of the integration segments is of order of Rh. However, the convergence rate of the method is entirely determined by the error estimates on the computational domain D_h.

5. A residual-based a posteriori error analysis

In this section we develop a reliable and quasi-efficient residual-based a posteriori error estimator for the Galerkin scheme (3.9). Throughout this section, we restrict ourself to the case where Γ_h is constructed by interpolating Γ by a picewise linear function and D_h is contained in Ω. In that case, the distance between Γ_h and Γ is of order h^2. We emphasize that the a priori error analysis in previous sections holds under the less restrictive assumption that $d(\Gamma_h, \Gamma)$ is of only order h. However, the corresponding a posteriori error analysis of the latter case is not trivial and is subject of ongoing work. In Section 5.3 we will comment how to deal with the case when D_h is not necessarily contained in Ω.

We start by introducing some useful notation and previous results. In what follows, h_e stands for the length of a given edge $e \in \mathcal{E}_h$. Moreover, for every $e \in \mathcal{E}_h$ we fix a unit normal vector $\mathbf{n}_e := (n_{e,1}, n_{e,2})^{\mathtt{t}}$ to the edge e, and let $\mathbf{t}_e := (-n_{e,2}, n_{e,1})^{\mathtt{t}}$ be the unit tangential vector along e. We define $\mathbf{n}_{\Gamma_e}$ and $\mathbf{t}_{\Gamma_e}$ similarly. In particular, for every $e \in \mathcal{E}_h^\partial$ (resp. $\Gamma_e \subset \Gamma$), we take $\mathbf{n}_e$ (resp. $\mathbf{n}_{\Gamma_e}$) as the vector pointing in the outward direction of Γ_h (resp. Γ) from D_h (resp. Ω). However, when no confusion arises we will simply write $\mathbf{n}$ and $\mathbf{t}$ instead of $\mathbf{n}_e$ and $\mathbf{t}_e$ (or, $\mathbf{n}_{\Gamma_e}$ and $\mathbf{t}_{\Gamma_e}$), respectively. Now, given an edge $e \in \mathcal{E}_h$, $\mathbf{v} \in \mathbf{L}^2(\Omega)$ and $\boldsymbol{\tau} \in \mathbb{L}^2(\Omega)$, such that $\mathbf{v}|_T \in [\mathcal{C}(T)]^2$ and $\boldsymbol{\tau}|_T \in [\mathcal{C}(T)]^{2\times 2}$ on each $T \in \mathcal{T}_h$, we let $[\![\mathbf{v}]\!]$ and $[\![\boldsymbol{\tau}\mathbf{t}]\!]$ be the corresponding jumps across e, that is,

$$[\![\mathbf{v}]\!] := \left(\mathbf{v}|_{T^+}\right)\big|_e - \left(\mathbf{v}|_{T^-}\right)\big|_e \quad \text{and} \quad [\![\boldsymbol{\tau}\mathbf{t}]\!] := \left\{\left(\boldsymbol{\tau}|_{T^+}\right)\big|_e - \left(\boldsymbol{\tau}|_{T^-}\right)\big|_e\right\}\mathbf{t},$$

where T^+ and T^- are two triangles of $\mathcal{T}_h$ having e as a common edge. Finally, if $\mathbf{v} := (v_i)_{i,j=1,2}$ and $\boldsymbol{\tau} := (\tau_{ij})_{i,j=1,2}$ are sufficiently smooth vector-valued and tensor-valued functions, respectively, we let

$$\underline{\mathbf{curl}}(\mathbf{v}) := \begin{pmatrix} \dfrac{\partial v_1}{\partial x_2} & -\dfrac{\partial v_1}{\partial x_1} \\ \dfrac{\partial v_2}{\partial x_2} & -\dfrac{\partial v_2}{\partial x_1} \end{pmatrix} \quad \text{and} \quad \operatorname{curl}(\boldsymbol{\tau}) := \begin{pmatrix} \dfrac{\partial \tau_{12}}{\partial x_1} - \dfrac{\partial \tau_{11}}{\partial x_2} \\ \dfrac{\partial \tau_{22}}{\partial x_1} - \dfrac{\partial \tau_{21}}{\partial x_2} \end{pmatrix}.$$

Let $(\boldsymbol{\sigma}_{0,h}, \mathbf{u}_h) \in \mathbb{H}_{0,h}(\mathrm{D}_h) \times \mathbf{Q}_h(\mathrm{D}_h)$ be the unique solution of (3.9) and $\boldsymbol{\sigma}_h$ be defined as in (3.28). For the forthcoming analysis we introduce an element-by-element postprocessed velocity $\mathbf{u}_h^\star$ being the unique function in $\prod_{T\in\mathcal{T}_h} \mathbf{P}_{k+1}(T)$, such that, for all $T \in \mathcal{T}_h$,

$$\begin{aligned} \int_T \nabla \mathbf{u}_h^\star : \nabla \mathbf{q} &= \frac{1}{2\mu} \int_T \boldsymbol{\sigma}_h^{\mathtt{d}} : \nabla \mathbf{q} \quad \forall\, \mathbf{q} \in \mathbf{P}_{k+1}(T), \\ \int_T \mathbf{u}_h^\star &= \int_T \mathbf{u}_h. \end{aligned} \tag{5.1}$$

It is immediate to check that $\mathbf{u}_h^\star$ is well-defined. Moreover, if we assume that $\mathbf{u} \in \mathbf{H}^{m+1}(\mathrm{D}_h)$ and $\boldsymbol{\sigma} \in \mathbb{H}^l(\mathrm{D}_h)$, with $m, l \in [1, k+1]$, it is not difficult to verify (see, e.g. [17, Theorem 5.2]) that

$$\|\mathbf{u} - \mathbf{u}_h^\star\|_{0,\mathrm{D}_h} \lesssim h^{\min\{l+1,m+1\}} \left(\|\boldsymbol{\sigma}\|_{l,\mathrm{D}_h} + \|\mathbf{u}\|_{m+1,\mathrm{D}_h}\right). \tag{5.2}$$

Therefore, the pair $(\boldsymbol{\sigma}_h, \mathbf{u}_h^\star)$ is an optimal convergent approximation of $(\boldsymbol{\sigma}, \mathbf{u}) \in \mathbb{H}_h(\mathrm{D}_h) \times \mathbf{Q}_h(\mathrm{D}_h)$. For the sake of simplicity, the extrapolation of $\mathbf{u}_h^\star$ on D_h^c (in the sense of (3.12)) will be denoted simply as $\mathbf{u}_h^\star$.

We introduce the following global a posteriori error estimator:

$$\Theta := \left(\sum_{T\in\mathcal{T}_h} \Theta_T^2\right)^{1/2}, \tag{5.3}$$

where Θ_T is the local error indicator defined for each $T \in \mathcal{T}_h$ by

$$\begin{aligned} \Theta_T^2 := {} & h_T^2 \left\| \operatorname{curl}\left\{\frac{1}{2\mu}\boldsymbol{\sigma}_h^{\mathtt{d}}\right\}\right\|_{0,T}^2 + \sum_{e\in\mathcal{E}(T)\cap\mathcal{E}_h^i} \left\{ h_e \left\| \left[\!\!\left[\frac{1}{2\mu}\boldsymbol{\sigma}_h^{\mathtt{d}}\mathbf{t}\right]\!\!\right] \right\|_{0,e}^2 + h_e^{-1} \|[\![\mathbf{u}_h^\star]\!]\|_{0,e}^2 \right\} \\ & + \left\| \frac{1}{2\mu}\boldsymbol{\sigma}_h^{\mathtt{d}} - \nabla \mathbf{u}_h^\star \right\|_{0,T}^2 + \|\mathbf{f} + \mathbf{div}\,\boldsymbol{\sigma}_h\|_{0,T}^2 + \sum_{e\in\mathcal{E}(T)\cap\mathcal{E}_h^\partial} \|\mathbf{f} + \mathbf{div}\,\boldsymbol{\sigma}_h\|_{0,\widetilde{T}_{ext}^e}^2 \\ & + \|\mathbf{u}_h - \mathbf{u}_h^\star\|_{0,T}^2 + \sum_{e\in\mathcal{E}(T)\cap\mathcal{E}_h^\partial} \|\mathbf{u}_h - \mathbf{u}_h^\star\|_{0,\widetilde{T}_{ext}^e}^2 + \mathbb{J}_T^2 + \mathbb{K}_T^2. \end{aligned} \tag{5.4}$$

Here, $\mathbb{J}_T$ and $\mathbb{K}_T$ are computable terms concerning the curved boundary Γ, which take the form

$$\mathbb{J}_T := \left(\sum_{e\in\mathcal{E}(T)\cap\mathcal{E}_h^\partial} h_e^{-1} \|\mathbf{g} - \mathbf{u}_h^\star\|_{0,\Gamma_e}^2 \right)^{1/2}, \tag{5.5}$$

and

$$\mathbb{K}_T := \left(\sum_{e\in\mathcal{E}(T)\cap\mathcal{E}_h^\partial} h_{T^e} \left\| \frac{d\mathbf{g}}{d\mathbf{t}} - \frac{1}{2\mu}\boldsymbol{\sigma}_h^{\mathrm{d}}\mathbf{t} \right\|_{0,\Gamma_e}^2 \right)^{1/2}. \tag{5.6}$$

Observe that, from the strong equations (2.4) and the regularity of the continuous weak solution, the residual character of each term defining (5.4) becomes clear. Note also that (5.6) requires that $d\mathbf{g}/d\mathbf{t} \in \mathbf{L}^2(\Gamma_e)$ for each curved edge Γ_e being part of the boundary Γ, which is overcome below by simply assuming that $\mathbf{g} \in \mathbf{H}^1(\Gamma)$. Moreover, since by (5.2) with $l = m = k+1$ the postprocessed $\mathbf{u}_h^\star$ converges to $\mathbf{u}$ with order $\mathcal{O}(h^{k+2})$ in the $\mathbf{L}^2(\mathrm{D}_h)$-norm, it should be expected, and this is verified in practice (cf. Section 6), that the global a posteriori error estimator Θ retains the rate of convergence of our method, i.e., $\mathcal{O}(h^{k+1})$, if the solution is smooth enough.

We are now in position of establishing the main result of this section.

Theorem 5.1. *Assume that $\mathbf{g} \in \mathbf{H}^1(\Gamma)$. Then, there exist positive constant C_{rel} and C_{eff}, both independent of the meshsizes and the continuous and discrete solutions, such that*

$$\|(\boldsymbol{\sigma} - \boldsymbol{\sigma}_h, \mathbf{u} - \mathbf{u}_h)\|_{\mathbb{H}(\mathbf{div};\Omega)\times\mathbf{L}^2(\Omega)} \le C_{\mathrm{rel}}\Theta, \tag{5.7}$$

and

$$C_{\mathrm{eff}}\Theta \le \|(\boldsymbol{\sigma} - \boldsymbol{\sigma}_h, \mathbf{u} - \mathbf{u}_h)\|_{\mathbb{H}(\mathbf{div};\Omega)\times\mathbf{L}^2(\Omega)} + \mathbb{B}, \tag{5.8}$$

where

$$\mathbb{B} := \left(\sum_{T\in\mathcal{T}_h} \mathbb{J}_T^2\right)^{1/2} + \left(\sum_{T\in\mathcal{T}_h} \mathbb{K}_T^2\right)^{1/2}, \tag{5.9}$$

and $\mathbb{J}_T$ and $\mathbb{K}_T$ are given by (5.5) and (5.6), respectively.

We recall from Section 4.2 that $\boldsymbol{\sigma}_h$ in D_h^c is obtained by (4.9) and satisfies $\int_\Omega \operatorname{tr}(\boldsymbol{\sigma}_h) = 0$. Then, since Γ_h is constructed by a picewise linear interpolation of Γ, it is clear that $\boldsymbol{\sigma}_h \in \mathbb{H}_0(\mathbf{div};\Omega)$, and hence the norm in the left hand side of (5.7) makes sense. In addition, we notice from (5.8) that Θ is efficient up to the term $\mathbb{B}$, which is usually referred as quasi-efficiency (see, e.g. [1, 34]). More importantly, the terms $\mathbb{J}_T$ and $\mathbb{K}_T$ lie on both sides of the inequality (5.8), which does not represent any problem since they provides computable estimates for the approximations $\mathbf{u}_h^\star$ and $(2\mu)^{-1}\boldsymbol{\sigma}_h^{\mathrm{d}}\mathbf{t}$ of the boundary data $\mathbf{g}$ and its tangential derivative along Γ, respectively. It should be noted, however, that $\mathbb{B}$ must have at least the same rate of convergence of the global error if the exact solution is smooth enough. In section 5.2 we treat this matter in more detail.

The proof of Theorem 5.1 is separated into several steps. In Section 5.1 we prove that Θ satisfies the reliability property (5.7), whereas the corresponding quasi-efficiency property (5.8) is derived in Section 5.2.

5.1. Reliability of the a posteriori error estimator

We proceed similarly as in [31] (see also [30, 32]), that is, we start by using the global inf-sup condition in (2.6). In fact, we have

$$\begin{aligned}
\|(\boldsymbol{\sigma} - \boldsymbol{\sigma}_h, \mathbf{u} - \mathbf{u}_h)\|_{\mathbb{H}(\mathbf{div};\Omega)\times\mathbf{L}^2(\Omega)} &\lesssim \|\mathbf{u}_h - \mathbf{u}_h^\star\|_{0,\Omega} + \|(\boldsymbol{\sigma} - \boldsymbol{\sigma}_h, \mathbf{u} - \mathbf{u}_h^\star)\|_{\mathbb{H}(\mathbf{div};\Omega)\times\mathbf{L}^2(\Omega)} \\
&\lesssim \|\mathbf{u}_h - \mathbf{u}_h^\star\|_{0,\Omega} + \sup_{\substack{(\boldsymbol{\tau},\mathbf{v})\in\mathbb{H}_0(\mathbf{div};\Omega)\times\mathbf{L}^2(\Omega)\\(\boldsymbol{\tau},\mathbf{v})\neq\mathbf{0}}} \frac{|a(\boldsymbol{\sigma} - \boldsymbol{\sigma}_h, \boldsymbol{\tau}) + b(\boldsymbol{\tau}, \mathbf{u} - \mathbf{u}_h^\star) + b(\boldsymbol{\sigma} - \boldsymbol{\sigma}_h, \mathbf{v})|}{\|(\boldsymbol{\tau},\mathbf{v})\|_{\mathbb{H}(\mathbf{div};\Omega)\times\mathbf{L}^2(\Omega)}},
\end{aligned}$$

from which

$$\|(\boldsymbol{\sigma}-\boldsymbol{\sigma}_h,\mathbf{u}-\mathbf{u}_h)\|_{\mathbb{H}(\mathbf{div};\Omega)\times\mathbf{L}^2(\Omega)} \lesssim \|\mathbf{u}_h-\mathbf{u}_h^\star\|_{0,\Omega}+\|\mathbf{f}+\mathbf{div}\,\boldsymbol{\sigma}_h\|_{0,\Omega}+\|\mathcal{R}\|_{\mathbb{H}_0(\mathbf{div};\Omega)'}, \tag{5.10}$$

where $\mathcal{R}:\mathbb{H}_0(\mathbf{div};\Omega)\to\mathbb{R}$ is the linear and bounded functional defined as

$$\mathcal{R}(\boldsymbol{\tau}) := \langle \boldsymbol{\tau}\mathbf{n}_\Gamma,\mathbf{g}\rangle_\Gamma - a(\boldsymbol{\sigma}_h,\boldsymbol{\tau}) - b(\boldsymbol{\tau},\mathbf{u}_h^\star) \quad \forall\,\boldsymbol{\tau}\in\mathbb{H}_0(\mathbf{div};\Omega). \tag{5.11}$$

In this way, to obtain the reliability estimate (5.7) it suffices to bound (5.11). We notice that in the case of mixed methods with Ω being polygonal, this is typically accomplished by using a stable Helmholtz decomposition of $\boldsymbol{\tau}$. In what follows, with the help of an auxiliary polygon different from D_h, we shall extend that idea to domains Ω with curved boundary.

Given $e\in\mathcal{E}_h^\partial$ such that $e\neq\Gamma_e$, we suppose that there exists an *auxiliary triangle* $\widetilde{T}^e_{aux}$, with diameter $h_{\widetilde{T}^e_{aux}}$, satisfying

(B1) $\widetilde{T}^e_{aux}$ has e as a boundary edge, $\Gamma_e\subset\widetilde{T}^e_{aux}$, $h_{\widetilde{T}^e_{aux}}\simeq h_{T^e}$, $|\Gamma_e|\simeq h_e$; and if $F=\overline{\widetilde{T}^{e_i}_{aux}}\cap\overline{\widetilde{T}^{e_j}_{aux}}$, with $e_i,\,e_j\in\mathcal{E}_h^\partial$, $i\neq j$, then F is either a common vertex or a common edge of $\widetilde{T}^{e_i}_{aux}$ and $\widetilde{T}^{e_j}_{aux}$; see an illustration in Figure 2.

We observe that in the case of $e=\Gamma_e$, we can simply take $\widetilde{T}^e_{aux}$ as T^e. For this reason, from now on we assume, without loss of generality, that for all $e\in\mathcal{E}_h^\partial$, $e\neq\Gamma_e$. By defining $\widetilde{\mathcal{T}}_h^{aux}:=\{\widetilde{T}^e_{aux}:\ e\in\mathcal{E}_h^\partial\}$, we further assume that

(B2) the triangulation $\mathcal{T}_h^*:=\mathcal{T}_h\cup\widetilde{\mathcal{T}}_h^{aux}$ is shape-regular.

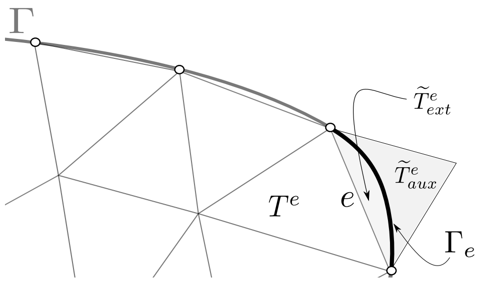

Figure 2: Example of *auxiliary triangle* $\widetilde{T}^e_{aux}$ (gray region).

These hypotheses are expected to be satisfied on sufficiently fine meshes since Γ_h is constructed through a picewise linear interpolation of Γ, even though, as we shall see later, the auxiliary triangles will not be used to compute our a posteriori error estimator. In this setting, it is straightforward to extend the Raviart–Thomas interpolation operator (cf. Section 3) to the polygonal region D_h^* induced by the triangularization $\mathcal{T}_h^*$, say $\overline{\mathrm{D}_h^*}=\cup\{T:\ T\in\mathcal{T}_h^*\}$. Therefore, the approximation properties of this operator also hold in $\mathcal{T}_h^*$.

Next, we denote by $\mathcal{I}_h:\mathrm{H}^1(\mathrm{D}_h^*)\to\{v\in\mathcal{C}\left(\overline{\mathrm{D}_h^*}\right):\ v|_T\in\mathrm{P}_1(T)\ \forall\,T\in\mathcal{T}_h^*\}$ the Clément interpolation operator [16]. From this operator we recall the following classical approximation properties.

Lemma 5.2. *Assume that* **(B1)**-**(B2)** *are satisfied. Then, for all $v\in\mathrm{H}^1(\mathrm{D}_h^*)$ there hold*

$$\|v-\mathcal{I}_h(v)\|_{0,T}\lesssim h_T|v|_{1,\Delta(T)} \quad \forall\,T\in\mathcal{T}_h^*, \tag{5.12}$$

and

$$\|v-\mathcal{I}_h(v)\|_{0,e}\lesssim h_e|v|_{1,\Delta(e)} \quad \forall\,\textit{edge } e \textit{ of } \mathcal{T}_h^*, \tag{5.13}$$

where $\Delta(T):=\cup\{T'\in\mathcal{T}_h^*:\ T\cap T'\neq\varnothing\}$ and $\Delta(e):=\cup\{T'\in\mathcal{T}_h^*:\ e\cap T'\neq\varnothing\}$.

Let us continue with the estimation of $\|\mathcal{R}\|_{[\mathbb{H}_0(\mathbf{div};\Omega)]'}$. To that end, we let (see, e.g. [30, Setion 4])t

$$\boldsymbol{\tau} = \boldsymbol{\zeta} + \underline{\mathbf{curl}}(\boldsymbol{\varphi}) \quad \text{in} \quad \Omega, \tag{5.14}$$

with $\boldsymbol{\chi} \in \mathbb{H}^1(\Omega)$ and $\boldsymbol{\varphi} \in \mathbf{H}^1(\Omega)$ satisfying the stability property

$$\|\boldsymbol{\zeta}\|_{1,\Omega} + \|\boldsymbol{\varphi}\|_{1,\Omega} \lesssim \|\boldsymbol{\tau}\|_{\mathbf{div},\Omega}. \tag{5.15}$$

In turn, following essentially the ideas in [30, Section 4.1] (see also the proof of Lemma 3.8 in [31]), we specify the discrete version of the identity in (5.14). First, we recall from [45] that for any $v \in \mathrm{H}^1(\Omega)$ there exists an extension $\mathscr{E}(v) \in \mathrm{H}^1(\mathbb{R}^2)$ such that $\mathscr{E}(v)|_\Omega = v$ and $\|\mathscr{E}(v)\|_{1,\mathbb{R}^2} \lesssim \|v\|_{1,\Omega}$. Then, we let

$$\boldsymbol{\zeta}_h := \boldsymbol{\Pi}_h^k \left(\boldsymbol{\mathscr{E}}(\boldsymbol{\zeta})|_{\mathrm{D}_h^*} \right) \quad \text{and} \quad \boldsymbol{\varphi}_h := \boldsymbol{\mathcal{I}}_h \left(\boldsymbol{\mathscr{E}}(\boldsymbol{\varphi})|_{\mathrm{D}_h^*} \right),$$

where $\boldsymbol{\Pi}_h^k$ is the Raviart–Thomas interpolation operator described before, whereas $\boldsymbol{\mathscr{E}}$ and $\boldsymbol{\mathcal{I}}_h$ are defined componentwise by the extension operator $\mathscr{E}$ and the Clément interpolant $\mathcal{I}_h$, respectively. Therefore, the aforementioned discrete Helmholtz decomposition is given by

$$\boldsymbol{\tau}_h := \boldsymbol{\zeta}_h + \underline{\mathbf{curl}}(\boldsymbol{\varphi}_h) + c_0 \mathbb{I} \quad \text{in} \quad \mathrm{D}_h^*, \tag{5.16}$$

with $c_0 := -\frac{1}{2|\Omega|} \int_\Omega \operatorname{tr}\left(\boldsymbol{\zeta}_h + \underline{\mathbf{curl}}(\boldsymbol{\varphi}_h)\right)$ chosen in such a way $\int_\Omega \operatorname{tr}(\boldsymbol{\tau}_h) = 0$. In this way, adding and subtracting $\boldsymbol{\tau}_h$ in the argument of $\mathcal{R}$ (cf. (5.11)), using the identities (5.14) and (5.16), noting that $c_0\mathbb{I}$ vanishes in the definition of $\mathcal{R}$ due to the compatibility condition (2.2), we have

$$\mathcal{R}(\boldsymbol{\tau}) = \mathcal{R}(\boldsymbol{\tau}_h) + \mathcal{R}(\boldsymbol{\zeta} - \boldsymbol{\zeta}_h) + \mathcal{R}(\underline{\mathbf{curl}}(\boldsymbol{\varphi} - \boldsymbol{\varphi}_h)). \tag{5.17}$$

In particular, from (5.11) and the identity $\boldsymbol{\sigma}_h^{\mathtt{d}} : \boldsymbol{\tau}_h^{\mathtt{d}} = \boldsymbol{\sigma}_h^{\mathtt{d}} : \boldsymbol{\tau}_h$, it follows that

$$\mathcal{R}(\boldsymbol{\tau}_h) = \sum_{e \in \mathcal{E}_h^\partial} \int_{\Gamma_e} \mathbf{g} \cdot (\boldsymbol{\tau}_h \mathbf{n}_{\Gamma_e}) - \frac{1}{2\mu} \int_\Omega \boldsymbol{\sigma}_h^{\mathtt{d}} : \boldsymbol{\tau}_h - \int_\Omega \mathbf{u}_h^\star \cdot \mathbf{div}\, \boldsymbol{\tau}_h. \tag{5.18}$$

By splinting the integrals over Ω into D_h and D_h^c, integrating by parts elementwise on each of these regions, and recalling that, for every $e \in \mathcal{E}_h^\partial$, the vector $\mathbf{n}_e$ is pointing outwards from D_h, there hold

$$\begin{aligned}
&\frac{1}{2\mu} \int_{\mathrm{D}_h} \boldsymbol{\sigma}_h^{\mathtt{d}} : \boldsymbol{\tau}_h + \int_{\mathrm{D}_h} \mathbf{u}_h^\star \cdot \mathbf{div}\, \boldsymbol{\tau}_h \\
&\quad = \sum_{T \in \mathcal{T}_h} \left\{ \int_T \left(\frac{1}{2\mu} \boldsymbol{\sigma}_h^{\mathtt{d}} - \nabla \mathbf{u}_h^\star \right) : \boldsymbol{\tau}_h + \int_{\partial T} \mathbf{u}_h^\star \cdot (\boldsymbol{\tau}_h \mathbf{n}) \right\} \\
&\quad = \sum_{T \in \mathcal{T}_h} \int_T \left(\frac{1}{2\mu} \boldsymbol{\sigma}_h^{\mathtt{d}} - \nabla \mathbf{u}_h^\star \right) : \boldsymbol{\tau}_h + \sum_{e \in \mathcal{E}_h^i} \int_e [\![\mathbf{u}_h^\star]\!] \cdot (\boldsymbol{\tau}_h \mathbf{n}_e) + \sum_{e \in \mathcal{E}_h^\partial} \int_e \mathbf{u}_h^\star \cdot (\boldsymbol{\tau}_h \mathbf{n}_e),
\end{aligned} \tag{5.19}$$

and

$$\begin{aligned}
&\frac{1}{2\mu} \int_{\mathrm{D}_h^c} \boldsymbol{\sigma}_h^{\mathtt{d}} : \boldsymbol{\tau}_h + \int_{\mathrm{D}_h^c} \mathbf{u}_h^\star \cdot \mathbf{div}\, \boldsymbol{\tau}_h \\
&\quad = \sum_{e \in \mathcal{E}_h^\partial} \left\{ \int_{\widetilde{T}_{ext}^e} \left(\frac{1}{2\mu} \boldsymbol{\sigma}_h^{\mathtt{d}} - \nabla \mathbf{u}_h^\star \right) : \boldsymbol{\tau}_h + \int_{\partial \widetilde{T}_{ext}^e} \mathbf{u}_h^\star \cdot (\boldsymbol{\tau}_h \mathbf{n}) \right\} \\
&\quad = \sum_{e \in \mathcal{E}_h^\partial} \left\{ \int_{\widetilde{T}_{ext}^e} \left(\frac{1}{2\mu} \boldsymbol{\sigma}_h^{\mathtt{d}} - \nabla \mathbf{u}_h^\star \right) : \boldsymbol{\tau}_h - \int_e \mathbf{u}_h^\star \cdot (\boldsymbol{\tau}_h \mathbf{n}_e) + \int_{\Gamma_e} \mathbf{u}_h^\star \cdot (\boldsymbol{\tau}_h \mathbf{n}_{\Gamma_e}) \right\}.
\end{aligned} \tag{5.20}$$

Combining (5.18), (5.19) and (5.20), and observing that $\mathbf{u}_h^\star$ coincides with its extrapolation along every edge $e \in \mathcal{E}_h^\partial$, we obtain

$$\begin{aligned}\mathcal{R}(\boldsymbol{\tau}_h) = &- \sum_{T\in\mathcal{T}_h} \int_T \left(\frac{1}{2\mu}\boldsymbol{\sigma}_h^{\mathtt{d}} - \nabla \mathbf{u}_h^\star\right) : \boldsymbol{\tau}_h - \sum_{e\in\mathcal{E}_h^i} \int_e [\![\mathbf{u}_h^\star]\!] \cdot (\boldsymbol{\tau}_h \mathbf{n}_e) \\ &+ \sum_{e\in\mathcal{E}_h^\partial} \left\{ \int_{\Gamma_e} (\mathbf{g} - \mathbf{u}_h^\star)\cdot(\boldsymbol{\tau}_h \mathbf{n}_{\Gamma_e}) - \int_{\widetilde{T}^e_{ext}} \left(\frac{1}{2\mu}\boldsymbol{\sigma}_h^{\mathtt{d}} - \nabla \mathbf{u}_h^\star\right) : \boldsymbol{\tau}_h \right\}.\end{aligned} \tag{5.21}$$

The following result plays an important role when estimating $|\mathcal{R}(\boldsymbol{\tau}_h)|$.

Lemma 5.3. *Suppose that* **(B1)-(B2)** *hold. Then, for every edge $e \in \mathcal{E}_h^\partial$ and each $\boldsymbol{\tau} \in \mathbb{H}^1(\widetilde{T}^e_{aux})$, there hold*

$$\|\boldsymbol{\tau}\mathbf{n}_{\Gamma_e}\|_{0,\Gamma_e} \lesssim h_{T^e}^{-1/2} \|\boldsymbol{\tau}\|_{1,\widetilde{T}^e_{aux}}, \tag{5.22}$$

$$\|(\boldsymbol{\tau} - \boldsymbol{\Pi}_h^k(\boldsymbol{\tau}))\mathbf{n}_{\Gamma_e}\|_{0,\Gamma_e} \lesssim h_{T^e}^{1/2} \|\boldsymbol{\tau}\|_{1,\widetilde{T}^e_{aux}}, \tag{5.23}$$

$$\|\boldsymbol{\tau} - \boldsymbol{\Pi}_h^k(\boldsymbol{\tau})\|_{0,\Gamma_e} \lesssim h_{T^e}^{1/2} \|\boldsymbol{\tau}\|_{1,\widetilde{T}^e_{aux}}. \tag{5.24}$$

Proof. Given an edge $e \in \mathcal{E}_h^\partial$, let F^e_{aux} be the usual ivertible affine mapping satisfying $F^e_{aux}(T_{ref}) = \widetilde{T}^e_{aux}$, with T_{ref} denoting the reference element. Then, we let Γ_{ref} be the corresponding inverse image of Γ_e. Let then $\boldsymbol{\tau} \in \mathbf{H}^1(\widetilde{T}^e_{aux})$ and define $\widehat{\boldsymbol{\tau}} := \boldsymbol{\tau} \circ F^e_{aux}$. In the present setting, according to Lemma 3 in [36], the following continuous trace inequality holds:

$$\|\widehat{\boldsymbol{\tau}}\|^2_{0,\Gamma_{ref}} \lesssim \|\widehat{\boldsymbol{\tau}}\|_{0,T_{ref}} \|\widehat{\boldsymbol{\tau}}\|_{1,T_{ref}},$$

from which standard scaling arguments gives

$$h_{\widetilde{T}^e_{aux}} \|\boldsymbol{\tau}\mathbf{n}_\Gamma\|^2_{0,\Gamma_e} \leq h_{\widetilde{T}^e_{aux}} \|\boldsymbol{\tau}\|^2_{0,\Gamma_e} \lesssim \|\boldsymbol{\tau}\|^2_{0,\widetilde{T}^e_{aux}} + \left(h_{\widetilde{T}^e_{aux}}\right)^2 \|\boldsymbol{\tau}\|^2_{1,\widetilde{T}^e_{aux}}. \tag{5.25}$$

Together with the assumption $h_{\widetilde{T}^e_{aux}} \simeq h_{T^e}$, this implies (5.22). The remaining two estimates (5.23) and (5.24) are a consequence of (5.25), the approximation properties of the Raviart–Thomas interpolation operator and the fact that $h_{\widetilde{T}^e_{aux}} \simeq h_{T^e}$ has been assumed, by just replacing $\boldsymbol{\tau}$ by $\boldsymbol{\tau} - \boldsymbol{\Pi}_h^k(\boldsymbol{\tau})$. □

Similarly, for every $e \in \mathcal{E}_h^\partial$ and all $\mathbf{v} \in \mathbb{H}^1(\mathrm{D}_h^*)$, we have

$$\|\mathbf{v} - \boldsymbol{\mathcal{I}}_h(\mathbf{v})\|_{0,\Gamma_e} \lesssim h_{T^e}^{1/2} \|\mathbf{v}\|_{1,\Delta(\widetilde{T}^e_{aux})}, \tag{5.26}$$

where $\boldsymbol{\mathcal{I}}_h$ is the vector Clément interpolant introduced above and $\Delta(\widetilde{T}^e_{aux})$ is the union of all the elements of $\mathcal{T}_h^*$ intersecting with $\widetilde{T}^e_{aux}$.

In the framework of Assumptions **(B1)-(B2)**, the following three lemmas provide upper bounds for $|\mathcal{R}(\boldsymbol{\tau}_h)|$, $|\mathcal{R}(\boldsymbol{\zeta} - \boldsymbol{\zeta}_h)|$ and $|\mathcal{R}(\underline{\mathbf{curl}}(\boldsymbol{\varphi} - \boldsymbol{\varphi}_h))|$ arising from (5.17).

Lemma 5.4. *There holds*

$$|\mathcal{R}(\boldsymbol{\tau}_h)| \lesssim \left(\sum_{T\in\mathcal{T}_h} \Theta^2_{0,T}\right)^{1/2} \|\boldsymbol{\tau}\|_{\mathbf{div},\Omega}, \tag{5.27}$$

where

$$\Theta_{0,T} := \left\|\frac{1}{2\mu}\boldsymbol{\sigma}_h^{\mathtt{d}} - \nabla\mathbf{u}_h^\star\right\|^2_{0,T} + \sum_{e\in\mathcal{E}(T)\cap\mathcal{E}_h^\partial} (h_{T^e})^{-1} \|\mathbf{g} - \mathbf{u}_h^\star\|^2_{0,\Gamma_e} + \sum_{e\in\mathcal{E}(T)\cap\mathcal{E}_h^i} (h_{T^e})^{-1} \|[\![\mathbf{u}_h^\star]\!]\|^2_{0,e}.$$

Proof. Applying the Cauchy–Schwarz inequality to each term in (5.21), and using (3.19), (5.22), the fact that $\|\cdot\|_{0,\widetilde{T}^e_{ext}} \lesssim \|\!|\cdot|\!\|_e$ holds for all $e \in \mathcal{E}^\partial_h$ (cf. Section 3.4), and the extrapolation constant (3.20), it follows that

$$
\begin{aligned}
|\mathcal{R}(\boldsymbol{\tau}_h)| \lesssim & \sum_{T\in\mathcal{T}_h} \left\| \frac{1}{2\mu}\boldsymbol{\sigma}^{\mathtt{d}}_h - \nabla \mathbf{u}^\star_h \right\|_{0,T} \|\boldsymbol{\tau}_h\|_{0,T} + \sum_{e\in\mathcal{E}^i_h} C^e_{eq}\,(h_{T^e})^{-1/2}\, \|[\![\mathbf{u}^\star_h]\!]\|_{0,e} \|\boldsymbol{\tau}_h\|_{\mathbf{div},\mathcal{K}(e)} \\
& + \sum_{e\in\mathcal{E}^\partial_h} \left\{ (h_{T^e})^{-1/2}\, \|\mathbf{g}-\mathbf{u}^\star_h\|_{0,\Gamma_e}\, \|\boldsymbol{\tau}_h\|_{1,\widetilde{T}^e_{aux}} + \widetilde{C}^e_{ext}(\widetilde{r}_e)^{1/2} \left\| \frac{1}{2\mu}\boldsymbol{\sigma}^{\mathtt{d}}_h - \nabla \mathbf{u}^\star_h \right\|_{0,T^e} \|\boldsymbol{\tau}_h\|_{0,\widetilde{T}^e_{ext}} \right\},
\end{aligned}
\tag{5.28}
$$

where

$$
\mathcal{K}(e) := \cup \{T' \in \mathcal{T}_h :\ e \in \mathcal{E}(T')\}\,. \tag{5.29}
$$

Notice that $\|\boldsymbol{\tau}_h\|_{0,\widetilde{T}^e_{ext}}$ can be bounded by $\|\boldsymbol{\tau}_h\|_{0,\widetilde{T}^e_{aux}}$ thanks to Assumption **(B1)**. Combining it with (5.28), using again the Cauchy–Schwarz inequality, and finally observing that (5.15) and (5.16) give $\|\boldsymbol{\tau}_h\|_{1,\mathrm{D}^*_h} \lesssim \|\boldsymbol{\tau}\|_{\mathbf{div},\Omega}$, we have

$$
\begin{aligned}
|\mathcal{R}(\boldsymbol{\tau}_h)| \lesssim \|\boldsymbol{\tau}\|_{\mathbf{div};\Omega} \Bigg(& \sum_{T\in\mathcal{T}_h} \left\| \frac{1}{2\mu}\boldsymbol{\sigma}^{\mathtt{d}}_h - \nabla \mathbf{u}^\star_h \right\|^2_{0,T} + \sum_{e\in\mathcal{E}^i_h} \left(C^e_{eq}\right)^2 (h_{T^e})^{-1} \|[\![\mathbf{u}^\star_h]\!]\|^2_{0,e} \\
& + \sum_{e\in\mathcal{E}^\partial_h} \left\{ (h_{T^e})^{-1} \|\mathbf{g}-\mathbf{u}^\star_h\|^2_{0,\Gamma_e} + \left(\widetilde{C}^e_{ext}\right)^2 \widetilde{r}_e \left\| \frac{1}{2\mu}\boldsymbol{\sigma}^{\mathtt{d}}_h - \nabla \mathbf{u}^\star_h \right\|^2_{0,T^e} \right\} \Bigg)^{1/2},
\end{aligned}
$$

where, by Assumption **(A1)**, $\widetilde{r}_e \leq C$ for all $e \in \mathcal{E}^\partial_h$. This completes the proof. $\square$

Lemma 5.5. *There holds*

$$
|\mathcal{R}(\boldsymbol{\zeta}-\boldsymbol{\zeta}_h)| \lesssim \left(\sum_{T\in\mathcal{T}_h} \Theta^2_{1,T} \right)^{1/2} \|\boldsymbol{\zeta}\|_{1,\Omega}, \tag{5.30}
$$

where

$$
\Theta_{1,T} := h^2_T \left\| \frac{1}{2\mu}\boldsymbol{\sigma}^{\mathtt{d}}_h - \nabla \mathbf{u}^\star_h \right\|^2_{0,T} + \sum_{e\in\mathcal{E}(T)\cap\mathcal{E}^\partial_h} h_{T^e} \|\mathbf{g}-\mathbf{u}^\star_h\|^2_{0,\Gamma_e} + \sum_{e\in\mathcal{E}(T)\cap\mathcal{E}^i_h} h_{T^e} \|[\![\mathbf{u}^\star_h]\!]\|^2_{0,e}.
$$

Proof. We first observe that, making use of the approximation properties of the Raviart–Thomas interpolation operator, we obtain, for every edge $e \in \mathcal{E}^\partial_h$,

$$
\|\boldsymbol{\zeta}-\boldsymbol{\zeta}_h\|_{0,\widetilde{T}^e_{ext}} \leq \|\boldsymbol{\mathscr{E}}(\boldsymbol{\zeta})-\boldsymbol{\zeta}_h\|_{0,\widetilde{T}^e_{aux}} \lesssim h_{T^e} \|\boldsymbol{\mathscr{E}}(\boldsymbol{\zeta})\|_{1,\widetilde{T}^e_{aux}}, \tag{5.31}
$$

since, by assumption, $\widetilde{T}^e_{ext} \subset \widetilde{T}^e_{aux}$ and $h_{\widetilde{T}^e_{aux}} \simeq h_{T^e}$. In this way, after replacing $\boldsymbol{\tau}_h$ by $(\boldsymbol{\zeta}-\boldsymbol{\zeta}_h)$ in (5.21), we can use similar arguments as in the previous lemma to obtain

$$
\begin{aligned}
|\mathcal{R}(\boldsymbol{\zeta}-\boldsymbol{\zeta}_h)| \lesssim & \sum_{T\in\mathcal{T}_h} h_T \left\| \frac{1}{2\mu}\boldsymbol{\sigma}^{\mathtt{d}}_h - \nabla \mathbf{u}^\star_h \right\|_{0,T} \|\boldsymbol{\zeta}\|_{1,T} + \sum_{e\in\mathcal{E}^i_h} h^{1/2}_e \|[\![\mathbf{u}^\star_h]\!]\|_{0,e} \|\boldsymbol{\zeta}\|_{1,\mathcal{K}(e)} \\
& + \sum_{e\in\mathcal{E}^\partial_h} \left\{ (h_{T^e})^{1/2} \|\mathbf{g}-\mathbf{u}^\star_h\|_{0,\Gamma_e} + \widetilde{C}^e_{ext} h_{T^e} (\widetilde{r}_e)^{1/2} \left\| \frac{1}{2\mu}\boldsymbol{\sigma}^{\mathtt{d}}_h - \nabla \mathbf{u}^\star_h \right\|_{0,T^e} \right\} \|\boldsymbol{\mathscr{E}}(\boldsymbol{\zeta})\|_{1,\widetilde{T}^e_{aux}}.
\end{aligned}
$$

The conclusion is therefore straightforward from the continuity of the extension operator $\boldsymbol{\mathscr{E}}$, Assumption **(A1)** and the Cauchy–Schwarz inequality. $\square$

Lemma 5.6. *Assume that* $\mathbf{g} \in \mathbf{H}^1(\Gamma)$*. Then, there holds*

$$|\mathcal{R}(\underline{\mathbf{curl}}(\boldsymbol{\varphi}-\boldsymbol{\varphi}_h))| \lesssim \left(\sum_{T\in\mathcal{T}_h} \Theta_{2,T}^2\right)^{1/2} \|\boldsymbol{\varphi}\|_{1,\Omega}, \tag{5.32}$$

where

$$\Theta_{2,T} := h_T^2 \left\|\operatorname{curl}\left\{\frac{1}{2\mu}\boldsymbol{\sigma}_h^{\mathtt{d}}\right\}\right\|_{0,T}^2 + \sum_{e\in\mathcal{E}(T)\cap\mathcal{E}_h^\partial} h_{T^e}\left\|\frac{d\mathbf{g}}{d\mathbf{t}} - \frac{1}{2\mu}\boldsymbol{\sigma}_{0,h}^{\mathtt{d}}\mathbf{t}\right\|_{0,\Gamma_e}^2 + \sum_{e\in\mathcal{E}(T)\cap\mathcal{E}_h^i} h_e \left\|\left[\!\left[\frac{1}{2\mu}\boldsymbol{\sigma}_h^{\mathtt{d}}\mathbf{t}\right]\!\right]\right\|_{0,e}^2.$$

Proof. We follow [30, Lemma 4.3] and use integration by parts formula, but more precisely the identities from [35, eq. 2.17 and Theorem 2.11], and the fact that $\underline{\mathbf{curl}}(\mathbf{v})\mathbf{n}_\Gamma = d\mathbf{v}/d\mathbf{t}$ for a sufficiently smooth vector-valued function $\mathbf{v}$, to obtain

$$\langle \underline{\mathbf{curl}}(\boldsymbol{\varphi}-\boldsymbol{\varphi}_h)\mathbf{n}_\Gamma, \mathbf{g}\rangle_\Gamma = -\sum_{e\in\mathcal{E}_h^\partial}\int_{\Gamma_e}\frac{d\mathbf{g}}{d\mathbf{t}}\cdot(\boldsymbol{\varphi}-\boldsymbol{\varphi}_h), \tag{5.33}$$

which holds true because $\mathbf{g}\in\mathbf{H}^1(\Gamma)$ has been assumed. In turn, from $\mathcal{R}(\underline{\mathbf{curl}}(\boldsymbol{\varphi}-\boldsymbol{\varphi}_h))$, using the identity $\mathbf{div}\,(\underline{\mathbf{curl}}(\boldsymbol{\varphi}-\boldsymbol{\varphi}_h)) = \mathbf{0}$, applying [35, Theorem 2.11] to integrate by parts elementwise the integrals over D_h and D_h^c separately, and then combining the resulting terms with (5.33), it follows that

$$\begin{aligned}
\mathcal{R}(\underline{\mathbf{curl}}(\boldsymbol{\varphi}-\boldsymbol{\varphi}_h)) &= -\sum_{e\in\mathcal{E}_h^\partial}\int_{\Gamma_e}\frac{d\mathbf{g}}{d\mathbf{t}}\cdot(\boldsymbol{\varphi}-\boldsymbol{\varphi}_h) - \frac{1}{2\mu}\int_\Omega \boldsymbol{\sigma}_h^{\mathtt{d}} : \underline{\mathbf{curl}}\,(\boldsymbol{\varphi}-\boldsymbol{\varphi}_h)\\
&= -\sum_{T\in\mathcal{T}_h}\int_T \operatorname{curl}\left\{\frac{1}{2\mu}\boldsymbol{\sigma}_h^{\mathtt{d}}\right\}\cdot(\boldsymbol{\varphi}-\boldsymbol{\varphi}_h) + \sum_{e\in\mathcal{E}_h^i}\int_e \left[\!\left[\frac{1}{2\mu}\boldsymbol{\sigma}_h^{\mathtt{d}}\mathbf{t}\right]\!\right]\cdot(\boldsymbol{\varphi}-\boldsymbol{\varphi}_h)\\
&\quad - \sum_{e\in\mathcal{E}_h^\partial}\left\{\int_{\widetilde{T}_{ext}^e}\operatorname{curl}\left\{\frac{1}{2\mu}\boldsymbol{\sigma}_h^{\mathtt{d}}\right\}\cdot(\boldsymbol{\varphi}-\boldsymbol{\varphi}_h) + \int_{\Gamma_e}\left(\frac{d\mathbf{g}}{d\mathbf{t}} - \frac{1}{2\mu}\boldsymbol{\sigma}_h^{\mathtt{d}}\mathbf{t}\right)\cdot(\boldsymbol{\varphi}-\boldsymbol{\varphi}_h)\right\}.
\end{aligned}$$

Next, applying the Cauchy-Schwarz inequality to each term above, noting that similarly to (5.31), one has

$$\|\boldsymbol{\varphi}-\boldsymbol{\varphi}_h\|_{0,\widetilde{T}_{ext}^e} \lesssim h_{T^e}\|\boldsymbol{\mathcal{E}}(\boldsymbol{\varphi})\|_{1,\Delta(\widetilde{T}_{aux}^e)} \quad \forall\, e\in\mathcal{E}_h^\partial,$$

using the extrapolation constant (3.20) in the same fashion as in the proof of Lemma 5.4, and making use of the approximation properties (5.12)-(5.13) and (5.26), we obtain

$$\begin{aligned}
|\mathcal{R}(\underline{\mathbf{curl}}(\boldsymbol{\varphi}-\boldsymbol{\varphi}_h))| &\lesssim \sum_{T\in\mathcal{T}_h} h_T\left\|\operatorname{curl}\left\{\frac{1}{2\mu}\boldsymbol{\sigma}_h^{\mathtt{d}}\right\}\right\|_{0,T}\|\boldsymbol{\varphi}\|_{1,\Delta(T)} + \sum_{e\in\mathcal{E}_h^i} h_e^{1/2}\left\|\left[\!\left[\frac{1}{2\mu}\boldsymbol{\sigma}_h^{\mathtt{d}}\mathbf{t}\right]\!\right]\right\|\|\boldsymbol{\varphi}\|_{1,\Delta(e)}\\
&+ \sum_{e\in\mathcal{E}_h^\partial}\left\{\widetilde{C}_{ext}^e h_{T^e}\,(\widetilde{r}_e)^{1/2}\left\|\operatorname{curl}\left\{\frac{1}{2\mu}\boldsymbol{\sigma}_h^{\mathtt{d}}\right\}\right\|_{0,T^e} + (h_{T^e})^{1/2}\left\|\frac{d\mathbf{g}}{d\mathbf{t}} - \frac{1}{2\mu}\boldsymbol{\sigma}_h^{\mathtt{d}}\mathbf{t}\right\|_{0,\Gamma_e}\right\}\|\boldsymbol{\mathscr{E}}(\boldsymbol{\varphi})\|_{1,\Delta(\widetilde{T}_{aux}^e)}.
\end{aligned}$$

In addition, owing to the shape-regularity of $\mathcal{T}_h^*$, the number of triangles in $\Delta(\widetilde{T}_{aux}^e)$, $\Delta(T)$ and $\Delta(e)$ are bounded, and thus the proof ends by using the same arguments as in the last two lemmas. □

Finally, from the identity (5.17), the estimates (5.27), (5.30), and (5.32), and the stability of the Helmholtz decomposition (cf. (5.15)), we have

$$\|\mathcal{R}\|_{[\mathbb{H}_0(\mathbf{div};\Omega)]'} \lesssim \left(\sum_{T\in\mathcal{T}_h}\sum_{i=0}^{2}\Theta_{i,T}^2\right)^{1/2}.$$

Then we combine it with (5.10), and then use the fact that $h_e \le h_{T^e}$ for all $e\in\mathcal{E}_h^\partial$, to conclude the reliability of Θ (cf. (5.7)).

5.2. Quasi-efficiency of the a posteriori error estimator

In order to prove the quasi-efficiency of our estimator Θ, in what follows we derive suitable upper bounds for each term defining the local error indicator Θ_T defined in (5.4). In particular, we briefly discuss at the end of this section the situation of $\mathbb{B}$ (cf. (5.9)) involving the Dirichlet datum $\mathbf{g}$ and the postprocessed velocity $\mathbf{u}_h^\star$.

We first notice that, using $\mathbf{div}\,\boldsymbol{\sigma} = -\mathbf{f}$ in Ω (see Lemma 2.1), there holds

$$\|\mathbf{f} + \mathbf{div}\,\boldsymbol{\sigma}_h\|_{0,T}^2 = \|\mathbf{div}\,(\boldsymbol{\sigma} - \boldsymbol{\sigma}_h)\|_{0,T}^2 \leq \|\boldsymbol{\sigma} - \boldsymbol{\sigma}_h\|_{\mathbf{div},T}^2 \quad \forall\, T \in \mathcal{T}_h, \tag{5.34}$$

and similarly,

$$\|\mathbf{f} + \mathbf{div}\,\boldsymbol{\sigma}_h\|_{0,\widetilde{T}^e_{ext}}^2 \leq \|\boldsymbol{\sigma} - \boldsymbol{\sigma}_h\|_{\mathbf{div},\widetilde{T}^e_{ext}}^2 \quad \forall\, e \in \mathcal{E}_h^\partial. \tag{5.35}$$

On the other hand, we have the following result for the terms involving the curl operator and the tangential jumps across the interior edges of $\mathcal{T}_h$.

Lemma 5.7. *There hold*

$$h_e^{-1}\left\|\left[\!\left[\frac{1}{2\mu}\boldsymbol{\sigma}_h^{\mathtt{d}}\mathbf{t}\right]\!\right]\right\|_{0,e}^2 \lesssim \|\boldsymbol{\sigma} - \boldsymbol{\sigma}_h\|_{0,\mathcal{K}(e)}^2 \quad \forall\, e \in \mathcal{E}_h^i, \tag{5.36}$$

and

$$h_T^2\left\|\mathrm{curl}\left\{\frac{1}{2\mu}\boldsymbol{\sigma}_h^{\mathtt{d}}\right\}\right\|_{0,T}^2 \lesssim \|\boldsymbol{\sigma} - \boldsymbol{\sigma}_h\|_{0,T}^2 \quad \forall\, T \in \mathcal{T}_h, \tag{5.37}$$

where $\mathcal{K}(e)$ is given by (5.29).

Proof. It follows by using similar arguments as in the proofs of Lemmas 6.3 and 6.4 in [15] (see also [7, Lemmas 4.3 and 4.4] or [30, Lemma 4.11]). We omit further details. □

Next, we exploit the properties of the postprocessed velocity $\mathbf{u}_h^\star$ (cf. (5.1)) and derive the local efficiency of $h_e^{-1}|[\![\mathbf{u}_h^\star]\!]\|_{0,e}^2$ for all $e \in \mathcal{E}_h^i$. In doing so, we follow here the approach of [24, Section 3.2]. Denoting by $\boldsymbol{\mathcal{P}}_h^0$ the $\mathbf{L}^2(\mathrm{D}_h)$-projection onto the piecewise constant functions on each edge, and then adding and subtracting a convenient term, we easily get

$$h_e^{-1}\|[\![\mathbf{u}_h^\star]\!]\|_{0,e}^2 \lesssim h_e^{-1}\|(\boldsymbol{I} - \boldsymbol{\mathcal{P}}_h^0)([\![\mathbf{u}_h^\star]\!])\|_{0,e}^2 + h_e^{-1}\|\boldsymbol{\mathcal{P}}_h^0([\![\mathbf{u}_h^\star]\!])\|_{0,e}^2, \tag{5.38}$$

where $\boldsymbol{I}$ denotes the identity operator. In this direction, our present goal reduces to bound each term in the right hand side of (5.38). The first of them is provided next.

Lemma 5.8. *For every edge $e \in \mathcal{E}_h^i$, we have*

$$h_e^{-1}\|(\boldsymbol{I} - \boldsymbol{\mathcal{P}}_h^0)[\![\mathbf{u}_h^\star]\!]\|_{0,e}^2 \lesssim \sum_{T\in\mathcal{K}(e)} \|\nabla(\mathbf{u} - \mathbf{u}_h^\star)\|_{0,T}^2. \tag{5.39}$$

Moreover, for each $T \in \mathcal{T}_h$, there holds

$$\left\|\frac{1}{2\mu}\boldsymbol{\sigma}_h^{\mathtt{d}} - \nabla\mathbf{u}_h^\star\right\|_{0,T}^2 \lesssim \|\boldsymbol{\sigma} - \boldsymbol{\sigma}_h\|_{0,T}^2. \tag{5.40}$$

Proof. With minor modification the proofs follows from Lemmas 3.5 and 3.7 in [24]. □

The next result establishes an upper bound for the last term in (5.38). The proof is similar to the one of Lemma 3.4 in [24], where the equations of the proposed hybridized Raviart-Thomas method and the posptocessed velocity are used to establish a relation between the residuals on elements and edges. For the sake of completeness and since we are not using hybrid-based methods, we include a detailed proof.

Lemma 5.9. *For each $e \in \mathcal{E}_h^i$, there holds*

$$h_e^{-1/2} \big\| \boldsymbol{\mathcal{P}}_h^0([\![\mathbf{u}_h^\star]\!]) \big\|_{0,e} \lesssim \sum_{T\in\mathcal{K}(e)} \Big\| \frac{1}{2\mu} \boldsymbol{\sigma}_h^{\mathtt{d}} - \nabla \mathbf{u}_h^\star \Big\|_{0,T}. \tag{5.41}$$

Proof. From the Galerkin scheme (3.9) and the equations defining the postprocessed velocity $\mathbf{u}_h^\star$ (cf. (5.1)), it is easy to check that

$$\begin{aligned}\sum_{e\in\mathcal{E}_h^\partial} \int_e \widetilde{\mathbf{g}}_h \cdot (\boldsymbol{\tau}_h \mathbf{n}_e) &= \int_{T\in\mathcal{T}_h} \left\{ \frac{1}{2\mu} \int_T \boldsymbol{\sigma}_h^{\mathtt{d}} : \boldsymbol{\tau}_h + \int_T \mathbf{u}_h \cdot \mathbf{div}\, \boldsymbol{\tau}_h \right\} \\ &= \sum_{T\in\mathcal{T}_h} \left\{ \int_T \left(\frac{1}{2\mu} \boldsymbol{\sigma}_h^{\mathtt{d}} - \nabla \mathbf{u}_h^\star \right) : \boldsymbol{\tau}_h + \int_{\partial T} \mathbf{u}_h^\star \cdot (\boldsymbol{\tau}_h \mathbf{n}) \right\}\end{aligned}$$

for all $\boldsymbol{\tau}_h$ in the space given by $\mathbb{H}_{0,h}(\mathrm{D}_h)$ with $k=0$ (cf. Section 3.3). After some algebraic manipulations, it yields

$$\sum_{T\in\mathcal{T}_h} \int_T \left(\frac{1}{2\mu} \boldsymbol{\sigma}_h^{\mathtt{d}} - \nabla \mathbf{u}_h^\star \right) : \boldsymbol{\tau}_h = - \sum_{e\in\mathcal{E}_h^i} \int_e [\![\mathbf{u}_h^\star]\!] \cdot \boldsymbol{\tau}_h \mathbf{n}_e + \sum_{e\in\mathcal{E}_h^\partial} \int_e (\widetilde{\mathbf{g}}_h - \mathbf{u}_h^\star) \cdot \boldsymbol{\tau}_h \mathbf{n}_e. \tag{5.42}$$

In particular, taking $\boldsymbol{\tau}_h$ such that, for a given edge $e' \in \mathcal{E}_h^i$ and each $T \in \mathcal{K}(e')$,

$$\begin{aligned} \int_e \boldsymbol{\tau}_h \mathbf{n}_T &= \mathbf{0} & &\forall\, e \in \mathcal{E}(T),\ e \neq e', \\ \int_{e'} \boldsymbol{\tau}_h \mathbf{n}_T &= \int_{e'} \boldsymbol{\mathcal{P}}_h^0([\![\mathbf{u}_h^\star]\!]) & &\text{for the edge } e', \end{aligned}$$

and for all $T \in \mathcal{T}_h \setminus \mathcal{K}(e')$,

$$\int_e \boldsymbol{\tau}_h \mathbf{n}_T = \mathbf{0} \quad \forall\, e \in \mathcal{E}(T),$$

we have that $\boldsymbol{\tau}_h|_T \equiv \mathbf{0}$ for all $T \in \mathcal{T}_h \setminus \mathcal{K}(e')$, and then (5.42) gives rise to

$$\sum_{T\in\mathcal{K}(e')} \int_T \left(\frac{1}{2\mu} \boldsymbol{\sigma}_h^{\mathtt{d}} - \nabla \mathbf{u}_h^\star \right) : \boldsymbol{\tau}_h = \int_{e'} [\![\mathbf{u}_h^\star]\!] \cdot \boldsymbol{\mathcal{P}}_h^0([\![\mathbf{u}_h^\star]\!]) = \big\| \boldsymbol{\mathcal{P}}_h^0([\![\mathbf{u}_h^\star]\!]) \big\|_{0,e'}^2.$$

In turn, applying the Cauchy–Schwarz inequality and observing that $\|\boldsymbol{\tau}_h\|_{0,T} \lesssim h_{e'}^{1/2} \|\boldsymbol{\tau}_h \mathbf{n}_{e'}\|_{0,e'}$ for all $T \in \mathcal{K}(e')$ (see, e.g. [24, Lemma A.1]), we obtain

$$\begin{aligned}\|\boldsymbol{\mathcal{P}}_h^0([\![\mathbf{u}_h^\star]\!])\|_{0,e'}^2 &\leq \sum_{T\in\mathcal{K}(e')} h_{e'}^{1/2} \Big\| \frac{1}{2\mu} \boldsymbol{\sigma}_h^{\mathtt{d}} - \nabla \mathbf{u}_h^\star \Big\|_{0,T} \|\boldsymbol{\tau}_h \mathbf{n}_{e'}\|_{0,e'} \\ &= \sum_{T\in\mathcal{K}(e')} h_{e'}^{1/2} \Big\| \frac{1}{2\mu} \boldsymbol{\sigma}_h^{\mathtt{d}} - \nabla \mathbf{u}_h^\star \Big\|_{0,T} \|\boldsymbol{\mathcal{P}}_h^0([\![\mathbf{u}_h^\star]\!])\|_{0,e'}.\end{aligned}$$

Clearly, this implies the claimed result. $\square$

Consequently, gathering (5.39) and (5.41) into (5.38) and employing the upper bound in (5.40), we conclude that, for each edge $e \in \mathcal{E}_h^i$,

$$h_e^{-1} \|[\![\mathbf{u}_h^\star]\!]\|_{0,e}^2 \lesssim \sum_{T\in\mathcal{K}(e)} \|\boldsymbol{\sigma} - \boldsymbol{\sigma}_h\|_{0,T}^2. \tag{5.43}$$

The following lemma deals with the corresponding upper bound for the estimator terms involving only the two velocity approximations.

Lemma 5.10. *For each $T \in \mathcal{T}_h$ and $h < 1$, there holds*

$$\|\mathbf{u}_h - \mathbf{u}_h^\star\|_{0,T}^2 \lesssim \|\boldsymbol{\sigma} - \boldsymbol{\sigma}_h\|_{0,T}^2 + \|\mathbf{u} - \mathbf{u}_h\|_{0,T}^2. \tag{5.44}$$

Moreover, for all $e \in \mathcal{E}_h^\partial$, we have

$$\|\mathbf{u}_h - \mathbf{u}_h^\star\|_{0,\widetilde{T}_{ext}^e}^2 \lesssim \|\boldsymbol{\sigma} - \boldsymbol{\sigma}_h\|_{0,T^e}^2 + \|\mathbf{u} - \mathbf{u}_h\|_{0,T^e}^2. \tag{5.45}$$

Proof. Let $\mathbf{w}_h := \mathbf{u}_h - \mathbf{u}_h^\star$. Denoting by $\boldsymbol{\mathcal{P}}_T^0$ the $\mathbf{L}^2(T)$-projection onto $\mathbf{P}_0(T)$, we have $\boldsymbol{\mathcal{P}}_T^0(\mathbf{w}_h|_T) = \mathbf{0}$ for all $T \in \mathcal{T}_h$, since $\mathbf{u}_h^\star$ solves (5.1). In this way, using the approximation property (3.14) with $k = 0$ and $l = 1$, and the fact that $\boldsymbol{\mathcal{P}}_T^0(\mathbf{w}_h|_T) = \boldsymbol{\mathcal{P}}_h^0(\mathbf{w}_h)|_T$, we obtain

$$\|\mathbf{w}_h\|_{0,T} = \left\|\mathbf{w}_h - \boldsymbol{\mathcal{P}}_h^0(\mathbf{w}_h)\right\|_{0,T} \le h_T |\mathbf{w}_h|_{1,T}.$$

Adding and subtracting $(2\mu)^{-1}\boldsymbol{\sigma}_h^{\mathtt{d}}$, and applying the triangle inequality, it follows that

$$\|\mathbf{w}_h\|_{0,T}^2 \lesssim \left\|\frac{1}{2\mu}\boldsymbol{\sigma}_h^{\mathtt{d}} - \nabla \mathbf{u}_h^\star\right\|_{0,T}^2 + h_T^2 \left\|\frac{1}{2\mu}\boldsymbol{\sigma}_h^{\mathtt{d}} - \nabla \mathbf{u}_h\right\|_{0,T}^2,$$

where we have used that $h < 1$. The first term in the right-hand side of the above inequality can be bounded by using (5.40). In turn, following the proof of Lemma 6.3 in [14] (see also [30, Lemma 4.13]), we easily get

$$h_T^2 \left\|\frac{1}{2\mu}\boldsymbol{\sigma}_h^{\mathtt{d}} - \nabla \mathbf{u}_h\right\|_{0,T}^2 \lesssim \|\boldsymbol{\sigma} - \boldsymbol{\sigma}_h\|_{0,T}^2 + \|\mathbf{u} - \mathbf{u}_h\|_{0,T}^2,$$

concluding (5.44).

On the other hand, using the extrapolation constant (cf. (3.20)) and the equivalence of the norms $\|\cdot\|_{0,\widetilde{T}_{ext}^e}$ and $|\!|\!|\cdot|\!|\!|_{0,e}$ for all $e \in \mathcal{E}_h^\partial$, we obtain $\|\mathbf{w}_h\|_{0,\widetilde{T}_{ext}^e} \lesssim (\widetilde{r}_e)^{1/2}\widetilde{C}_{ext}^e\|\mathbf{w}_h\|_{0,T^e}$, which together with the Assumption **(A1)** and the estimate (5.44), implies (5.45). $\square$

Therefore, the quasi-efficiency property of the estimator Θ is a consequence of the upper bounds given by (5.34)-(5.37) and (5.43)-(5.45).

Having established (5.8), as already mentioned at the beginning of this section, the mayor issue is the convergence rate of $\mathbb{B}$ given by (5.9). If $\mathbf{g}$ were piecewise polynomial on a polygonal boundary Γ, it would be possible to apply the results given by Lemmas 4.14 and 4.15 in [30], which are based on standard tools including the usual localization technique of bubble functions and inverse inequalities, to deduce that the convergence order of $\mathbb{B}$ is at least $\mathcal{O}(h^{k+1})$ owing to the approximations properties of the postprocessed velocity $\mathbf{u}_h^\star$. Otherwise, assuming that $\mathbf{g}$ is sufficiently smooth, the previous estimate is actually valid with possible further high order terms arising from Taylor approximations of the data. The extension of this idea to curved domains is an ongoing work. However, our numerical results below allow us to conjecture that $\mathbb{B}$ has the above mentioned optimal convergence property.

5.3. Extending the estimator Θ to more complicated geometries

When defining the computational boundary as in the previous section, it would be possible to have $\omega := \Omega^c \cap \mathrm{D}_h \neq \varnothing$. Indeed, this certainly happens if we consider nonconvex curved domains Ω, even though some regions having boundaries that are not completely curved, as for instance the pacman-shaped domain, could be the exception. Thus, our intention here is to propose a way of extending the previous analysis to that situation. In what follows, we assume that the solution $(\boldsymbol{\sigma}, \mathbf{u})$ of (2.5) can be extended to ω, with $\boldsymbol{\sigma} \in \mathbb{H}(\mathbf{div}; \omega \cup \Omega)$, but not necessarily satisfying $\int_{\omega\cup\Omega} \mathrm{tr}\,(\boldsymbol{\sigma}) = 0$.

Now, since $\boldsymbol{\sigma}$ solves (2.5), which ensures that $\int_\Omega \mathrm{tr}\,(\boldsymbol{\sigma}) = 0$, we can write

$$\boldsymbol{\sigma} = \boldsymbol{\sigma}_0 - \frac{1}{2|\mathrm{D}_h|}\left(\int_{\mathrm{D}_h^c} \mathrm{tr}\,(\boldsymbol{\sigma}) - \int_\omega \mathrm{tr}\,(\boldsymbol{\sigma})\right)\mathbb{I} \quad \text{in} \quad \mathrm{D}_h,$$

where $\boldsymbol{\sigma}_0 \in \mathbb{H}_0(\mathbf{div}; \mathrm{D}_h)$. Similarly, the tensor $\boldsymbol{\sigma}_h$ could be defined as in (3.28), by replacing γ_h in (3.30) by

$$\gamma_h := -\int_{\mathrm{D}_h^c} \mathrm{tr}\left(\mathbf{E}_h(\boldsymbol{\sigma}_{0,h}) - \frac{1}{2|\Omega|}\left(\int_{\mathrm{D}_h^c} \mathrm{tr}\,(\mathbf{E}_h(\boldsymbol{\sigma}_{0,h})) - \int_{\omega} \mathrm{tr}\,(\mathbf{E}_h(\boldsymbol{\sigma}_{0,h}))\right)\mathbb{I}\right), \tag{5.46}$$

from which we easily obtain that $\boldsymbol{\sigma}_h \in \mathbb{H}_0(\mathbf{div}; \Omega)$, provided $\boldsymbol{\sigma}_{0,h} \in \mathbb{H}_{0,h}(\mathrm{D}_h)$. As a consequence, the a priori error bounds in Section 4 still valid on the larger region $\omega \cup \Omega$. Moreover, whenever $T^e \cap \omega \neq \varnothing$ we consider $\widetilde{T}^e_{aux} = T^e$ (cf. Section 5.1) and define the global a posteriori error estimator Θ as in (5.3), with the only difference that $\boldsymbol{\sigma}_h$ is now computed in terms of (5.46).

6. Numerical results

We now present a series of numerical examples devised to illustrate the good performance of our discrete scheme (3.9), to validate the reliability and quasi-efficiency of the a posteriori error estimator Θ defined in (5.3), and to show the behavior of the associated adaptive algorithm. Our implementation is based on a MATLAB code along with the direct linear solver UMFPACK [26]. All our examples were carry out using the finite element spaces $\mathbb{H}_{0,h}(\mathrm{D}_h)$ and $\mathbf{Q}_h(\mathrm{D}_h)$ with $k \in \{0, 1, 2, 3\}$ (cf. Section 3.3). In turn, the condition $\int_{\mathrm{D}_h} \mathrm{tr}\,(\boldsymbol{\tau}_h) = 0$ for $\boldsymbol{\tau}_h \in \mathbb{H}_{0,h}(\mathrm{D}_h)$ was imposed as usual, that is, via a real Lagrange multiplier. Regarding the basis functions of high order, they were computed using the *hierarchical basis* for the local Raviart–Thomas space of order k, as presented in [8], and the *Dubiner basis* (see, e.g. [27]) for the local polynomial space of degree less or equal to k.

In what follows, we denote by N the total number of elements defining the mesh $\mathcal{T}_h$ associated to the computational domain D_h. Denoting by $\mathbf{u}_h$ the solution of the problem (3.4), and by $\boldsymbol{\sigma}_h$, p_h and $\mathbf{u}_h^\star$ the postprocessed solutions given by (3.28), (3.29) and (5.1), respectively, the individual errors are defined as

$$\mathrm{e}(\mathbf{u}) := \|\mathbf{u} - \mathbf{u}_h\|_{0,\Omega}, \quad \mathrm{e}^\star(\mathbf{u}) := \|\mathbf{u} - \mathbf{u}_h^\star\|_{0,\Omega},$$
$$\mathrm{e}(p) := \|p - p_h\|_{0,\Omega}, \quad \text{and} \quad \mathrm{e}(\boldsymbol{\sigma}) := \left(\|\boldsymbol{\sigma} - \boldsymbol{\sigma}_h\|^2_{\mathbf{div},\mathrm{D}_h} + \|\boldsymbol{\sigma} - \boldsymbol{\sigma}_h\|^2_{\mathbf{div},\widetilde{\mathcal{T}}_h}\right)^{1/2},$$

where the approximations in D_h^c are those specified in Section 4.2. According to Theorem 5.1, the global error is computed as

$$\mathrm{e}(\boldsymbol{\sigma}, \mathbf{u}) := \left(\mathrm{e}(\mathbf{u})^2 + \mathrm{e}(\boldsymbol{\sigma})^2\right)^{1/2},$$

whereas the quality of the posteriori error estimator Θ is measured by using the effectivity index $\mathtt{eff}(\Theta) := \Theta/\mathrm{e}(\boldsymbol{\sigma}, \mathbf{u})$. In order to explore the convergence properties of $\mathbb{B}$ (cf. (5.9)), we also introduce the estimator terms

$$\mathbb{J} := \left(\sum_{T\in\mathcal{T}_h} \mathbb{J}_T^2\right)^{1/2} \quad \text{and} \quad \mathbb{K} := \left(\sum_{T\in\mathcal{T}_h} \mathbb{K}_T^2\right)^{1/2},$$

where $\mathbb{J}_T$ and $\mathbb{K}_T$ are given by (5.5) and (5.6), respectively. In addition, suppose that $\mathtt{e}$ and $\mathtt{e}'$ are any of the above quantities for two consecutive meshes with N and N' number of elements, respectively. Then, by using the fact that $h \simeq N^{-1/2}$, we consider the experimental rate of convergence given by

$$\mathtt{r} := -2\frac{\log(\mathrm{e}/\mathrm{e}')}{\log(N/N')} \quad \text{for quasi-uniform/adaptive refinements.}$$

The examples to be considered in this section are summarized in Table 1. For the examples that include adaptivity, we use the following algorithm:

1. Start with a coarse mesh $\mathcal{T}_h$ of $\overline{\mathrm{D}_h}$.
2. Solve the discrete problem (3.9) on the current mesh $\mathcal{T}_h$.
3. Compute Θ_T for each $T \in \mathcal{T}_h$.

4. Check the stopping criterion and decide whether to finish or go to next step.
5. Use *red-green-blue* procedure to refine each $T' \in \mathcal{T}_h$ satisfying $\Theta_{T'} \geq 0.5\,(\max_{T\in\mathcal{T}_h}\Theta_{\mathrm{T}})$.
6. Project every new vertex $\mathbf{x}$ of Γ_h onto the closest point $\widetilde{\mathbf{x}}$ of Γ by using the transferring paths.
7. Define the resulting mesh as the current mesh $\mathcal{T}_h$, and go to step 2.

While Steps 1–5 are applied to refine polygonal meshes (see, e.g. [47]), the 6*th* step is added to improve the approximation of the curved boundary (see, e.g. [46]) and also to expect the Assumption **(A2)** of Section 3.4 to hold. In fact, without including the 6*th* step, the region D_h^c remains unchanged when updating $\mathcal{T}_h$.

Example	$d(\Gamma,\Gamma_h)$	Exact solution	Ω	$\Omega^c\cap\mathrm{D}_h$	Adaptivity
1	$\mathcal{O}(h)$	smooth	nonconvex	$\varnothing$	no
2	$\mathcal{O}(h^2)$	smooth	convex	$\varnothing$	no
3	$\mathcal{O}(h^2)$	smooth	convex	$\varnothing$	yes
4	$\mathcal{O}(h^2)$	with a singularity	nonconvex	$\varnothing$	yes
5*	$\mathcal{O}(h^2)$	smooth	nonconvex	$\neq\varnothing$	yes

Table 1: *It is carried out with the help of the considerations made in Section 5.3.

Example 1. This test is aimed at evaluating the performance of the method when the computational boundary is as far from Γ as the theory allows. To that end, we consider the kidney-shaped domain Ω whose boundary satisfies

$$\left(2\left[(x_1+0.5)^2+x_2^2\right]-x_1-0.5\right)^2-\left[(x_1+0.5)^2+x_2^2\right]+0.1=0.$$

In turn, we take the viscosity $\mu=1$, and $\mathbf{f}$ and $\mathbf{g}$ such that the exact solution is given by

$$\mathbf{u}(x_1,x_2):=\begin{pmatrix}-2x_2\sin(x_1)\\(x_1^2+x_2^2)\cos(x_1)+2x_1\sin(x_1)\end{pmatrix}\quad\text{and}\quad p(x_1,x_2):=\sin\left(x_1^2+x_2^2\right)-p_0(x_1,x_2),$$

where $p_0\in\mathbb{R}$ is chosen such that $p\in\mathrm{L}_0^2(\Omega)$. In practice, p_0 is computed numerically employing a extremely fine polygonal mesh approximating Ω. The precise construction of D_h is given next. Following [21, Section 2.1], we consider a uniform Cartesian background grid $\mathcal{B}_h$ of a square domain $\mathcal{B}$ such that $\Omega\subset\mathcal{B}$, and then set D_h as the union of all elements that are inside Ω; see an example in the left panel of Figure 3. Here, the index $h>0$, refers to the meshsize of $\mathcal{B}_h$. By construction, the distance $d(\Gamma_h,\Gamma)$ is only of order h, which increases the complexity for the implementation of the transferring paths. However, as we have already seen in Section 3.2, this task is reduced to find those paths associated to the vertices $\mathbf{p}_1$ and $\mathbf{p}_2$ of every edge $e\in\mathcal{E}_h^\partial$. To that end, we use the algorithm proposed in [21, Section 2.4.1] that uniquely determines a point $\widetilde{\mathbf{p}}_i$ $(i=1,2)$ in Γ as the closest point to $\mathbf{p}_i$ such that $\mathscr{C}(\mathbf{p}_i)$ does not intersect any other path and does not intersect the interior of the domain D_h; computed paths are shown in the right panel of Figure 3. In Table 2 we present the convergence history obtained for this example under a sequence of uniform triangulations of the background mesh detailed before. We observe there that the convergence rate predicted by Theorem 4.7, namely $\mathcal{O}(h^{k+1})$, is attained by $\mathrm{e}(\mathbf{u})$, $\mathrm{e}(\boldsymbol{\sigma})$ and $\mathrm{e}(p)$. In addition, the error $\mathrm{e}^\star(\mathbf{u})$ is clearly converging like $\mathcal{O}(h^{k+2})$, that is, it is superconvergent, which corresponds to the theoretical error bound (5.2) with $l=m=k+1$. On the other hand, the approximate pseudostress component $\sigma_{11,h}$ obtained with $N=654$ and $k=2$ is depicted in Figure 4. The good accuracy of the approximation suggests that the Assumption **(A2)** (cf. Section 5) holds true, event though it is not entirely verifiable because some of the quantities involved cannot be calculable explicitly.

Example 2. Next, the accuracy of the proposed scheme (3.9) is tested under a sequence of quasi-uniform triangulations satisfying the hypotheses in Section 5. The main goal is to asses the properties of the posteriori error estimator Θ (cf. (5.3)) via the effectivity index $\mathrm{eff}(\Theta)$. We choose Ω as a disc centered at the origin with radius 2, the viscosity $\mu=1$ and the smooth solution to the problem (2.4) given by

$$\mathbf{u}(x_1,x_2):=\begin{pmatrix}-\pi\cos(\pi x_2)\sin(\pi x_1)\\\pi\cos(\pi x_1)\sin(\pi x_2)\end{pmatrix}\quad\text{and}\quad p(x_1,x_2):=x_2\exp(x_1)-p_0(x_1,x_2),$$

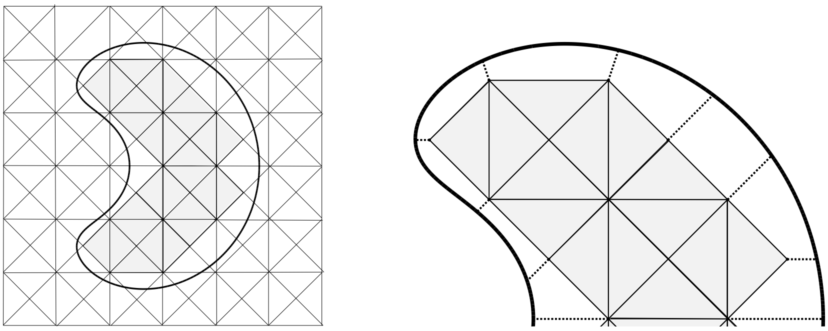

Figure 3: Left: the domain Ω defined in EXAMPLE 1, its boundary Γ (solid line), the first background mesh $\mathcal{B}_h$ under consideration, and the corresponding computational domain D_h (gray color). Right: computed transferring paths (dotted lines) associated to the vertices of the computational boundary; they were obtained by using the algorithm introduced in [21, Section 2.4.1].

k	N	h	d.o.f	$\mathrm{e}(\mathbf{u})$	$\mathtt{r}$	$\mathrm{e}^\star(\mathbf{u})$	$\mathtt{r}$	$\mathrm{e}(\boldsymbol{\sigma})$	$\mathtt{r}$	$\mathrm{e}(p)$	$\mathtt{r}$
0	28	0.263	159	$3.98e-02$	–	$2.02e-02$	–	$8.40e-01$	–	$3.09e-01$	–
	146	0.131	769	$2.50e-02$	0.56	$3.87e-03$	2.00	$3.81e-01$	0.96	$1.21e-01$	1.14
	654	0.066	3355	$1.39e-02$	0.78	$8.99e-04$	1.95	$1.76e-01$	1.03	$5.16e-02$	1.14
	3068	0.031	15497	$6.90e-03$	0.90	$2.88e-04$	1.47	$7.57e-02$	1.10	$2.02e-02$	1.21
	12579	0.016	63205	$3.52e-03$	0.96	$7.66e-05$	1.88	$3.63e-02$	1.04	$9.28e-03$	1.10
	50877	0.008	255007	$1.78e-03$	0.98	$1.90e-05$	1.99	$1.77e-02$	1.03	$4.51e-03$	1.03
1	28	0.263	485	$5.23e-03$	–	$2.06e-03$	–	$2.08e-01$	–	$1.09e-01$	–
	146	0.131	2413	$1.42e-03$	1.58	$1.80e-04$	2.95	$2.64e-02$	2.50	$7.78e-03$	3.20
	654	0.066	10633	$3.70e-04$	1.79	$4.22e-05$	1.94	$7.05e-03$	1.76	$2.88e-03$	1.33
	3068	0.031	49401	$9.54e-05$	1.75	$2.52e-06$	3.65	$1.20e-03$	2.29	$4.18e-04$	2.50
	12579	0.016	201883	$2.40e-05$	1.95	$2.65e-07$	3.19	$2.58e-04$	2.18	$7.49e-05$	2.44
	50877	0.008	815275	$6.04e-06$	1.98	$2.57e-08$	3.34	$5.35e-05$	2.25	$1.21e-05$	2.61
2	28	0.263	979	$3.15e-04$	–	$3.09e-04$	–	$2.13e-02$	–	$1.41e-02$	–
	146	0.131	4933	$1.48e-05$	3.70	$1.29e-05$	3.85	$1.41e-03$	3.29	$8.30e-04$	3.43
	654	0.066	21835	$6.52e-06$	1.10	$6.03e-06$	1.02	$1.03e-03$	0.42	$6.89e-04$	0.25
	3068	0.031	101713	$1.40e-07$	4.97	$6.56e-08$	5.85	$1.40e-05$	5.56	$8.44e-06$	5.70
	12579	0.016	416035	$1.62e-08$	3.06	$3.48e-09$	4.16	$1.35e-06$	3.31	$7.88e-07$	3.36
	50877	0.008	1680805	$2.02e-09$	2.98	$2.04e-10$	4.06	$1.03e-07$	3.69	$5.63e-08$	3.78
3	28	0.263	1641	$6.78e-05$	–	$6.74e-05$	–	$5.78e-03$	–	$3.88e-03$	–
	146	0.131	8329	$1.68e-06$	4.48	$1.66e-06$	4.49	$1.73e-04$	4.25	$1.11e-04$	4.31
	654	0.066	36961	$1.35e-07$	3.36	$1.35e-07$	3.35	$2.58e-05$	2.54	$1.67e-05$	2.52
	3068	0.031	172433	$1.27e-09$	6.04	$3.97e-10$	7.54	$1.77e-07$	6.45	$1.06e-07$	6.55
	12579	0.016	705661	$7.68e-11$	3.97	$1.18e-11$	4.99	$8.33e-09$	4.33	$4.69e-09$	4.42
	50877	0.008	2851597	$4.77e-12$	3.98	$2.86e-13$	5.32	$3.46e-10$	4.55	$2.01e-10$	4.51

Table 2: EXAMPLE 1: Convergence history of the individual errors under uniform refinement.

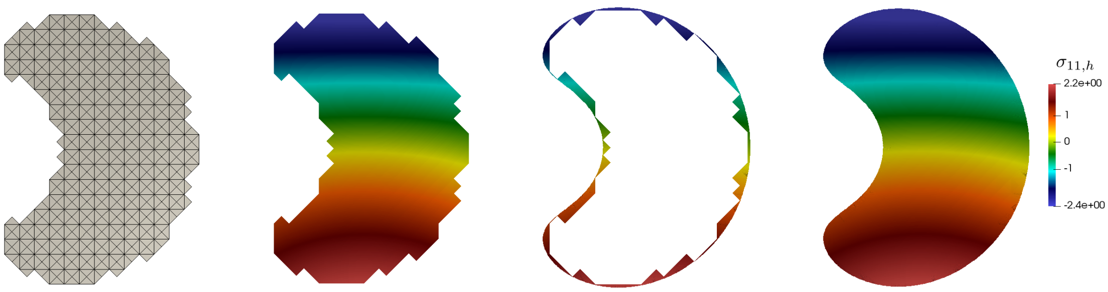

Figure 4: EXAMPLE 1: Approximate pseudostress component $\sigma_{11,h}$ obtained with $N = 654$ and $k = 2$.

where p_0 satisfies the same as that required by the previous example, in terms of which we define the corresponding source term $\mathbf{f}$ and the Dirichlet data $\mathbf{g}$. Let us now specify the domain D_h. Given $h > 0$, let Γ_h be the computational boundary constructed through a piecewise linear interpolation of Γ, such that the length of each segment is of order h. We define D_h as the region enclosed by Γ_h and then set $\mathcal{T}_h$ as a quasi-uniform triangulation of D_h with meshsize h. The transferring paths associated to the interior points of a boundary edge e can be chosen so that they are perpendicular to e, we have $d(\Gamma, \Gamma_h) = \mathcal{O}(h^2)$ and actually the assumptions of Section 3.4 hold for h small enough. Also, all the geometrical hypotheses required by the a posteriori error analysis (cf. Section 5) are satisfied. The results reported in Table 3 are in accordance with the theoretical bounds established in (5.2) and Theorem 4.7. In addition, from Table 4, we can conclude that both estimator terms $\mathbb{J}$ and $\mathbb{K}$ yield a convergence $\mathcal{O}(h^{k+3/2})$, which, together with the fact that, for each $k \in \{0, 1, 2, 3\}$, the effectivity index $\mathtt{eff}(\Theta)$ remains bounded, verifies not only the reliability of the a posteriori error estimator Θ, but also suggests its efficiency. In turn, the effectivity index increases as k does, which is not surprising since, according to Theorem 5.1, the reliability constant depends on the polynomial degree, and more specifically on the extrapolation constant defined in (3.20).

k	N	d.o.f	$\mathrm{e}(\mathbf{u})$	$\mathtt{r}$	$\mathrm{e}^\star(\mathbf{u})$	$\mathtt{r}$	$\mathrm{e}(\boldsymbol{\sigma})$	$\mathtt{r}$	$\mathrm{e}(p)$	$\mathtt{r}$
0	36	191	$5.82e+00$	–	$4.89e+00$	–	$2.31e+02$	–	$2.15e+01$	–
	138	721	$3.51e+00$	0.75	$1.55e+00$	1.72	$1.40e+02$	0.75	$1.23e+01$	0.83
	528	2721	$1.78e+00$	1.01	$4.31e-01$	1.90	$7.20e+01$	0.99	$6.15e+00$	1.03
	2120	10713	$8.86e-01$	1.01	$1.01e-01$	2.09	$3.59e+01$	1.00	$3.03e+00$	1.02
	8696	43737	$4.43e-01$	0.98	$2.49e-02$	1.99	$1.79e+01$	0.98	$1.53e+00$	0.97
	34612	173573	$2.21e-01$	1.00	$6.30e-03$	1.99	$8.98e+00$	1.00	$7.63e-01$	1.01
1	36	597	$3.30e+00$	–	$1.69e+00$	–	$1.27e+02$	–	$1.19e+01$	–
	138	2269	$8.85e-01$	1.96	$2.12e-01$	3.09	$3.40e+01$	1.96	$4.41e+00$	1.48
	528	8609	$2.46e-01$	1.91	$2.88e-02$	2.98	$9.98e+00$	1.83	$1.16e+00$	1.99
	2120	34145	$5.86e-02$	2.06	$3.34e-03$	3.10	$2.41e+00$	2.04	$2.75e-01$	2.07
	8696	139649	$1.44e-02$	1.99	$4.12e-04$	2.97	$5.95e-01$	1.98	$6.85e-02$	1.97
	34612	554817	$3.60e-03$	2.00	$5.12e-05$	3.02	$1.49e-01$	2.00	$1.71e-02$	2.01
2	36	1219	$1.08e+00$	–	$4.44e-01$	–	$4.51e+01$	–	$5.66e+00$	–
	138	4645	$1.67e-01$	2.78	$2.10e-02$	4.54	$6.73e+00$	2.83	$7.78e-01$	2.95
	528	17665	$2.17e-02$	3.04	$1.66e-03$	3.78	$8.96e-01$	3.01	$1.15e-01$	2.85
	2120	70297	$2.61e-03$	3.05	$8.91e-05$	4.21	$1.08e-01$	3.04	$1.36e-02$	3.07
	8696	287737	$3.29e-04$	2.93	$5.46e-06$	3.96	$1.36e-02$	2.94	$1.65e-03$	2.99
	34612	1143733	$4.10e-05$	3.02	$3.39e-07$	4.02	$1.70e-03$	3.02	$2.07e-04$	3.00
3	36	2057	$3.08e-01$	–	$1.43e-01$	–	$1.41e+01$	–	$1.98e+00$	–
	138	7849	$2.09e-02$	4.01	$3.43e-03$	5.56	$8.69e-01$	4.15	$1.26e-01$	4.10
	528	29889	$1.89e-03$	3.58	$1.24e-04$	4.94	$7.68e-02$	3.62	$8.06e-03$	4.10
	2120	119169	$1.01e-04$	4.22	$3.64e-06$	5.08	$4.13e-03$	4.21	$4.57e-04$	4.13
	8696	488001	$6.34e-06$	3.92	$1.19e-07$	4.85	$2.61e-04$	3.91	$2.95e-05$	3.88
	34612	1940321	$3.93e-07$	4.03	$3.66e-09$	5.04	$1.61e-05$	4.03	$1.80e-06$	4.05

Table 3: Example 2: Convergence history of the individual errors with quasi-uniform refinement.

Example 3. We set the fluid domain Ω, the computational domain D_h, the transferring paths and the viscosity as in the previous example. However, this time, the manufactured exact solution adopts the form

$$\mathbf{u}(x_1, x_2) := \begin{pmatrix} x_1 \sin(x_2) - \sin(x_1) \\ \cos(x_2) + x_2 \cos(x_1) \end{pmatrix} \quad \text{and} \quad p(x, y) := \frac{1}{x_1^2 + x_2^2 - 2.05^2} - p_0(x_1, x_2),$$

with $p_0 \in \mathbb{R}$ being chosen as before. Notice that p has high gradients near the boundary Γ and thus, in addition to the accuracy of the method, we now asses the performance of the a posteriori error estimator Θ by using both quasi-uniform and adaptive refinement strategies. In Figure 5, we display the total error decay with respect to the total number of elements using both refinement strategies and different polynomial

k	N	d.o.f	$\mathbb{J}$	r	$\mathbb{K}$	r	$\mathrm{e}(\boldsymbol{\sigma},\mathbf{u})$	r	Θ	r	eff(Θ)
0	36	191	$6.23e+00$	–	$2.51e+01$	–	$2.31e+02$	–	$2.26e+02$	–	0.981
	138	721	$2.20e+00$	1.55	$1.02e+01$	1.34	$1.40e+02$	0.75	$1.43e+02$	0.69	1.021
	528	2721	$7.30e-01$	1.65	$4.76e+00$	1.14	$7.20e+01$	0.99	$7.42e+01$	0.97	1.031
	2120	10713	$4.00e-01$	0.87	$1.90e+00$	1.32	$3.59e+01$	1.00	$3.70e+01$	1.00	1.032
	8696	43737	$1.23e-01$	1.67	$6.63e-01$	1.49	$1.80e+01$	0.98	$1.85e+01$	0.98	1.031
	34612	173573	$4.38e-02$	1.50	$2.36e-01$	1.50	$8.98e+00$	1.00	$9.26e+00$	1.00	1.031
1	36	597	$2.13e+00$	–	$4.89e+01$	–	$1.27e+02$	–	$1.86e+02$	–	1.468
	138	2269	$4.45e-01$	2.33	$5.66e+00$	3.21	$3.40e+01$	1.96	$5.73e+01$	1.75	1.687
	528	8609	$6.60e-02$	2.84	$8.89e-01$	2.76	$9.98e+00$	1.83	$1.60e+01$	1.91	1.599
	2120	34145	$1.51e-02$	2.12	$1.81e-01$	2.29	$2.41e+00$	2.04	$3.88e+00$	2.04	1.607
	8696	139649	$2.20e-03$	2.73	$2.79e-02$	2.65	$5.95e-01$	1.98	$9.96e-01$	1.93	1.673
	34612	554817	$4.08e-04$	2.44	$5.26e-03$	2.42	$1.49e-01$	2.00	$2.47e-01$	2.02	1.657
2	36	1219	$7.90e-01$	–	$2.83e+01$	–	$4.51e+01$	–	$9.32e+01$	–	2.067
	138	4645	$4.44e-02$	4.28	$1.01e+00$	4.95	$6.73e+00$	2.83	$1.29e+01$	2.95	1.911
	528	17665	$2.94e-03$	4.05	$9.89e-02$	3.47	$8.96e-01$	3.01	$2.17e+00$	2.65	2.418
	2120	70297	$3.98e-04$	2.88	$1.19e-02$	3.05	$1.08e-01$	3.04	$2.47e-01$	3.12	2.287
	8696	287737	$2.75e-05$	3.79	$8.85e-04$	3.68	$1.36e-02$	2.94	$3.11e-02$	2.94	2.279
	34612	1143733	$2.48e-06$	3.48	$7.87e-05$	3.50	$1.70e-03$	3.02	$3.88e-03$	3.01	2.285
3	36	2057	$1.98e-01$	–	$9.05e+00$	–	$1.41e+01$	–	$3.08e+01$	–	2.175
	138	7849	$5.06e-03$	5.46	$1.93e-01$	5.73	$8.70e-01$	4.15	$2.76e+00$	3.59	3.176
	528	29889	$1.56e-04$	5.18	$6.55e-03$	5.05	$7.68e-02$	3.62	$1.99e-01$	3.92	2.594
	2120	119169	$1.05e-05$	3.88	$4.38e-04$	3.89	$4.13e-03$	4.21	$1.13e-02$	4.13	2.729
	8696	488001	$2.83e-07$	5.12	$1.46e-05$	4.82	$2.61e-04$	3.91	$7.61e-04$	3.82	2.920
	34612	1940321	$1.30e-08$	4.46	$7.46e-07$	4.31	$1.61e-05$	4.03	$4.61e-05$	4.06	2.855

Table 4: EXAMPLE 2: Convergence history of some estimator terms and the total error with quasi-uniform refinement.

degrees. In all cases, the errors of the adaptive refinement are considerably smaller than the quasi-uniform ones considering the same number of elements $N > 500$, and it is also able to achieve the optimal convergence order for the total error $\mathrm{e}(\boldsymbol{\sigma},\mathbf{u})$, namely $\mathcal{O}(h^{k+1})$. Some snapshots of the adapted meshes obtained with $k = 0$ and $k = 2$ are depicted in Figure 6, and it is concluded from there that the adaptive procedure is marking where is needed. Moreover, it is clear that the case $k = 2$ produces a very accurate approximate pseudostress component $\sigma_{22,h}$ with a considerable less number of triangles than its counterpart of lowest order.

Example 4. The next example is on the pacman-shaped domain

$$\Omega := \left\{(x_1,x_2) \in \mathbb{R}^2 : \ x_1^2 + x_2^2 < 1\right\} \setminus (0,1)\times(-1,0),$$

with $\mu = 1/2$ and the manufactured exact solution given, in polar coordinates, by

$$\mathbf{u}(r,\lambda) := \begin{pmatrix} r^{2/3}\sin\left(\frac{2\lambda}{3}\right) \\ r^{2/3}\cos\left(\frac{2\lambda}{3}\right) \end{pmatrix} \quad \text{and} \quad p(r,\lambda) = 0,$$

satisfying $\mathbf{f} = \mathbf{0}$. We notice that the partial derivatives of the components of $\mathbf{u}$ have a singularity at the origin, and then a convergence $\mathcal{O}(h^{2/3})$ should be expected from Theorem 4.7. The construction of the domain D_h and transferring paths are the same as that indicated in the last two examples. We point out that, since the nonconvex part of $\overline{\Omega}$ is only including the straight segments $\{0\}\times(-1,0)$ and $(0,1)\times\{0\}$, on which the boundaries Γ_h and Γ coincide, the requirement $\mathrm{D}_h \subset \Omega$ holds true. In Table 5 we report the convergence history of the total error for $k = 0$ using the quasi-uniform refinement strategy, where the total error is converging like $\mathcal{O}(h^{2/3})$, as expected. In turn, it can be observed from Figure 7 that in all cases the adaptive algorithm reduces significantly the magnitude of the total error and also restores the

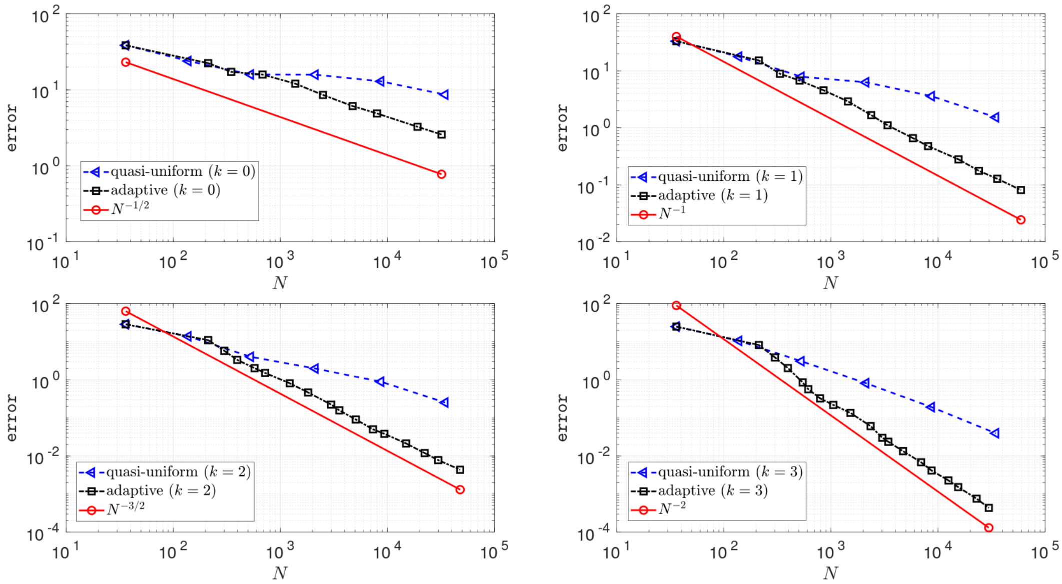

Figure 5: EXAMPLE 3: Log-log plot of $\mathrm{e}(\boldsymbol{\sigma}, \mathbf{u})$ vs N for quasi-uniform/adaptive refinements and $k = 0, 1, 2, 3$.

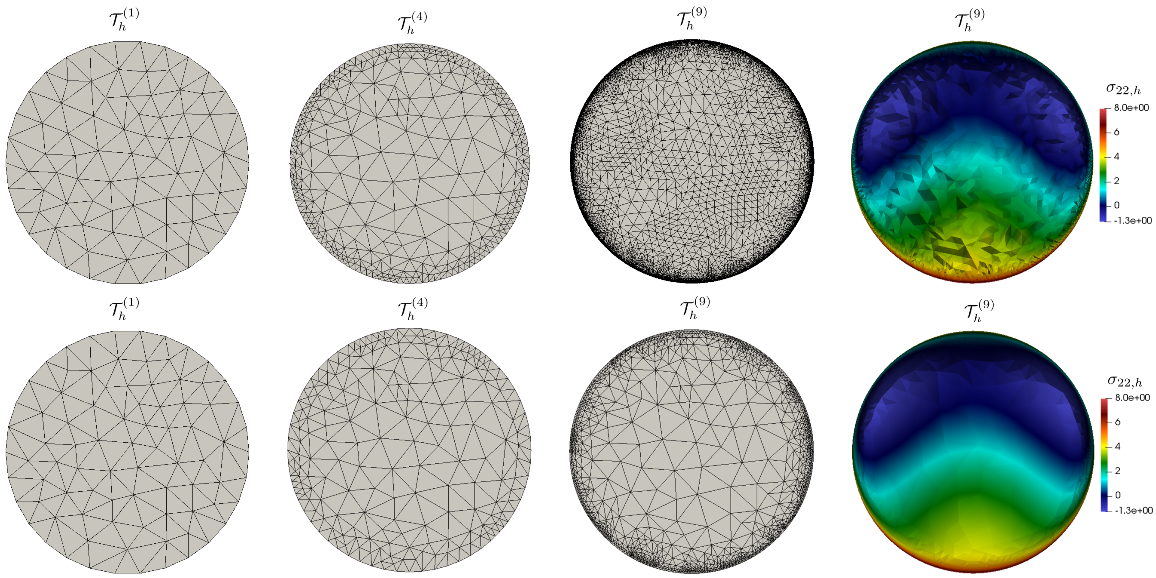

Figure 6: EXAMPLE 3: Initial mesh and two adapted meshes according to the residual-based a posteriori error estimator Θ with $k = 0$ (first row) and $k = 2$ (second row), and comparative view of the approximate pseudostress component $\sigma_{22,h}$ obtained in the $9th$ iteration.

k	N	d.o.f	$\mathrm{e}(\boldsymbol{\sigma}, \mathbf{u})$	r
0	65	349	2.62e-01	–
	257	1331	1.58e-01	0.73
	1037	5273	1.01e-01	0.65
	4143	20873	6.32e-02	0.67
	16583	83333	4.08e-02	0.63

Table 5: EXAMPLE 4: Convergence history of the total error with quasi-uniform refinement.

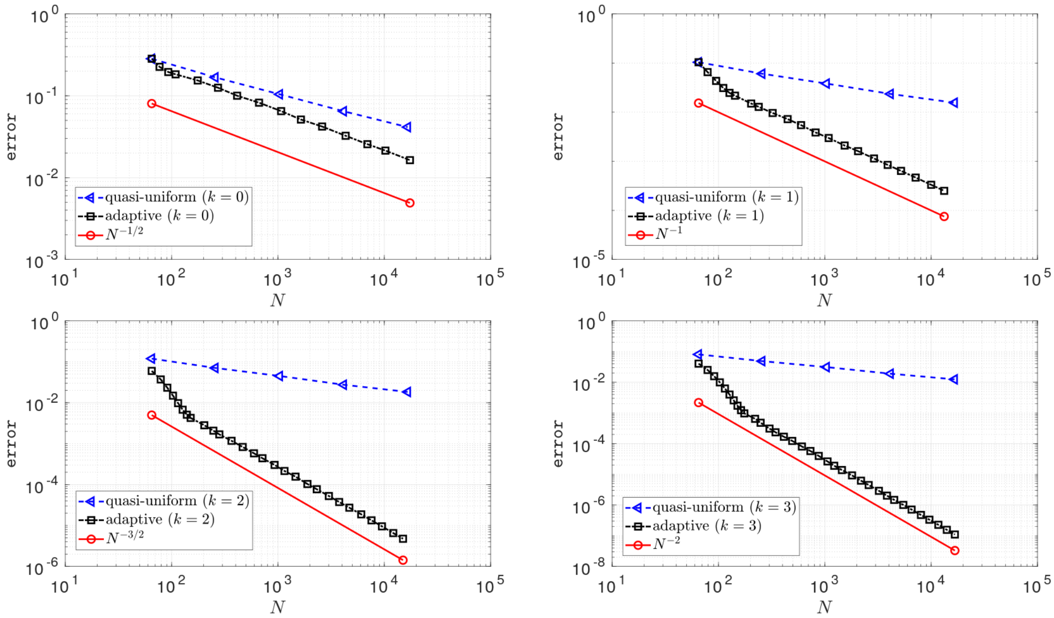

Figure 7: EXAMPLE 4: Log-log plot of $\mathrm{e}(\boldsymbol{\sigma}, \mathbf{u})$ vs N for quasi-uniform/adaptive refinements and $k = 0, 1, 2, 3$.

optimal convergence order. Again, very accurate approximations are obtained with a few elements when the polynomial degree is increased as Figure 8 shows.

Example 5. To conclude, we choose Ω to be the annular domain consisting in two concentric circles of radius 0.5 and 2, respectively. Here the computational boundary is also constructed through a piecewise linear interpolation of Γ, implying $\omega := \Omega^c \cap \mathrm{D}_h \neq \varnothing$. In order to asses the accuracy of the Galerkin scheme (3.9) we use both quasi-uniform and adaptive refinement strategies and adopt the considerations made in Section 5.3. To that end, we take $\mu = 1$ and the manufactured exact solution such that

$$\mathbf{u}(x_1, x_2) := \begin{pmatrix} \dfrac{x_2}{x_1^2 + x_2^2 - 2.2^2} - \pi \cos(\pi x_2) \sin(\pi x_1) \\ -\dfrac{x_1}{x_1^2 + x_2^2 - 2.2^2} + \pi \cos(\pi x_1) \sin(\pi x_2) \end{pmatrix}$$

and

$$p(x_1, x_2) = \frac{1}{\exp(x_1^2 + x_2^2 - 0.45^2) - 1} - p_0(x_1, x_2),$$

with $p_0 \in \mathbb{R}$ being chosen so that $p \in \mathrm{L}_0^2(\Omega)$. As a result, the fluid pressure has high gradients near the boundary of the circle of radius 0.5, whereas the components of the fluid velocity have high gradients near the circle of radius 2. The decay of the total error with respect to the total number of elements using both refinement strategies is depicted in Figure 9. In all cases, although the adaptive procedure is able to recognize the regions where there exist high gradients of the solution, the error convergence is oscillatory for small values of N, which could be explained by the fact that the region ω is too big when starting the mesh refinement process as shown in Figure 10. After that, the adaptive refinement strategy is much superior that the quasi-uniform one because it reduces the magnitude of the total error with optimal convergence $\mathcal{O}(h^{k+1})$. We also present in Figure 10 the approximate velocity component $u_{1,h}$ and the approximate pressure p_h obtained with the adaptive procedure and $k = 2$.

References

[1] R. ARAYA, T. P. BARRIOS, G. N. GATICA, AND N. HEUER, *A posteriori error estimates for a mixed-fem formulation of a non-linear elliptic problem*, Computer methods in applied mechanics and engineering, 191 (2002), pp. 2317–2336.

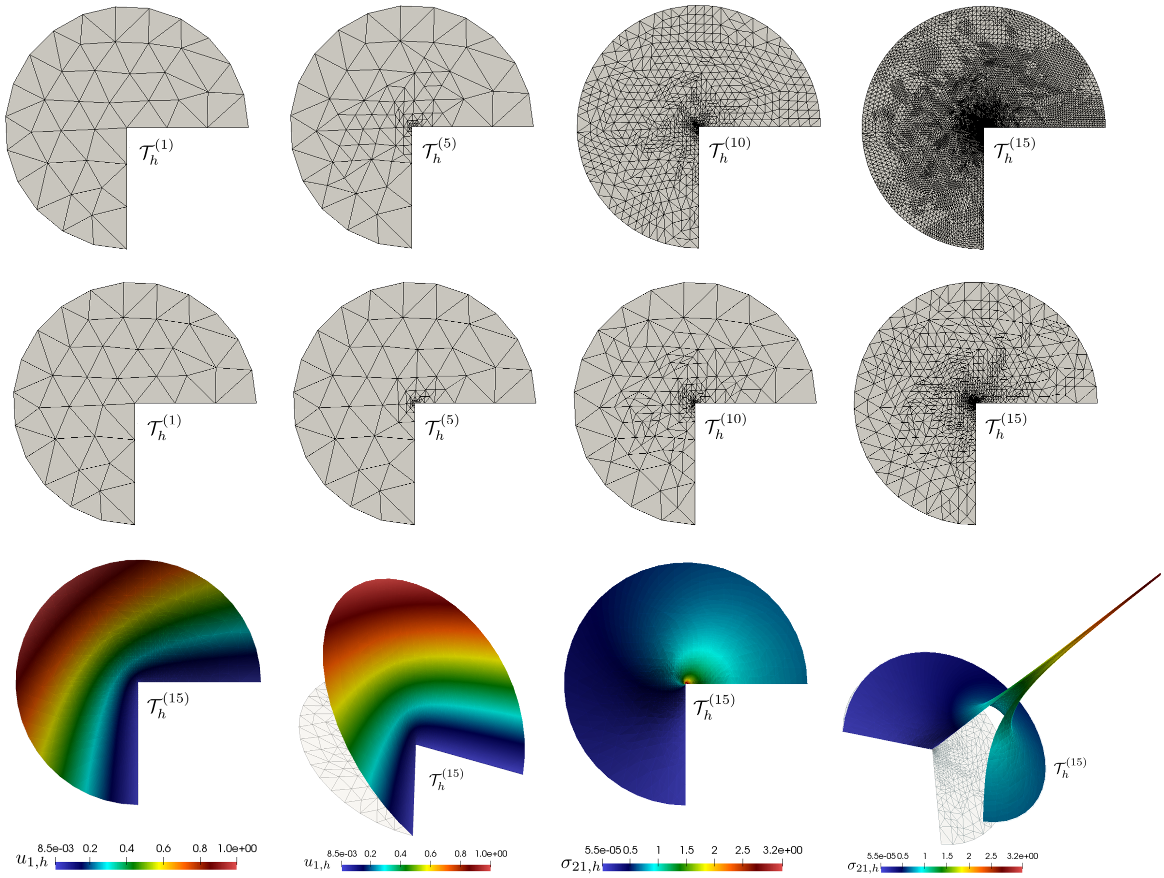

Figure 8: Example 4: Initial mesh and three adapted meshes according to residual-based a posteriori error estimator Θ with $k = 0$ (first row) and $k = 1$ (second row), approximate velocity component $u_{1,h}$ and approximate pseudostress component $\sigma_{21,h}$ obtained in the 15th iteration with $k = 1$ and $N = 2055$ (third row).

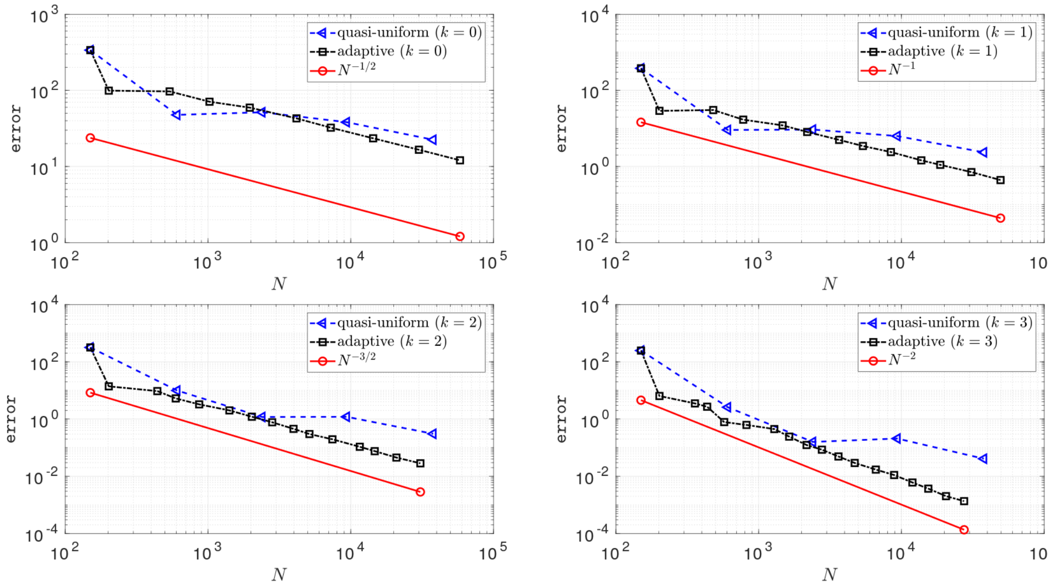

Figure 9: Example 5: Log-log plot of $\mathrm{e}(\boldsymbol{\sigma}, \mathbf{u})$ vs N for quasi-uniform/adaptive refinements and $k = 0, 1, 2, 3$.

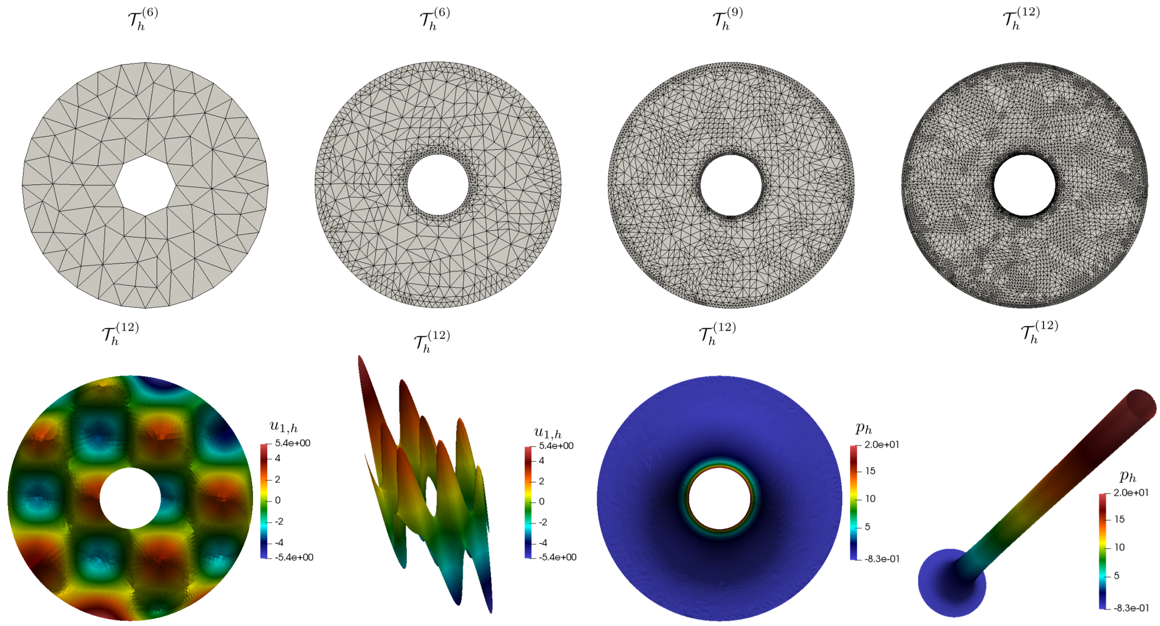

Figure 10: Example 5: Initial mesh and three adapted meshes according to the residual-based a posteriori error estimator Θ with $k = 2$ (first row), approximate velocity component $u_{1,h}$ and approximate pressure p_h obtained in the $12th$ iteration with $k = 2$ and $N = 11571$ (second row).

[2] M. G. Armentano, C. Padra, and M. Scheble, *An hp finite element adaptive scheme to solve the Poisson problem on curved domains*, Comput. Appl. Math., 34 (2015), pp. 705–727.

[3] D. N. Arnold, F. Brezzi, and J. Douglas, Jr., *PEERS: a new mixed finite element for plane elasticity*, Japan J. Appl. Math., 1 (1984), pp. 347–367.

[4] D. N. Arnold, J. Douglas, Jr., and C. P. Gupta, *A family of higher order mixed finite element methods for plane elasticity*, Numer. Math., 45 (1984), pp. 1–22.

[5] D. N. Arnold, R. S. Falk, and R. Winther, *Mixed finite element methods for linear elasticity with weakly imposed symmetry*, Math. Comp., 76 (2007), pp. 1699–1723.

[6] I. Babuška and M. R. Dorr, *Error estimates for the combined h and p versions of the finite element method*, Numer. Math., 37 (1981), pp. 257–277.

[7] T. P. Barrios, G. N. Gatica, M. González, and N. Heuer, *A residual based a posteriori error estimator for an augmented mixed finite element method in linear elasticity*, M2AN Math. Model. Numer. Anal., 40 (2006), pp. 843–869 (2007).

[8] S. Beuchler, V. Pillwein, and S. Zaglmayr, *Sparsity optimized high order finite element functions for $H(\mathrm{div})$ on simplices*, Numer. Math., 122 (2012), pp. 197–225.

[9] S. C. Brenner and L. R. Scott, *The mathematical theory of finite element methods*, vol. 15 of Texts in Applied Mathematics, Springer, New York, third ed., 2008.

[10] F. Brezzi and M. Fortin, *Mixed and hybrid finite element methods*, vol. 15 of Springer Series in Computational Mathematics, Springer-Verlag, New York, 1991.

[11] E. Burman, S. Claus, P. Hansbo, M. G. Larson, and A. Massing, *CutFEM: discretizing geometry and partial differential equations*, Internat. J. Numer. Methods Engrg., 104 (2015), pp. 472–501.

[12] Z. Cai, B. Lee, and P. Wang, *Least-squares methods for incompressible Newtonian fluid flow: linear stationary problems*, SIAM J. Numer. Anal., 42 (2004), pp. 843–859.

[13] Z. Cai and Y. Wang, *Pseudostress-velocity formulation for incompressible Navier-Stokes equations*, Internat. J. Numer. Methods Fluids, 63 (2010), pp. 341–356.

[14] C. Carstensen, *A posteriori error estimate for the mixed finite element method*, Math. Comp., 66 (1997), pp. 465–476.

[15] C. Carstensen and G. Dolzmann, *A posteriori error estimates for mixed FEM in elasticity*, Numer. Math., 81 (1998), pp. 187–209.

[16] P. Clément, *Approximation by finite element functions using local regularization*, Rev. Française Automat. Informat. Recherche Opérationnelle Sér., 9 (1975), pp. 77–84.

[17] B. Cockburn, J. Gopalakrishnan, and F.-J. Sayas, *A projection-based error analysis of HDG methods*, Math. Comp., 79 (2010), pp. 1351–1367.

[18] B. Cockburn, D. Gupta, and F. Reitich, *Boundary-conforming discontinuous Galerkin methods via extensions from subdomains*, J. Sci. Comput., 42 (2010), pp. 144–184.

[19] B. Cockburn, W. Qiu, and M. Solano, *A priori error analysis for HDG methods using extensions from subdomains to achieve boundary conformity*, Math. Comp., 83 (2014), pp. 665–699.

[20] B. Cockburn, F.-J. Sayas, and M. Solano, *Coupling at a distance HDG and BEM*, SIAM J. Sci. Comput., 34 (2012), pp. A28–A47.

[21] B. Cockburn and M. Solano, *Solving Dirichlet boundary-value problems on curved domains by extensions from subdomains*, SIAM J. Sci. Comput., 34 (2012), pp. A497–A519.

[22] B. Cockburn and M. Solano, *Solving convection-diffusion problems on curved domains by extensions from subdomains*, J. Sci. Comput., 59 (2014), pp. 512–543.

[23] B. Cockburn and W. Zhang, *A posteriori error estimates for HDG methods*, J. Sci. Comput., 51 (2012), pp. 582–607.

[24] B. Cockburn and W. Zhang, *An a posteriori error estimate for the variable-degree Raviart-Thomas method*, Math. Comp., 83 (2014), pp. 1063–1082.

[25] E. Colmenares, G. N. Gatica, and R. Oyarzúa, *Analysis of an augmented mixed-primal formulation for the stationary Boussinesq problem*, Numer. Methods Partial Differential Equations, 32 (2016), pp. 445–478.

[26] T. A. Davis, *Algorithm 832: UMFPACK V4.3—an unsymmetric-pattern multifrontal method*, ACM Trans. Math. Software, 30 (2004), pp. 196–199.

[27] S. Deng and W. Cai, *Analysis and application of an orthogonal nodal basis on triangles for discontinuous spectral element methods*, Applied Numerical Analysis & Computational Mathematics, 2 (2005), pp. 326–345.

[28] D. A. Di Pietro and A. Ern, *Mathematical aspects of discontinuous Galerkin methods*, vol. 69 of Mathématiques & Applications (Berlin) [Mathematics & Applications], Springer, Heidelberg, 2012.

[29] G. N. Gatica, *A simple introduction to the mixed finite element method*, Theory and Applications. Springer Briefs in Mathematics. Springer, London, (2014).

[30] G. N. Gatica, A. Márquez, and M. A. Sánchez, *Analysis of a velocity–pressure–pseudostress formulation for the stationary stokes equations*, Computer Methods in Applied Mechanics and Engineering, 199 (2010), pp. 1064–1079.

[31] G. N. Gatica, R. Oyarzúa, and F.-J. Sayas, *A residual-based a posteriori error estimator for a fully-mixed formulation of the Stokes-Darcy coupled problem*, Comput. Methods Appl. Mech. Engrg., 200 (2011), pp. 1877–1891.

[32] G. N. Gatica, R. Oyarzúa, and F.-J. Sayas, *A twofold saddle point approach for the coupling of fluid flow with nonlinear porous media flow*, IMA J. Numer. Anal., 32 (2012), pp. 845–887.

[33] G. N. Gatica, R. Ruiz-Baier, and G. Tierra, *A mixed finite element method for Darcy's equations with pressure dependent porosity*, Math. Comp., 85 (2016), pp. 1–33.

[34] G. N. Gatica and E. P. Stephan, *A mixed-FEM formulation for nonlinear incompressible elasticity in the plane*, Numer. Methods Partial Differential Equations, 18 (2002), pp. 105–128.

[35] V. Girault and P.-A. Raviart, *Finite element methods for Navier-Stokes equations*, vol. 5 of Springer Series in Computational Mathematics, Springer-Verlag, Berlin, 1986. Theory and algorithms.

[36] A. Hansbo and P. Hansbo, *An unfitted finite element method, based on nitsches method, for elliptic interface problems*, Computer methods in applied mechanics and engineering, 191 (2002), pp. 5537–5552.

[37] R. Hiptmair, *Finite elements in computational electromagnetism*, Acta Numerica, 11 (2002), pp. 237–339.

[38] M. Lenoir, *Optimal isoparametric finite elements and error estimates for domains involving curved boundaries*, SIAM J. Numer. Anal., 23 (1986), pp. 562–580.

[39] R. Oyarzúa, M. Solano, and P. Zúñiga, *A High Order Mixed-FEM for Diffusion Problems on Curved Domains*, J. Sci. Comput., 79 (2019), pp. 49–78.

[40] W. Qiu, M. Solano, and P. Vega, *A high order HDG method for curved-interface problems via approximations from straight triangulations*, J. Sci. Comput., 69 (2016), pp. 1384–1407.

[41] J. E. Roberts and J.-M. Thomas, *Mixed and hybrid methods*, in Handbook of numerical analysis, Vol. II, Handb. Numer. Anal., II, North-Holland, Amsterdam, 1991, pp. 523–639.

[42] T. Sánchez-Vizuet and M. E. Solano, *A Hybridizable Discontinuous Galerkin solver for the Grad–Shafranov equation*, Comput. Phys. Commun., 235 (2019), pp. 120–132.

[43] M. Solano and F. Vargas, *An unfitted HDG method for Oseen equations*, Preprint 2019-8, Centro de Investigación en Ingeniería Matemática (CI^{2}MA), Universidad de Concepción, Chile, Preprint available at `https://ci2ma.udec.cl/publicaciones/prepublicaciones/prepublicacion.php?id=358`.

[44] M. Solano and F. Vargas, *A high order HDG method for Stokes flow in curved domains*, J. Sci. Comput., (2019), doi:10.1007/s10915-018-00901-2.

[45] E. M. Stein, *Singular integrals and differentiability properties of functions*, Princeton Mathematical Series, No. 30, Princeton University Press, Princeton, N.J., 1970.

[46] R. Verfürth, *A posteriori error estimators for the Stokes equations*, Numer. Math., 55 (1989), pp. 309–325.

[47] R. Verfürth, *A Review of A Posteriori Error Estimation and Adaptive Mesh-Refinement Techniques*, Wiley Teubner (Chichester), 1996.

[48] R. Verfürth, *A posteriori error estimation techniques for finite element methods*, Numerical Mathematics and Scientific Computation, Oxford University Press, Oxford, 2013.

Centro de Investigación en Ingeniería Matemática (CI²MA)

PRE-PUBLICACIONES 2019

2019-04 Eligio Colmenares, Gabriel N. Gatica, Sebastian Moraga: *A Banach spaces-based analysis of a new fully-mixed finite element method for the Boussinesq problem*

2019-05 Antoine J. Cerfon, Tonatiuh Sanchez-Vizuet, Manuel Solano: *Adaptive Hybridizable Discontinuous Galerkin discretization of the Grad-Shafranov equation by extension from polygonal subdomains*

2019-06 Rommel Bustinza, Jonathan Munguia: *An HHO formulation for a Neumann problem on general meshes*

2019-07 Raimund Bürger, Gerardo Chowell, Leidy Y. Lara-Diaz: *Comparative analysis of phenomenological growth models applied to epidemic outbreaks*

2019-08 Manuel Solano, Felipe Vargas: *An unfitted HDG method for Oseen equations*

2019-09 Raimund Bürger, Stefan Diehl, María Carmen Martí: *A system of conservation laws with discontinuous flux modelling flotation with sedimentation*

2019-10 Andrea Cangiani, Mauricio Munar: *A posteriori error estimates for mixed virtual element methods*

2019-11 Alfredo Bermúdez, Bibiana López-Rodríguez, Rodolfo Rodríguez, Pilar Salgado: *Numerical analysis of a penalty approach for the solution of a transient eddy current problem*

2019-12 Javier A. Almonacid, Gabriel N. Gatica, Ricardo Ruiz-Baier: *Ultra-weak symmetry of stress for augmented mixed finite element formulations in continuum mechanics*

2019-13 Mario Álvarez, Gabriel N. Gatica, Ricardo Ruiz-Baier: *A mixed-primal finite element method for the coupling of Brinkman-Darcy flow and nonlinear transport*

2019-14 Marcelo Cavalcanti, Wellington Correa, Türker Özsari, Mauricio Sepúlveda, Rodrigo Véjar: *Exponential stability for the nonlinear Schrödinger equation with locally distributed damping*

2019-15 Ricardo Oyarzúa, Manuel Solano, Paulo Zuñiga: *A priori and a posteriori error analyses of a high order unfitted mixed-FEM for Stokes flow*

Para obtener copias de las Pre-Publicaciones, escribir o llamar a: Director, Centro de Investigación en Ingeniería Matemática, Universidad de Concepción, Casilla 160-C, Concepción, Chile, Tel.: 41-2661324, o bien, visitar la página web del centro: http://www.ci2ma.udec.cl




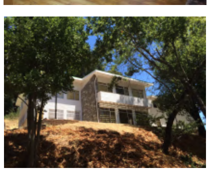

Centro de Investigación en
Ingeniería Matemática (CI²MA)
Universidad de Concepción

Casilla 160-C, Concepción, Chile
Tel.: 56-41-2661324/2661554/2661316
http://www.ci2ma.udec.cl